EFFECTS OF SALINE WATER ON
MECHANICAL PROPERTIES OF CONCRETE

BURIN THONGKLIANG

A Thesis Submitted in Partial Fulfillment of the Requirements for the

Degree of Master of Engineering in Civil, Transportation

and Geo-resources Engineering

Suranaree University of Technology

Academic Year 2023

ผลกระทบของน้ำเค็มต่อสมบัติทางกลของคอนกรีต

นางสาวบุรินทร์ ทองเกลี้ยง

EFFECTS OF SALINE WATER ON
MECHANICAL PROPERTIES OF CONCRETE

Suranaree University of Technology has approved this thesis submitted in partial fulfillment of the requirements for a Master's Degree.

Thesis Examining Committee

....
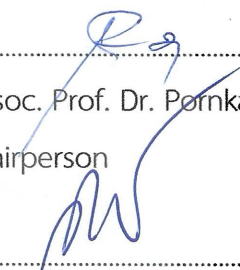
(Assoc. Prof. Dr. Pornkasem Jongpradist)

Chairperson

....

(Asst. Prof. Dr. Decho Phueakphum)

Member (Thesis Advisor)

....

(Asst. Prof. Dr. Prachya Tepnarong)

Member

....
(Assoc. Prof. Dr. Yupaporn Ruksakulpiwat)
Vice Rector for Academic Affairs and Quality
Assurance

....
(Assoc. Prof. Dr. Pornsiri Jongkol)
Dean of Institute of Engineering

บุรินทร์ ทองเกลี้ยง: ผลกระทบของน้ำเค็มต่อสมบัติทางกลของคอนกรีต (EFFECTS OF SALINE WATER ON MECHANICAL PROPERTIES OF CONCRETE) อาจารย์ที่ปรึกษา : ผู้ช่วยศาสตราจารย์ ดร.เดโช เผือกภูมิ, 102 หน้า

คำสำคัญ: ความเค็ม/ความแข็งแรง/การเสื่อมสภาพของคอนกรีต/การดูดซับน้ำ/ความเร็วคลื่นอัลตราโซนิค

วัตถุประสงค์ของการศึกษานี้คือการประเมินคุณสมบัติในระยะยาวของคอนกรีตที่แช่อยู่ใน น้ำเค็ม ตัวอย่างคอนกรีตทรงกระบอก (เส้นผ่าศูนย์กลาง = 15 เซนติเมตร และความยาว = 30 เซนติเมตร) และตัวอย่างมอร์ตาร์ทรงลูกบาศก์ (5 x 5 x 5 เซนติเมตร) ถูกเตรียมไว้เพื่อทดสอบในห้องปฏิบัติการ ตัวอย่างจะถูกแช่ในน้ำที่มีความเค็มต่าง ๆ (0, 25, 50, 75, และ 100%) เป็นเวลา 0, 1, 2, 3, 6, และ 12 เดือน การทดสอบกำลังอัดทั้งทางตรงและทางอ้อมถูกดำเนินการกับตัวอย่างที่ผ่านการแช่ในน้ำเค็มเพื่อ ประเมินการเสื่อมสภาพโดยการวัดคุณสมบัติเชิงกล ตัวอย่างที่ผ่านการทดสอบนี้ได้ถูกนำไปวิเคราะห์โดย ใช้เทคนิควิเคราะห์การเลี้ยวเบนของรังสีเอ็กซ์ ส่วนตัวอย่างมอร์ตาร์ ถูกนำไปวัดการดูดซึมของน้ำเค็มและ ความเร็วของคลื่นอัลตราโซนิก ผลทดสอบพบว่ากำลังอัดของคอนกรีตที่ผ่านการบ่มมีค่าเพิ่มขึ้นอย่าง รวดเร็วภายใน 7 วันแรก จากนั้นค่อย ๆ เพิ่มขึ้นและมีค่าสูงสุดหลังจากบ่มเป็นเวลา 28 วัน กำลังอัดและ ความยืดหยุ่นของคอนกรีตลดลงเมื่อความเค็มและเวลาที่แช่ในน้ำเค็มเพิ่มขึ้น การลดของความแข็งแรงและ ความยืดหยุ่นนี้ เกิดจากการแทรกซึมของไอออนคลอไรด์เข้าไปสู่ตัวอย่าง และทำให้เกิดปฏิกิริยาทางเคมี ระหว่างไอออนคลอไรด์กับ C_2S, C_3S, C_3A, และ C_4AF ทำให้เกิดการเสื่อมสภาพของคอนกรีต โดยที่ C_3S และ C_2S ลดลงเมื่อความเค็มเพิ่มขึ้น ในขณะที่ C_3A และ C_4AF เพิ่มขึ้น ส่วนการดูดซึมของน้ำเค็มมี แนวโน้มที่จะลดลงในขณะที่ความหนาแน่นมีแนวโน้มที่จะเพิ่มขึ้นตามเวลาแช่นานขึ้นและความเค็มสูงขึ้น ด้วยการแช่ในน้ำเกลือเป็นเวลานานและระดับความเค็มที่สูงจะมีแนวโน้มที่จะมีการลดลงของการดูดซึม น้ำเกลือและทำให้ความหนาแน่นมากมากขึ้นเนื่องจากการตกผลึกภายในช่องว่างของตัวอย่าง ความเร็ว ของคลื่นปฐมภูมิและทุติยภูมิมีการเพิ่มขึ้นแบบเอกซ์โพเนนเชียลเมื่อมีการแช่เวลาและความเค็มเพิ่มขึ้น โดยการเพิ่มขึ้นนี้เป็นผลให้ค่าอัตราส่วนปัวซองค์แบบไดนามิกมีค่าเพิ่มขึ้น ในขณะที่สัมประสิทธิ์ความ ยืดหยุ่นแบบไดนามิกมีค่าลดลง สมการทางคณิตศาสตร์ที่พัฒนาในงานวิจัยนี้สามารถประยุกต์ใช้คำนวณ กำลังอัดของคอนกรีตที่แช่ในน้ำเกลือที่เวลาใด ๆ และนำไปทำนายอายุของคอนกรีตได้

สาขาวิชา เทคโนโลยีธรณี

ปีการศึกษา 2566

ลายมือชื่อนักศึกษา ....

ลายมือชื่ออาจารย์ที่ปรึกษา ....

BURIN THONGKLIANG: EFFECTS OF SALINE WATER ON MECHANICAL PROPERTIES OF CONCRETE. THESIS ADVISOR: ASST.PROF. DECHO PHUEAKPHUM, PH.D., 102 PP.

The aim of this study is to assess the long-term properties of concrete immersing in saline water. Cylindrical concrete specimens (diameter = 15 cm and length = 30 cm) and cubic mortar specimens (5 x 5 x 5 cm) were prepared for laboratory tests. The specimens were immersed in saline water of varied salinity (0, 25, 50, 75, and 100%) for 0, 1, 2, 3, 6, and 12 months. Direct and indirect compression tests are conducted on samples that have been immersed in salt water to evaluate the deterioration of concrete by examining changes in mechanical properties. Post-tested samples were then subsequently analyzed using X-ray diffraction. Mortar samples were subjected to measurement of saltwater absorption and ultrasonic wave velocity. Test results reveal that the compressive strength of cured concrete notably increased rapidly within the initial 7 days, then gradually increased, and reached its peak at the end of 28 days. Concrete's compressive strength and elasticity decreased with increasing saline concentration and immersion time. This reduction in strength and elasticity is due to the infiltration of chloride ions into the sample and causes chemical reactions between chloride ions and C_2S, C_3S, C_3A, and C_4AF, contributing to concrete deterioration. C3S and C_2S content decreases as salinity increases, while C_3A and C_4AF increase. Saline absorption tends to decrease, while density tends to increase with increasing immersion time and salinity. With prolonged immersion time and higher salinity levels, there is a tendency for saline absorption to decrease, accompanied by an increase in density due to crystallization within voids. P- and S-wave velocities exhibited an exponential increase with increasing immersion time and salinity. Simultaneously, there was a concurrent rise in the dynamic Poisson's ratio while the dynamic elastic modulus decreased. The empirical equations correlating compressive strength with immersion time under various saline concentrations provide practical insights into predicting the concrete's lifespan.

School of Geotechnology
Academic Year 2023

Student's Signature ....Burin.................
Advisor's Signature ....D.Phuakphum.........

ACKNOWLEDGEMENTS

I would like to express my deepest thanks to Asst. Prof. Dr. Decho Phueakphum, the thesis advisor, gave a critical review. Furthermore, I appreciate the encouragement, suggestions, and comments during the research period. I would like to express my sincere thanks to Assoc. Prof. Dr. Pornkasem Jongpradist, and Asst. Prof. Dr. Prachya Tepnarong for their valuable suggestions and comments on my research works as a thesis committee member. Thanks are given to all staff of the Geomechanics Research Unit, Institute of Engineering who supported my work.

Finally, I most appreciatively acknowledge my parents, and my friends for all their supported throughout the period of this study.

Burin Thongkliang

TABLE OF CONTENTS

Page

TABLE OF CONTENTS (Continued)

TABLE OF CONTENTS (Continued)

TABLE OF CONTENTS (Continued)

LIST OF TABLES

LIST OF FIGURES

LIST OF FIGURES (Continued)

LIST OF FIGURES (Continued)

LIST OF FIGURES (Continued)

SYMBOLS AND ABBREVIATIONS

C_2S =   Dicalcium silicate

C_3S =   Tricalcium silicate

C_3A =   Tricalcium aluminate

C_4AF =   Tetra calcium alumino ferrite

UCS   =   Uniaxial compressive strength test

XRD   =   X-Ray diffractometer

CSH   =   Calcium hydrosilicate

C_3AH_6 =   Aluminate hydrate

SEM   =   Scanning electron microscope

w/c   =   Water-to-cement ratio

PSA   =   Physical salt attack

NaCl   =   Sodium chloride

RHA   =   Rice husk ash

OPC   =   Ordinary Portland cement

Cl^- =   Chloride ion

Na^+ =   Sodium cation

ASR   =   Alkali-silica reactivity

K^+ =   Potassium cation

OH^- =   Hydroxide

pH   =   Power of hydrogen

TPCs   =   Ternary Portland cements

AFt   =   Ettringite

CH   =   Calcium hydroxide

SYMBOLS AND ABBREVIATIONS (Continued)

AFm = Mono-sulfate

FS = Friedel's salt

KS = Kuzel's salt

CaO = Calcium oxide

H_2O = Water

Al_2O_3 = Aluminum oxide

R = Rebound number

σ_C = Uniaxial compressive strength

P = Maximum pressure measured at the failure point of sample

A = Original cross-sectional area of the concrete sample

ε = Axial strain

E = Elastic modulus

ΔL = Change in the length of the concrete sample

L = Original length

ν = Poisson's ratio

W = Weight of mortar samples soaked in saturated brine

D = Dry weight of the mortar sample

°C = Degree Celsius

V_P = Primary wave velocity

V_S = Secondary wave velocity

λ, G = Lame's constants

ρ = Density

UPV = Ultrasonic pulse velocity

V_d = Dynamic Poisson's ratio

SYMBOLS AND ABBREVIATIONS (Continued)

E_d = Elastic modulus dynamic

σ'_{C0} = Normalized compressive strength

σ = Compressive stress

R^2 = R-Squared

t = Immersion time

α = Empirical constant for equation (6.3)

β = Empirical constant for equation (6.4)

α' = Empirical constant for equation (6.8)

β' = Empirical constant for equation (6.9)
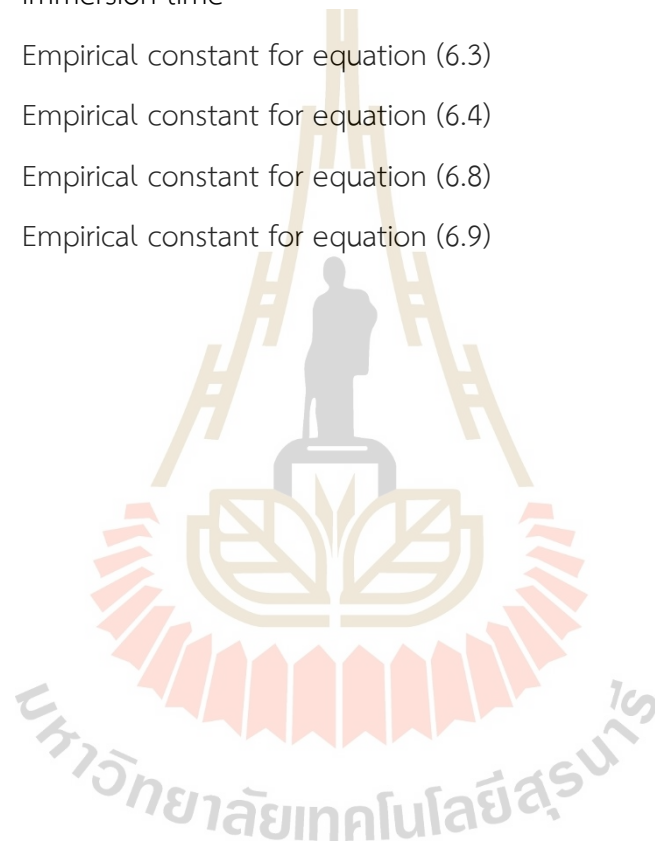
CHAPTER I

INTRODUCTION

1.1   Background and Rationale

Concrete serves as a fundamental building material due to its cost-effectiveness and remarkably high compressive strength properties. It is utilized in various construction projects, including buildings, roads, dams, bridges, monuments, and other structures in general construction work. It is crucial to comprehend how concrete reacts and deteriorates under varying environmental conditions. Concrete deterioration occurs due to various factors, primarily influenced by environmental elements such as chloride-rich saline solutions, leading to corrosion within the concrete matrix and embedded materials (Vassuoni and Rahmam, 2016; Yang et al., 2022; Cao et al., 2019). This degradation causes observable effects such as cracking, fading, and reduced strength, significantly impacting structural integrity (Liu et al., 2014; Wang et al., 2019; Qasim et al., 2020; Qiao et al., 2018). The cumulative effect poses substantial risks to both human life and property, underscoring the necessity to study and mitigate concrete deterioration for sustainable and safe infrastructure development.

Environmental factors, especially saline solutions containing chloride ions, pose a significant threat to concrete integrity. Understanding these effects is vital to assess potential risks and ensure the longevity of concrete structures. Deterioration in concrete structures compromises safety, risking both human life and property. Investigating the impact of saline solutions aids in evaluating these risks and implementing preventive measures. Analyzing the effects of saline solutions helps in devising strategies to enhance the durability and resilience of concrete structures, ensuring sustainable infrastructure development.

This research contributes to practical applications, guiding construction practices, material selection, and maintenance strategies in areas prone to high salinity, ultimately improving infrastructure reliability. Overall, studying the effect of saline solutions on concrete deterioration aligns with ensuring safety, sustainability, and longevity in construction practices, addressing real-world challenges, and fostering safer and more resilient infrastructure.

The study area conducted is in Nakhon Ratchasima Province. Thongwat et al. (2018) illustrate the accumulation of chloride within Nakhon Ratchasima province's groundwater, as shown in Figure 1.1. The study's objective is to comprehend concrete deterioration in chloride-rich settings, with a focus on determining the lifetime of concrete. This effort aims to bolster the assurance of individuals residing near such structures. It necessitated a comprehensive exploration of salinity effects on diverse concrete structures and properties. The outcomes will culminate in mathematical models estimating concrete lifespan or degradation in saline groundwater conditions.
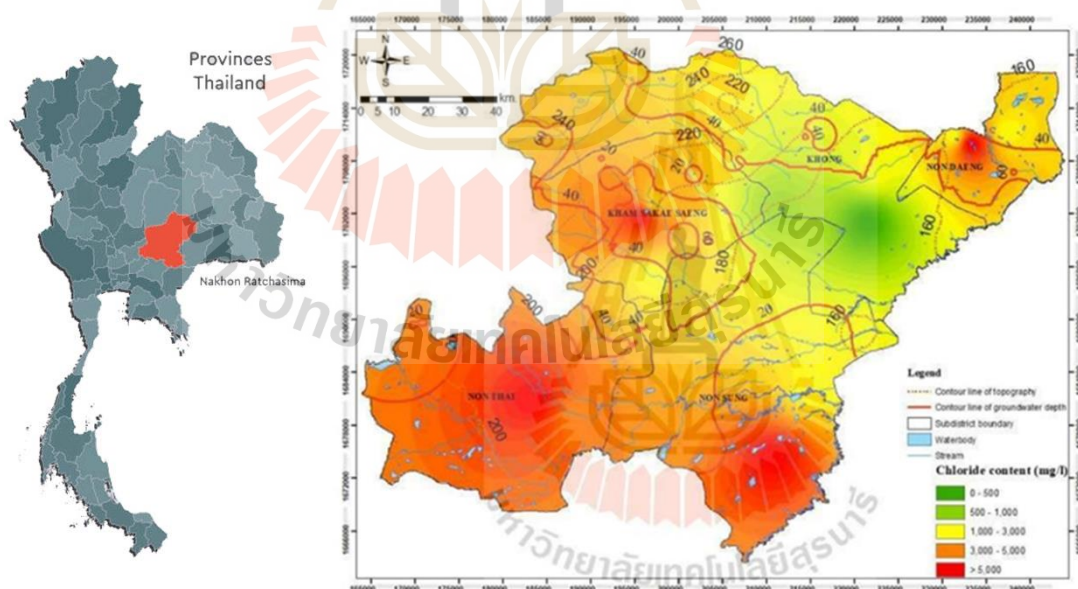
Figure 1.1   Map of chloride content of surface water in Nakhon Ratchasima province (Thongwat et al., 2018).

1.2   Research Objective

The objectives of this study are to study the effect of saline concentration on physical and engineering properties of concrete, including compressive strength, water absorption, porosity, and mineral composition of concrete.   Uniaxial compressive strength test results are used to formulate the empirical equations for predicting the long-term compressive strength of concrete under immersion into various saline concentrations.

1.3   Scope and Limitations

The scope and limitations of the study are as follows:

1) The dimension of the core specimen is 150 mm in diameter and a length of 300 mm in length and the nominal dimensions of rectangular specimens is 50×50×50 mm³.
2) The uniaxial compression test procedure follows the ASTM C31, ASTM C39, ASTM C109, ASTM C617, and ASTM C1231 standard practices.
3) Concrete is prepared from Ordinary Portland Cement (Type 1) mixed with cement, fine aggregate, coarse aggregate and water in a ratio of 1:2:4:0.5.
4) Mortar is prepared from Ordinary Portland Cement (Type 1) mixed with cement, fine aggregate, and water in a ratio of 1:2.75:0.5.
5) The salinity conditions of the total immersion varied in five levels: 0%, 25%, 50%, 75%, and 100%.
6) The direct and indirect compressive strength are conducted on cylindrical shape concrete sample.
7) X-ray diffraction analysis to determine the mineral composition is conducted on the post-tested concrete samples from the uniaxial compression test.
8) Saline absorption and ultrasonic pulse velocity are measured on mortar samples to explain the physical properties change during the deterioration of concrete.

9) Saline absorption and ultrasonic pulse velocity measurements are conducted on mortar samples to explain the alterations in physical properties occurring throughout the concrete's deterioration process.

10) All tests are performed under immersion brine conditions and ambient temperature.

1.4   Research Methodology

This research methodology (Figure 1.2) comprises 6 steps: literature review, sample collection and preparation, laboratory tests, analysis, discussions, conclusions, and thesis writing.
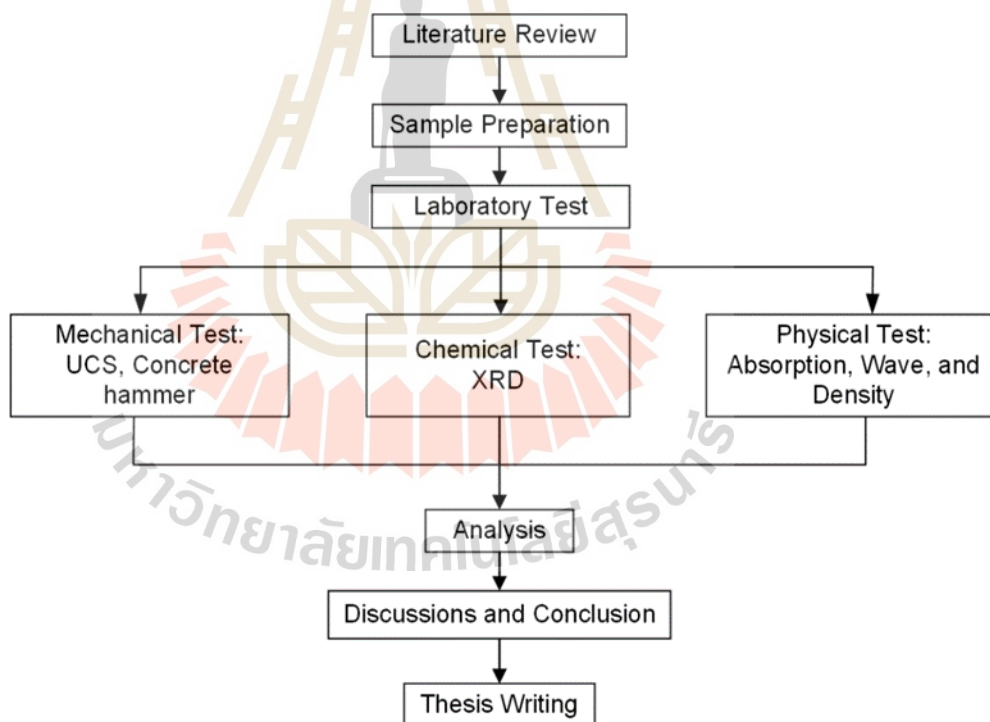
Figure 1.2 Research methodology.

1.4.1 Literature Reviews

The previous studies and review on the causes of concrete deterioration, factors affecting concrete erosion, the effects of saline water on concrete, the impact of salt immersion time on concrete properties, and the influence of saline concentration on the mechanical properties of concrete. The sources of information for this review are drawn from journals, technical reports, and conference papers. A summary of the literature review is provided in the thesis.

1.4.2 Sample preparation

The concrete cone samples are prepared in the laboratory at Suranaree University of Technology, Nakhon Ratchasima Province, typically have dimensions of diameter 150 mm × length 300 mm. A cubic mortar samples measure 50 x 50 x 50 mm. The concrete samples were prepared using Ordinary Portland Cement (Type 1) mixed with cement, fine aggregate, coarse aggregate, and water in a ratio of 1:2:4:0.5. Mortar samples were prepared using Ordinary Portland Cement (Type 1) mixed with cement, fine aggregate, and water at a ratio of 1:2.75:0.5.

After 24 hours of sample preparation, the concrete samples were cured in water for a duration of 28 days. Following this, the concrete samples were immersed in water. The water is conditioned to varied salinity concentrations at specified time intervals of 0, 1, 2, 3, 6, and 12 months. The concrete samples were assessed for maximum compressive strength, water absorption, and mineral changes.

1.4.3 Laboratory test

Laboratory tests were divided into 3 groups: mechanical tests, chemical tests, and physical tests.

1) The mechanical test, a uniaxial compressive strength test (UCS) and a concrete hammer test were performed on water-saturated concrete samples.

2) The chemical test, the failure samples from the uniaxial compressive test were analyzed for mineral composition using X-Ray diffractometer (XRD).

3) The physical test involved water-saturated mortar samples, which were tested for brine adsorption and density. Afterward, the mortar samples were dried and tested for wave velocity.

1.4.4 Analysis of test results

Uniaxial compression tests are performed to determine the compressive strength of concrete and mortar with varied salinity concentrations. Saline water absorption is analyzed to understand the change in mineral composition. The results are analyzed to determine the relationship between time and uniaxial compressive strength. Mathematical equations are developed for estimating the service life and corrosion of concrete conditions to long-term exposure to brine groundwater using SPSS statistical software.

1.4.5 Discussions, conclusions, and thesis writing

All study activities, methods, and results are documented and compiled in the thesis.

1.5 Thesis Contents

Chapter 1 describes the objectives, problems, rationale, and methodology of the research. Chapter 2 presents the results of the literature review to improve an understanding of the physical and engineering properties of concrete in a state of submersion in brine. Chapter 3 describes the specimen preparation. Chapter 4 describes the laboratory test and method. Chapter 5 describes the test results. Chapter 6 describes the analysis of test results. Chapter 7 presents discussions, conclusions, and recommendations for future studies.

CHAPTER II

LITERATURE REVIEW

2.1   Introduction

This chapter provides an understanding of the types of Portland cement, the causes of concrete deterioration, the saline water effect on concrete, the saline water exposure effect on concrete properties and the saline concentration effect on the mechanical properties of concrete. The relevant knowledge is reviewed to support these conclusions and discussions.

2.2   Types of Portland cement

Portland cement, categorized by ASTM C-150, has the following main types:

1) Type I ordinary Portland cement is commonly used in general construction work, offering high strength within a short timeframe and producing moderate heat. Type I is employed to construct building elements for various structures, such as columns, beams, and standard foundations.

2) Type II modified Portland cement is a type of cement that does not generate excessive heat and exhibits a slower heating rate than Type I cement. Presently, this cement variety is not widely accessible in Thailand. In the United States, Type I and II cement are often combined and called Type I and II.

3) Type III High early-strength Portland cement is characterized by its rapid solidification upon mixing with water. The heat generated during the hydration reaction is significantly higher than that of Type I cement. The compressive strength of concrete made from this cement reaches the same level at three days as that of concrete made from aged Type I cementitious cement at seven days.

4) Type IV low-heat Portland cement characterized by its minimal heat generation during hydration reactions, attributed to its low tri-calcium silicate (C_3S) content averaging 30% relative to high di-calcium silicate (C_2S) content averaging 46%. However, the presence of C_3S imparts significant early-stage strength (within 28 days), making it well-suited for substantial concrete projects such as dam construction, among others.

5) Type V sulfate-resisting Portland cement is characterized by its low tri-calcium aluminate (C_3A) content, typically not exceeding 5%. It causes a higher C_3A content leading to susceptibility to sulfate attacks. Thus, minimizing the C_3A content prevents reactions with sulfate, reducing the potential for corrosion.

2.3   Cement mixing processes

The mechanical process is related to deflocculation. Immediately after the cement powder is exposed to water, the chemical process starts resulting in the formation of hydrosilicates. The hydration component of silicate phases is calcium hydrosilicate (CSH) (Saleh et al.,2019). The major components of cement crystalline phases are:

1) C_3S-Tri-Calcium Silicate

2) C_2S-Di-Calcium Silicate

3) C_3A-Tri-Calcium Aluminate

4) C_4AF-Tetra-Calcium Aluminoferrite

The hydration of C_3A is very rapid compared to the hydration of tri-calcium silicate. This quick reaction dissipates hydro aluminum precipitates (C_3AH_6), which causes premature stiffening of slurry often described as a flash set (Gauffine-Garrault, 2012). In the first few seconds of cement exposure, tricalcium silicates come into contact and form a connected structure. With more CSH precipitation, the structure reinforces which makes it very difficult to break the gel (Figure 2.1, Nonat and Mutin, 1992). This process is irreversible. Hydration

kinetics are primarily dominated by silicate hydration since it is the primary cement constituent. Several hydration stages are outlined in Figure. 2.2. These stages include dissolution (stage 1), induction (stage 2), acceleration (stage 3), deceleration (stage 4), and diffusion (stage 5) (Nelson and Guillot, 2006). Early cement strength is impacted by tricalcium silicate whereas the final strength of cement is impacted by dicalcium silicate (Fink, 2015, Barret et al., 1983). Gutteridge and Dalziel (1990) studied the hydration behavior of cement for 100 days. Their studies showed exponential behavior of the hydration reaction plot with time, except for C_2S. During the first 40 days, most of the reactions occur as shown in Figure 2.3. It can be observed that hydration is very active in the first few days when many cement phases have steep hydration curves.
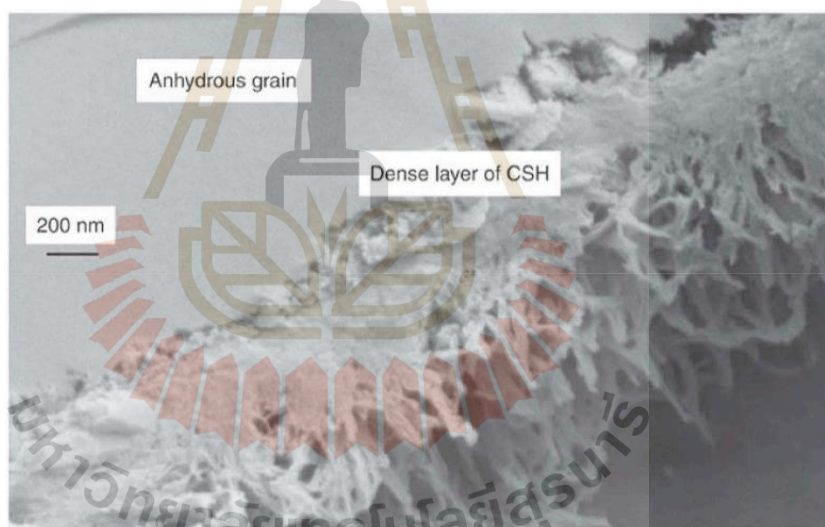
Figure 2.1 Close view of a tricalcium silicate hydrated grain and CSH. SEM image shows a dense layer of CSH around the anhydrous grain. This dense layer corresponds to the hydrate layer formed during the first stage of hydration (Gauffine-Garrault, 2012).
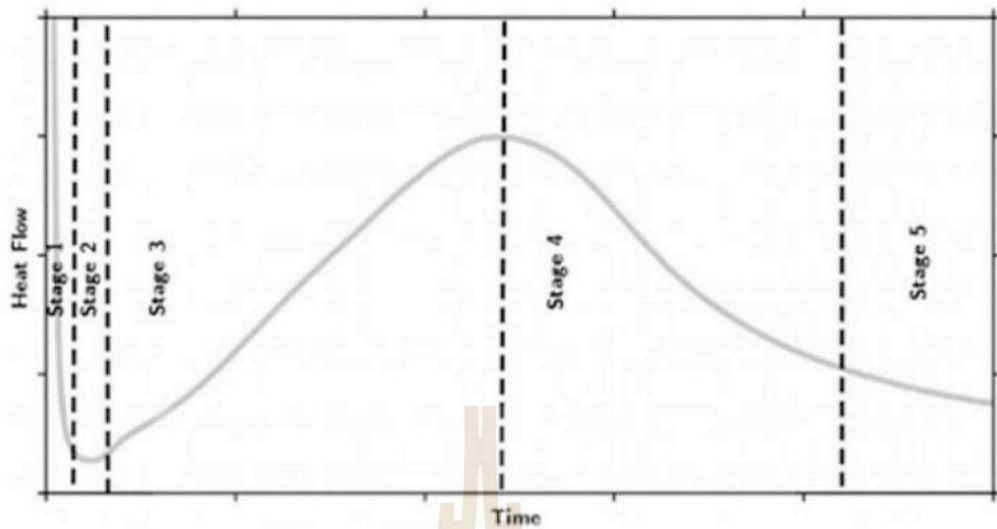
Figure 2.2 Heat flow versus hydration time in cement. Five stages of hydration can be
seen. These stages include dissolution (stage 1), induction (stage 2),
acceleration (stage 3), deceleration (stage 4), and diffusion (stage 5) (Nelson
and Guillot, 2006).
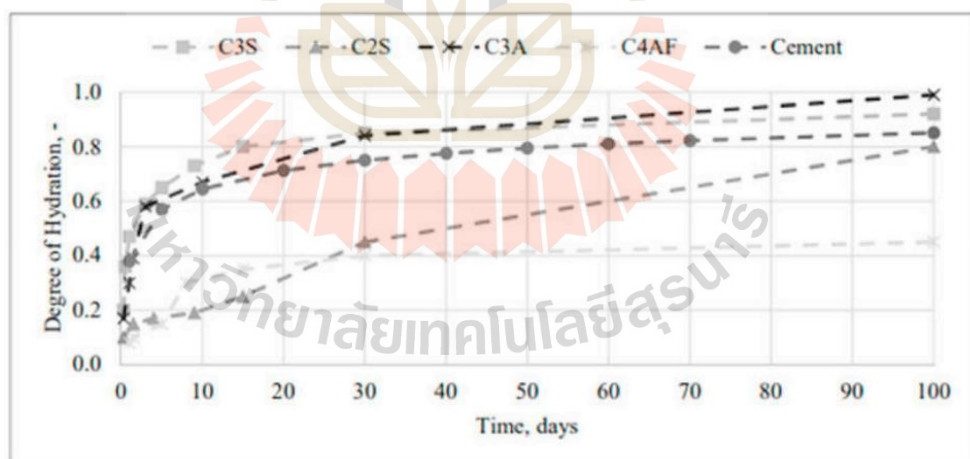
Figure 2.3 Cement hydration with time. The initial period of hydration is characterized
by dissolution and rapid reactions between C_3S and water that begin
immediately upon wetting (Gutteridge and Dalziel, 1990).

2.4   Causes of concrete deterioration

The Product and Building Materials Co., Ltd. (2023) has summarized the general causes of damage in concrete into three main categories: mechanical causes, chemical causes, and physical causes, as shown in Figure 2.4.

Most mechanical causes occur in concrete areas such as floors, roads, and airstrips that are subject to constant abrasion. In concrete structures in submerged conditions, erosion can occur when water flows and carries gravel or sand leading to the enlargement of cavities. In addition, water pressure from the entry of water into the concrete gap causes an increase in hollow space (cavitation).

There are many chemical causes of concrete deterioration and the severity of each case varies. The chemical environments can significantly degrade high-quality concrete. Common chemicals that have a negative effect on concrete include sulfate (such as calcium sulfate), sodium sulfate, and magnesium sulfate (with solubility in water of 1.20, 240, and 300 g/l, respectively; magnesium sulfate has the greatest effect). Various acids, the reaction between alkali and aggregate in concrete, carbon dioxide, chloride, bacterial action, and seawater can also contribute to concrete deterioration. The extent of the damage will depend on the main constituents involved and the quality of the concrete. Aggressive chemicals must be present in the solution and exceed the minimum concentration to cause significant damage to concrete.

The physical cause is that tensile stress in the concrete results in increased cracking, making it more susceptible to chemical deterioration. The physical causes of concrete degeneracy include ice damage, heat, fire, equal alternating wet and dry conditions, excessive loads, fatigue, and accidents.

```
                      ┌─────────────────────────────┐
                      │  Causes of damage in concrete │
                      └─────────────────────────────┘
```

Physical causes	Chemical cause	Mechanical causes
Damaged by frost and ice	Sulfate corrosion	Abrasion
Damaged by fire	Acid corrosion	Erosion
Dry and wet alternating damage	The reaction between the alkali and the rock	Cavitation
Damage by payload	Seawater	
Fatigue damage	Carbon dioxide	
Accidental damage	Action of bacteria	
	Chloride	
	Steel reinforcement corrosion	

Figure 2.4 The causes of concrete deterioration come from 3 main factors: physical, chemical, and mechanical (The Product and Building Materials Co., Ltd., 2023).

2.5   Factors affecting concrete erosion

Homwuttiwong (2022) summarized the factors affecting the erosion of concrete, or the ability to resist erosion. The erosion of concrete depends on numerous factors related to the concrete environment, structural characteristics, usage, and every step of the concrete production process. Each of these factors has a different influence on concrete erosion. The main factors to consider are the compressive strength of concrete, aggregates, finishing the surface of fresh concrete, concrete curing and the number of cavities or voids in the concrete.

2.5.1 Compressive strength of concrete

Compressive strength is a crucial factor in determining the resistance of concrete to erosion. It has been observed that concrete with high compressive strength exhibits better resistance to erosion. Achieving high compressive strength can be accomplished through the use of a high cement content in the mix or by employing a low water-to-cement ratio (w/c).

The higher cement content ensures that the cement paste evenly coats and binds the fine particles. It results in a strong bond within the concrete. Additionally, when the water content in the concrete mixture is minimized (low w/c ratio), excess water is avoided, leading to fewer cavities or gaps in the concrete. Consequently, the concrete's density is increased, and the presence of cavities that might promote erosion is reduced. Thus, concrete with low water content exhibits higher density and enhanced resistance to abrasion.

2.5.2 Aggregates

The type and quality of aggregate are used in the study. It has a significant impact on the wear-resistance properties of concrete. This effect is particularly pronounced in low-strength concrete but becomes less prominent as the concrete's compressive strength increases. Previous studies have shown that when mixing concrete, the coarse aggregate should possess sufficient strength and its maximum size should not exceed 25 mm in diameter. Concrete made with smaller coarse aggregates generally exhibits higher wear resistance compared to concrete made with larger coarse aggregates.

Regarding fine aggregates, it is essential that they are clean and have a well-balanced mix ratio and distribution. The correct quantity and composition between coarse and fine aggregates are maintained, avoiding excessive use of either type. Taking these factors into consideration will lead to concrete with improved abrasion resistance.

2.5.3 Finishing the surface of fresh concrete

Finishing the surface of fresh concrete involves various techniques, including polishing, rough scrubbing, and exfoliation, all of which enhance the strength of the concrete surface compared to unpolished concrete. In practice, achieving a polished surface may require an increased amount of cement in the concrete mix or a reduction in the water content. Conversely, for rough polishing, special cement or surface coating materials are used to enhance the strength of the concrete surface, especially in applications like industrial plant floors.

However, if the concrete is mixed with an excess amount of water, it can lead to lower abrasion resistance once it hardens. The higher water-to-cement ratio at the surface of the concrete reduces the strength of the paste, causing the concrete surface and aggregate particles to detach. This can result in surface flaking, particularly noticeable on roads or driveways, where the top layer may wear away, exposing the underlying rock or coarse aggregates.

2.5.4 Concrete curing

Concrete curing involves maintaining water or moisture in the concrete to facilitate the hydration reaction. The formation of cement particles during hydration contributes to the development of concrete strength as it ages. Therefore, well-cured concrete exhibits higher strength compared to uncured concrete. Increased concrete strength is also associated with enhanced corrosion resistance.

Curing can also involve controlling the temperature of the concrete. Shoukry et al. (2011) found that higher temperatures and moisture levels can decrease concrete strength because the elevated temperature accelerates the hydration reaction, leading to rapid early strength gain. However, this acceleration may have adverse effects on the long-term properties of the concrete.

Curing wet concrete for 28 days before subjecting it to physical attack can reduce surface scaling as it increases the solid content and decreases concrete porosity (Nehdi et al., 2014). Proper curing plays a crucial role in achieving durable and resilient concrete structures.

2.5.5 The number of cavities or voids in the concrete

Concrete with a high number of voids will exhibit reduced resistance to abrasion. Insufficient coating or bonding of fine aggregate particles by the cement paste makes these particles prone to slipping off when subjected to force. Additionally, when erosion begins and the concrete surface extends deeper, the presence of cavities or spaces within the concrete accelerates the increase in erosion depth, leading to rapid damage.

Concrete containing air-entraining additives or having high porosity is not suitable for use in structures that will be subjected to severe corrosive conditions. Such concrete is more vulnerable to erosion and may not provide the necessary durability and longevity in harsh environments. Therefore, it is important to use concrete with proper density and bonding to ensure its resistance to abrasion and other adverse conditions.

2.6   Saline water effect on concrete

Haynes and Bassuoni (2011) conducted a study on the deterioration of concrete caused by the physical salt attack (PSA) by investigating salt crystallization in the pores near the concrete surface. The salts responsible for PSA in concrete are sodium sulfate, sodium carbonate, and sodium chloride, with sodium sulfate being the most severe (Figure 2.5).

The permeability and diffusion of salt solutions play a significant role in controlling PSA, as the salt crystallization pressure is directly related to the pore size of the concrete. Changes in cement composition and hydrate microstructure can impact the durability of cementitious materials in environments rich in salts (Nadelman and Kurtis, 2019).

Depending on the type and concentration of salt, typical characteristics of concrete deterioration include the formation of crystals or powder upon water loss (efflorescence), delamination, and, in some cases, increased cracking that can compromise the material's structural integrity. These damages are often observed on the surface of materials in direct contact with soil or groundwater and can affect critical structural elements like foundations, structures, and dams. The severity of the damage is closely related to the pore structure of the material (Lee and Kurtis, 2017).

Over the years, many researchers have studied the effect of saltwater on concrete properties using a mixture of sodium chloride solution to prepare concrete or mortar samples. For example, Mbadikea and Elinwab (2011) prepared all 90 concrete samples for compressive strength testing. They divided the sampling into two

groups: group 1 cast using fresh water and group 2 model using saltwater, with all groups consisting of 45 samples. The concrete samples were immersed in water for a variety of durations of 7, 21, 28, 60, and 90 days. From the test, the chloride and sulfate solutions in water result in the strength of concrete is reduced.

Similarly, Abalaka and Babalage (2011) investigated the effect of 5% and 10% NaCl as the curing medium on the compressive strength of concrete samples containing 5% rice husk ash (RHA) for curing periods of 3, 7, 14, 21, and 28 days. After the curing period, the samples were tested for compressive strength. Figure 2.6 shows that concrete samples containing 5% RHA in NaCl solution exhibited a reduction in compressive strength, with the strength loss being more significant at early stages of 3 days and 7 days. At 28 days, the concrete samples with 5% RHA incubated in NaCl solution showed higher strength loss compared to other days, indicating a long-term loss of compressive strength. This study revealed that RHA-containing concrete was more susceptible. The attack of NaCl solution compared to conventional concrete.

Figure 2.5 After 104 weeks, concrete samples of partial immersion in (a) 5% sodium sulfate solution, (b) 5% sodium carbonate solution and (c) 5% sodium chloride solution (Haynes and Bassuoni, 2011).
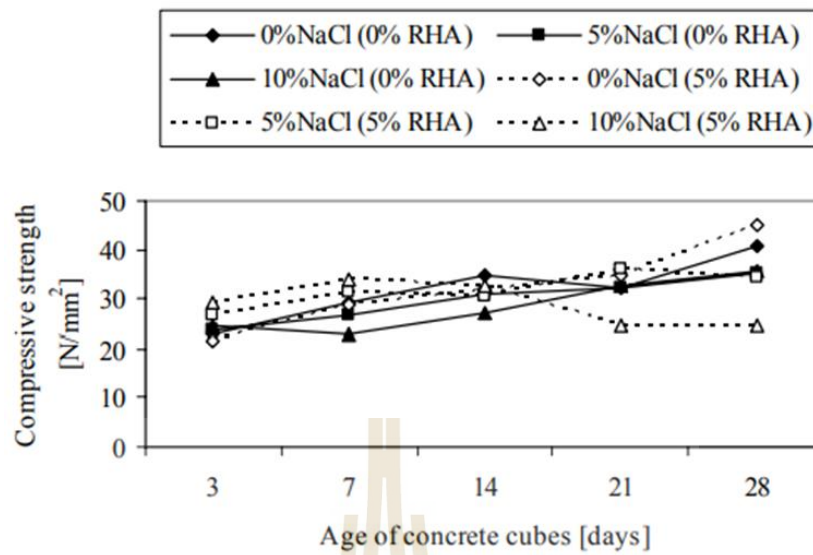
Figure 2.6 The relationship between the compressive strength of concrete and the sample curing time (Abalaka and Babalage, 2011).

Guo et al. (2018) investigated the possibility of substituting saltwater in concrete mixtures during curing to increase the strength of various concrete grades. The coarse aggregate in the concrete samples was crushed stone with a particle size ranging from 15 to 20 mm, and the binder was regular Portland cement (OPC). Sand with a particle size larger than 0.25 mm was employed as a fine aggregate. A total of 192 samples of concrete, each measuring 100 x 100 x 100 mm, were produced for testing. Concrete samples were put through uniaxial compression testing at ages 7, 14, 28, and 90 days to gauge their compressive strength. Concrete test samples were compressed at a continuous rate of 4.0 kN/sec until cracking appeared. According to the study's findings, using saltwater when mixing or curing concrete has an effect on its strength. Although it initially increased the early strength, it ultimately led to a decrease in the total strength of the concrete samples.

Dhondy et al. (2021) conducted a study to examine the impact of concrete admixture water salinity on the short-term properties of reinforced concrete. The salinity concentrations varied from 0% to 250% of the world average. The study found that the shrinkage rate of concrete increased with the salinity of the mixed water,

particularly within the first 21 days after casting. At 90 days, the shrinkage of concrete mixed with saline water at a salinity of 66 g/l was twice as high as that of concrete mixed with tap water. In Figure 2.7, it was observed that water salinity had a slightly negative effect on the compressive strength of concrete after 14 days, with concrete mixed with 33 g/l of saline water showing higher one-day strength compared to tap water. However, over a 90-day period, the compressive strength of concrete mixed with salt water at 49.5 g/l was lower than that of concrete mixed with tap water.

The high concentration of salts, particularly NaCl in salt water can harm concrete constructions. The potential effects of saltwater on concrete include the following: corrosion of cement paste, increased permeability, scaling, spalling, and changes in hydration products.

2.6.1 Corrosion of cement plain

Niamluang et al. (2018) studied the deterioration of an irrigation building structure based on its external appearance and conducted compressive strength tests. They found that most of the structure decay was characterized by the degeneration of concrete, but it did not affect the building's load-bearing capacity. Additionally, water samples were tested, and the water in the deteriorated irrigation area had higher salinity, sulfate, and chloride content than other areas.

2.6.2 Absorption

Chandra and Xu (1992) tested mortar samples using freeze-thaw cycles. Found that sample expansion depends on the salt concentration gradient. Condition of the saline adsorption rate by weight increases with the concentration of NaCl.

Saline water can increase the absorption of concrete, allowing more water and harmful substances to penetrate the material, increasing damage caused by freeze-thaw cycles, chemical attacks, and other environmental factors.
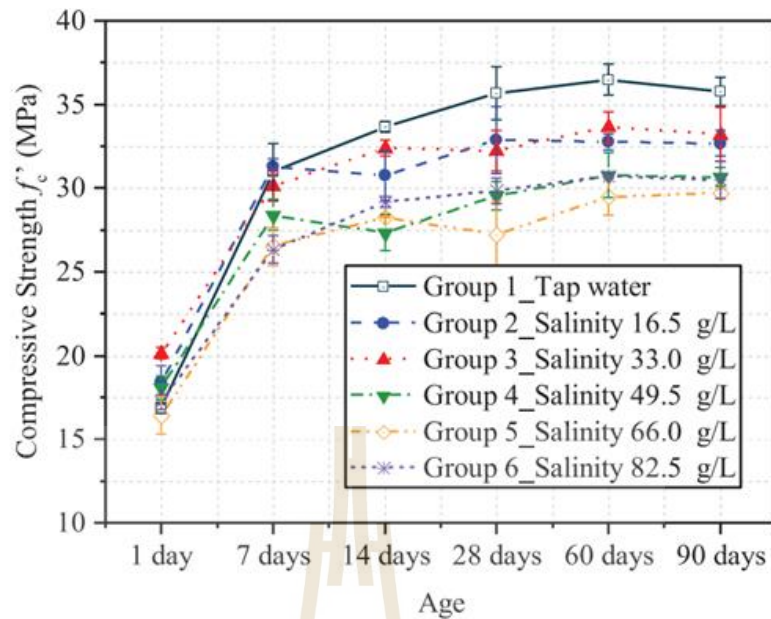
Figure 2.7 Strength development of concrete (Dhondy et al., 2021).

2.6.3   Scaling and Spalling

Sakr and Bassuoni (2018) investigated the potential use of some surface treatments to prevent the triggering conditions of PSA. It found that damage generally occurs due to the combined physical and chemical action of a sulfate attack. However, for uncoated samples, most deterioration occurs due to PSA.

Exposure to salt water can contribute to the scaling and spalling of concrete surfaces. The salt crystals formed within the concrete pores expand during freeze-thaw cycles, leading to the detachment of thin layers of concrete and surface deterioration.

2.6.4   Hydration products

Yang et al. (2022) found that the main corrosion products were ettringite crystals, gypsum crystals, and Friedel's salt calcium and carbonate crystals. In general, gypsum and ettringite exhibit volume expansion, which has two effects on the internal structure of the concrete. First of all, these two crystals grow in the original porosity of the concrete, increasing its density and compressive strength. Second, when these two crystals have completely filled the original porosity of the concrete, the continuous

formation of crystals induces internal pressure on the inner wall of the pore. When the internal pressure is greater than the concrete's tensile limit, small cracks will form, leading to concrete deterioration and a reduction in its strength. Moreover, Friedel's salt is formed by the reaction of Cl- and cement hydration products, and there is no synchronization feature. Therefore, the formation of Friedel's salt results in a decrease in the cementitious ability of the concrete. It was shown that the corrosion effect caused an initial increase in the compressive strength of concrete, followed by a decrease.

2.7 Saline water exposure effect on concrete properties

Be´rube et al. (2003) examined the effects of NaCl on alkali-silica reactivity (ASR) at different depths in concrete tank samples. The results indicated that the Cl- and Na+ ion concentrations increased in the pore solution of the subsurface layer of the concrete exposed to the NaCl solution, while the K+ and OH- ion concentrations and the pH decreased. The NaCl solution did not change the chemical properties of the pore solution at depths greater than 60-80 mm. In Figure 2.8, a sample continuously immersed in 6% NaCl began to expand over time at a higher rate than other samples. It may be indicating that NaCl can accelerate ASR over the long term. For samples immersed in NaCl solution continuously or intermittently, there is a possibility that the overall expansion of the concrete components will increase in the long time.

Xiong and Yu (2015) investigated the mechanical properties of cement in a sodium sulfate solution and NaCl. They test on the uniaxial compressive strength and measured the ultrasonic pulse velocity. The research found that the compressive strength of cement first increases and then decreases with increasing immersion time.

He et al. (2020) studied the compressive strength development of mortar samples under different immersion conditions. During the immersion period before 28 days, the compressive strength of the mortar samples immersed in seawater was higher than that of mortar immersed in fresh water. However, after 28 days, the compressive strength of the cement samples under immersion in seawater decreased, while the samples under immersion in freshwater showed a slow increase as the immersion period increased, as shown in Figure 2.9.
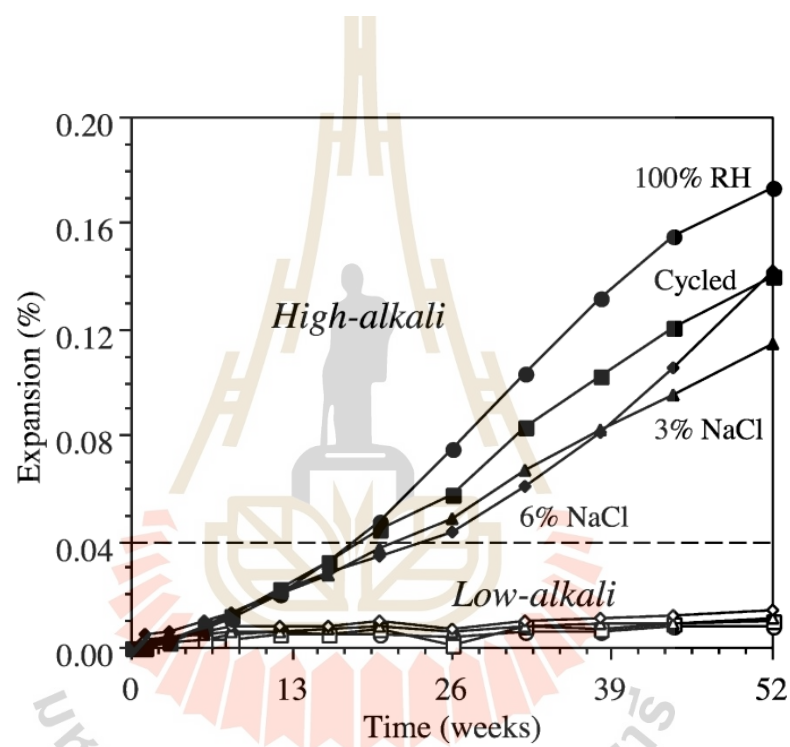
Figure 2.8 Expansion results for the laboratory cylinders (Bérube et al., 2003).
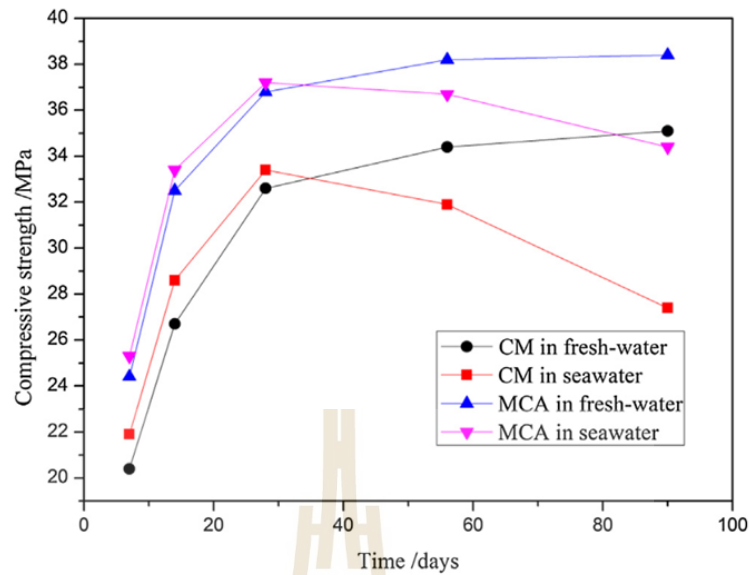
Figure 2.9 Compressive strength development of mortar with ion chelator (MCA) and control mortar (CM) submerged in seawater and freshwater over time. (He et al., 2020).

Vassuoni and Rahmam (2016) studied the physical salt attack (PSA) that causes durability problems when concrete is exposed to salt and cyclic environments. PSA damage on concrete manifests as scaling and surface peeling. The deterioration occurs due to salt crystallization, with potential chemical reactions between salt ions and cement hydrates depending on the material composition and the type of salt present. The results can be summarized as follows: The mass loss and microstructure properties showed that in a simulated PSA test on concrete over a period of 120 days, the deterioration of the concrete mix was mainly due to the crystallization of soluble salts. Thermal, mineralogical, and microstructural analyses revealed salt deposits with limited availability of ettringite and gypsum.

Bai et al. (2021) studied the hygroscopic changes of cement mortar under salt attack. The results showed that with a higher salt concentration and a longer holding time, the moisture absorption increased initially at the beginning of the experiment and then gradually decreased. Eventually, the moisture absorption reached a constant level in the subsequent period.

Rozgonyi-Boissinot et al. (2021) studied the speed of ultrasonic waves (P and S waves) due to salt crystallization in limestone samples according to DIN EN 12370. An increase in the ultrasonic wave speed will be observed during the initial salt crystallization cycles. However, with additional salt crystallization cycles, the pulse speed will reduce. The negative change in wave velocity is linked to the opening of small cracks.

Sui et al. (2023) studied the mechanism of the influence of chloride on the hydration kinetics of interface materials using chloride-rich raw materials. The hydration rate was accelerating and increasing for both peak silicate and aluminate in the presence of chloride. The change in silicate peaks is attributed to the effect of chloride ions in the porous solution.

2.8   Saline concentration effect on the mechanical properties of concrete

The effect of salinity on the mechanical properties of concrete can be significant or detrimental. Salinity refers to the presence of salts, particularly chloride ions, in the environment surrounding the concrete. Here are the effects of salinity on the mechanical properties of concrete: compressive strength, elastic modulus, and permeability.

2.8.1 Compressive strength

Ming et al. (2017) studied the durability of concrete in a salt environment under freeze-thaw and wet-dry cycles. The results showed that the compressive strength of concrete decreases with increasing salt concentration and soaking time.

Qasim et al. (2020) studied the effects of salt and fresh water on concrete properties. The proportion of NaCl was divided into 0, 10, 20, 30, 40, and 50 g/l and incubated for 7, 14, and 28 days, respectively. Compressive strength decreases with increasing salt content. The results from the experiment showed that after salt curing for 14 days, the concrete samples had an increase in compressive strength of

1%–2% of the salt content. However, the experimental tests also showed that while there was an initial increase in concrete properties at certain curing levels, in the end, the strength of concrete was reduced by salt curing for 28 days.

Althoey (2021) studied the interaction between NaCl solution and cement paste, highlighting chemical changes that may occur with a corresponding reduction in compressive strength. The cement paste had a water-to-cement ratio of 0.5, with NaCl concentrations varying at 0, 1, 2, 3, and 4 mol/l at 5 and 25 °C. The damage to cement exposed to NaCl solutions was temperature-dependent. No calcium hydroxide leaching was observed in contact with sodium chloride, indicating that the calcium hydroxide phase is stable in the NaCl solution. Friedel's salts formed in the cement paste in contact with the sodium chloride solution, and the amount will increase with increasing salt concentration, as shown in Figure 2.10. The corresponding volume change in hydrated cement at NaCl concentrations determines the stability of Friedel's salt and calcium hydroxide at the focus of the NaCl solution. The volumetric expansion of the sample is the main reason for the decrease in compressive strength. The results were consistent with Qiao et al. (2018) conclusion that the damage was primarily caused by the crystallization pressure associated with Friedel's salt in the porosity. The initial chemical reaction between hydrated cement and NaCl involves the formation of Friedel salts (Shi et al., 2011; Sutter et al., 2006; Qiao et al., 2018), as shown in equations (2.1) and (2.2).

$$3CaO \cdot Al_2O_3 + Ca\,(OH)_2 + 2NaCl + 10H_2O \longrightarrow Ca_4Al_2(OH)_{12}Cl_2 \cdot 4H2O + 2NaOH$$

$$(2.1)$$

$$Ca_4Al_2(OH)_{12}SO_4 \cdot 6H_2O + 2NaCl \longrightarrow Ca_4Al_2(OH)_{12}Cl_2 \cdot 4H_2O + Na_2SO_4 + 2H_2O$$

$$(2.2)$$
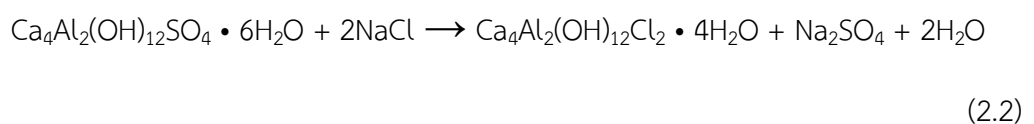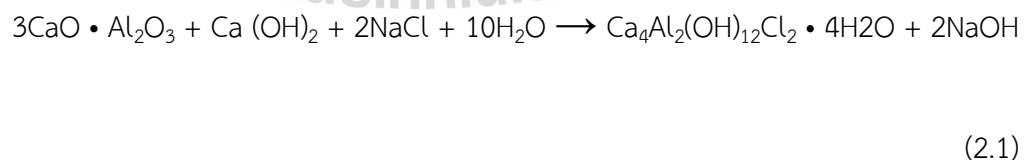
Considering the equation was a slight volume change. The mechanism of chemical damage is hypothesized to be the crystallization pressure of Friedel's salt (Qiao et al., 2018). Valenza et al. (2005) observed volumetric expansion resulting from the crystallization pressure of Friedel's salt.

High salinity, especially chloride ions, can significantly reduce the compressive strength of concrete. Chloride ions penetrate the concrete and disrupt the hydration process of the cement, leading to the formation of weaker reaction products. This weakens the overall structure of the concrete and diminishes its ability to resist compressive forces.

2.8.2 Elastic modulus

Su and Zhang (2014) stated that the dynamic elastic modulus of concrete tends to deteriorate over time with prolonged soaking. The dynamic elastic modulus of concrete immersed in water undergoes minimal degradation due to the equivalence of water immersion to curing. In the case of concrete soaked in a salt solution, the dynamic elastic modulus initially experiences an increase in the process, followed by a subsequent decrease. This trend suggests that the mechanisms of salt crystallization and chemical reactions are not immediately evident in the short term. However, over time, the volume expands due to salt crystallization, leading to the small emergence of cracks in the concrete. Consequently, the concrete's properties gradually decline, and its dynamic elastic modulus enters a phase of decomposition.

Althoey and Farnam (2020) examine ordinary Portland cement (OPC) and calcium aluminate cement. OPC shows chemical interactions with high concentrations of NaCl solutions, mainly due to tribalism aluminate (C_3A) and mono-sulfate (AFm) phases. These phases may be destructive chemical phase changes during cycling and heating, which leads to the development of damage and a decrease in the dynamic modulus of elasticity.

Salinity can lower the elastic modulus of concrete, which reflects its stiffness or rigidity. Salts can disrupt the structure of the hydrated cement paste, resulting in a less compact and weaker matrix. Consequently, the concrete exhibits a lower elastic modulus, making it more deformable under stress.

2.8.3 Permeability

Liu et al. (2014) found that for OPC, calcium was the main parameter controlling the pore structure evolution. Although solid hydration products were growing during the immersion stage, the condition of calcium leaching was obvious. This conclusion is consistent with the study of Wang et al. (2019), which states that calcium leaching and salt crystallization coincide with the process of NaCl solution absorption, while the amount of leaching and loss of strength will change in a fluctuating characteristic with the concentration of the solution. The amount of crystallized salt increases with the certain of the resolution. Figure 2.11 shows the SEM images of concrete saturated in deionized water and NaCl solution. The observation was that the surface of cement products under saturation with deionized water was noticeably rough (Figure 2.11a), with little pores and notches. However, chloride saturation may lead to different observations. Figure 2.11b shows a smooth surface and dense structure within the concrete. The results are consistent with findings from a previous study (Shi et al., 2011), which proposed that NaCl can chemically react with partially hydrated cement and form new products in the concrete matrix.

Cao et al. (2019) studied the effect of salt concentration on chloride-sulfate interactions. The water-to-cement ratio was determined to be 0.48 after 28 days of cured with water. The mortar samples were sealed with epoxy (to determine one-dimensional diffusion), and then the samples were immersed in a salt solution. In the experiments, Cl^- first reacted with hydration products to form Friedel's salt in the mortar. At the same time, the invasion of ions into the mortar reduces its porosity.

Salinity increases the permeability of concrete according to the ingress of water and other aggressive substances. Chloride ions can penetrate the concrete matrix and reach the reinforcement, initiating and accelerating corrosion. The increased permeability also facilitates the movement of moisture, which compromises the durability and mechanical properties of the concrete.
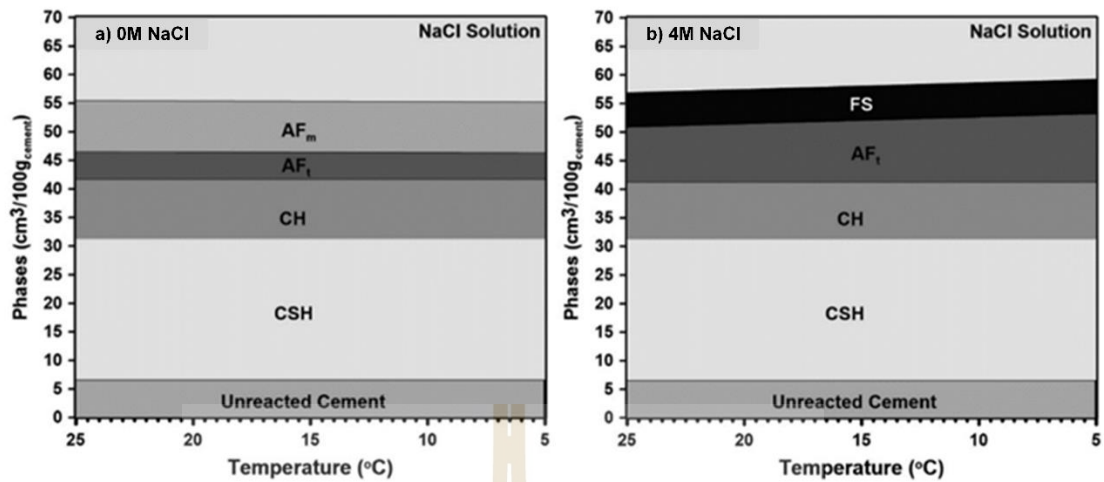
Figure 2.10 Phase assemblages and total volume of solids for cement paste exposed
to temperature variations between 25 °C and 5 °C (a) for 0 M NaCl solution
and (b) for 4 M NaCl solution. CSH: calcium-silicate-hydrate; AFt.: ettringite;
CH: calcium hydroxid; AFm: monosulfate; FS: Friedel's salt; KS: Kuzel's salt.
(Althoey, 2021).

Figure 2.11 Comparison of scanning electron microscopy (SEM) images of the
specimens immersed with different solutions: (a) Saturated in deionised
water; (b) Saturated in NaCl solution. (Liu et al., 2021).

CHAPTER III

SPECIMEN PREPARATION

3.1   Introduction

This chapter describes the sample preparation for examining the effects of sodium chloride (NaCl) solutions (hereby referred to as saline solutions) on concrete deterioration. The investigation involves immersing concrete samples into saline solutions with varying concentrations (0%, 25%, 50%, 75%, and 100%) for varying immersion duration. To comprehensively understand the chemical degradation of concrete, two distinct sample types—cylindrical and cubical specimens—are prepared for different testing methodologies. Three meticulously prepared samples represent each immersion period and salt concentration, ensuring a robust and comprehensive evaluation of the concrete's response to these specified environmental conditions. This chapter additionally outlines the granular composition of aggregates, provides the findings from a slump test conducted on liquid concrete, and details the density measurements of both concrete and mortar specimens.

3.2   Laboratory test plan

The laboratory testing is divided into two groups, focusing on examining properties pertaining to aggregates, concrete, and mortar.

3.2.1 Aggregate properties test

The aggregates used for sample preparation consist of coarse aggregates (3/4-inch crushed stone) and fine aggregates (sand). These materials are tested to examine basic physical properties such as grain size distribution and specific gravity, which require comprehensive examination.

3.2.2 Concrete and mortar properties test

This group of testing comprehensively assesses fundamental concrete properties, including concrete weight, slump value, and compressive strength during a curing period extending up to 28 days. Following the 28-day curing period, the samples undergo immersion in NaCl solutions for varying concentrations and durations. The subsequent evaluation involves testing the compressive strength to evaluate the degree of deterioration. Furthermore, concrete samples undergo X-ray diffraction (XRD) analysis to discern alterations in mineral composition resulting from hydration reactions. Additionally, prepared mortar samples are subject to testing for saline absorption capacity and ultrasonic wave velocity, providing valuable insights into concrete degradation.

3.3   Materials for concrete and mortar samples, and saline solutions preparation

Materials used in the preparation of concrete and mortar samples consisted of:

1) Portland cement type I (according to ASTM C39 standards) from "INSEE" brand, manufactured by Siam City Cement Public Company Limited (SCCC).
2) Fine aggregates, specifically river sand (meeting ASTM C33 standards), recognized for its cleanliness and suitability for general construction purposes.
3) Coarse aggregate (according to ASTM C33) with a maximum size of 3/4 inches.
4) Tap water devoid of acids, alkalis, oils, and any other organic substances in quantities detrimental to concrete, ensuring its suitability for use in sample preparation.

Figure 3.1 illustrates the materials used for preparing concrete and mortar samples. The brine preparation involved the utilization of rock salt (Figure 3.2) sourced from Nakhon Ratchasima province. Dissolving salt in water: 0.00, 89.75, 179.50, 269.25, and 359.00 grams/liter (by weight) represent different salinity levels from 0%, 25%, 50%, 75%, and 100% respectively, were prepared for testing. The solubility is 100% at 25℃. The salinity levels were measured using a reflectometer. The saline concentration levels were varied to 0.00, 89.75, 179.50, 269.25, and 359.00 ppt to cover the study area.
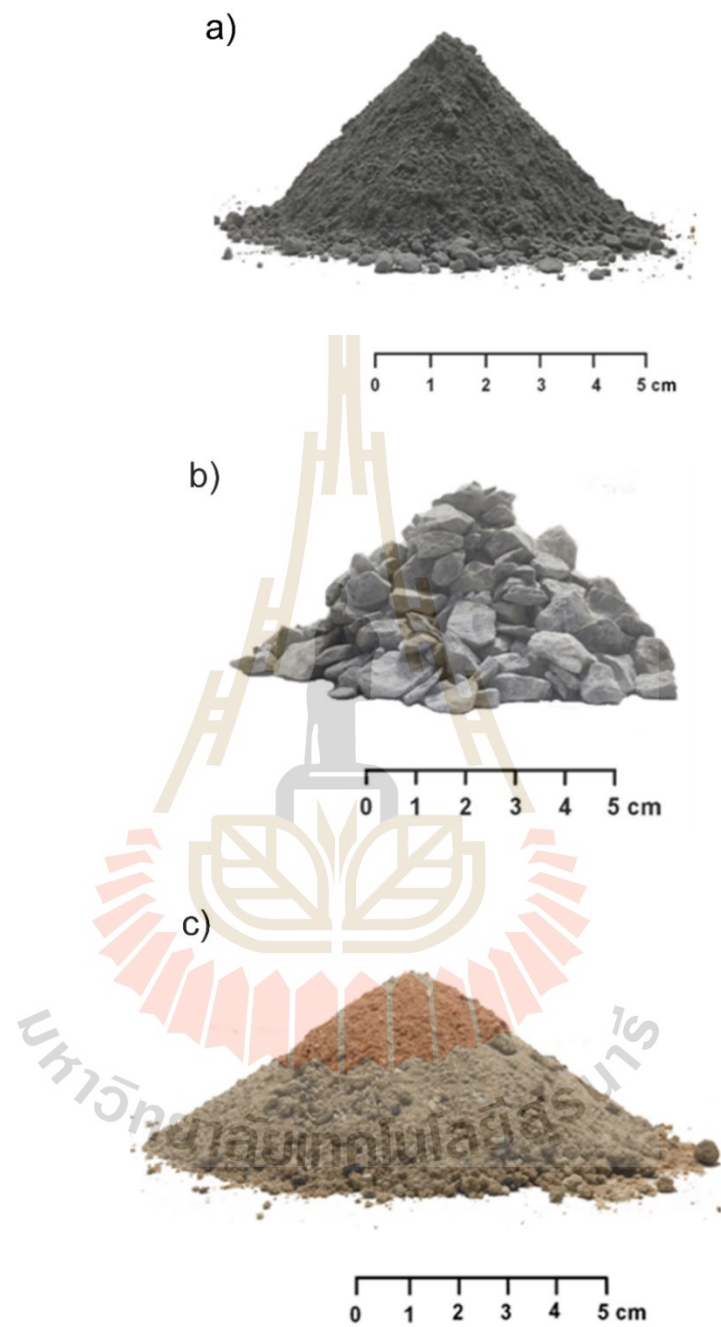
Figure 3.1   Portland cement type I (a), 3/4-inch coarse aggregate (b), and fine aggregate
            (c) used to prepare concrete and mortar samples.

3.4   Sample preparation and measurement of basic properties

3.4.1   Coarse and fine aggregate

Fine and coarse aggregates were washed to eliminate any clay coating on their outer surface. Subsequently, these aggregates were placed in an oven for drying. Sieve analysis was performed to classify the particle sizes in compliance with ASTM C136 standards. Vibrators and a series of sieve sizes—ranging from 3/4", 1/2", 3/8", No. 4, 8, 16, 30, 50, 100, 200, and a tray (illustrated in Figure 3.3)—were employed for this determination.

3.4.2   Concrete and mortar samples

The samples were formed by blending Portland cement type I with cleaned fine and coarse aggregates and tap water. The mixture ratio (cement: fine aggregate: coarse aggregate: water) is approximately 1:2:4:0.5 by weight. Fine and coarse aggregates were mixed using a concrete mixer (Figure 3.4) for approximately 10 minutes. Subsequently, water was added to the mixture until the designated quantity was attained. Once thoroughly blended, the liquid concrete was poured into the cleaned cylindrical mold (Figure 3.5). These cylindrical molds had a diameter of 15 cm and a length of 30 cm, according to ASTM C39 standards.

Figure 3.2   Rock salt used to prepare saline solution for laboratory tests.

Figure 3.3   Analysis of the particle sizes in both the fine and coarse aggregates was
              conducted using a vibrator and sieve method in accordance with ASTM
              C136 standards. This analysis was performed before the aggregates were
              mixed with cement and water.

Figure 3.6 shows the pouring of liquid concrete into the concrete molds. The pouring process is divided into three layers, and each layer is compacted using a 4-pound steel rod (Figure 3.7) with a cross-sectional area of 1 square inch and rounded ends. The rod is pressed 35 times per layer to remove air bubbles and prevent voids from forming. After pouring the last layer, the surface is smoothed (Figure 3.8). The concrete surface is then left to dry. Hemp sacks soaked with water are placed over the concrete surfaces (Figure 3.9) to prevent the concrete from drying too quickly. After casting the concrete samples for 24 hours, they are carefully removed from the formwork (Figure 3.10). The concrete samples are then cured in water for 28 days, as shown in Figure 3.11.

Furthermore, rectangular mortar samples with nominal dimensions of 5x5x5 cm3 were prepared. These samples were made from ordinary Portland cement (type 1) mixed with fine aggregate (sand) and water, using a cement-sand-water ratio of 1:2.75:0.5. The process involved thoroughly hand-mixing clean sand, cement, and water for approximately 10 minutes. Subsequently, the mixtures were carefully poured into the mortar mold and left undisturbed for 24 hours before removal (Figure 3.12). Similar to the preparation of concrete samples, all mortar samples were then cured in water for 28 days. Figure 3.13 shows the concrete and mortar samples prepared for laboratory testing.

Figure 3.4 Blending cement with fine aggregate, coarse aggregate, and water was accomplished using a concrete mixer.

Figure 3.5   Preparing the concrete molds involved scrubbing them with a wire brush and applying oil to the formwork, facilitating the easier removal of the concrete samples from the molds.

Figure 3.6   The liquid concrete is systematically poured into the cylindrical mold in three layers until it reaches the brim, effectively filling the mold.

Figure 3.7   Steel rods are used to prod the liquid concrete, eliminating air bubbles, and ensuring complete filling within the mold.

Figure 3.8   Smoothing the surface of the concrete mold is crucial to ensure optimal contact surfaces, necessary for conducting precise compressive strength tests on the concrete samples.

Figure 3.9   After casting, the samples are covered with a hemp sack and left to set before being removed from the mold.

Figure 3.10 Removing concrete samples from concrete mold.

Figure 3.11   The concrete samples were submerged in tap water for a curing period of up to 28 days.

Figure 3.12   Removing the mortar sample from the mold.
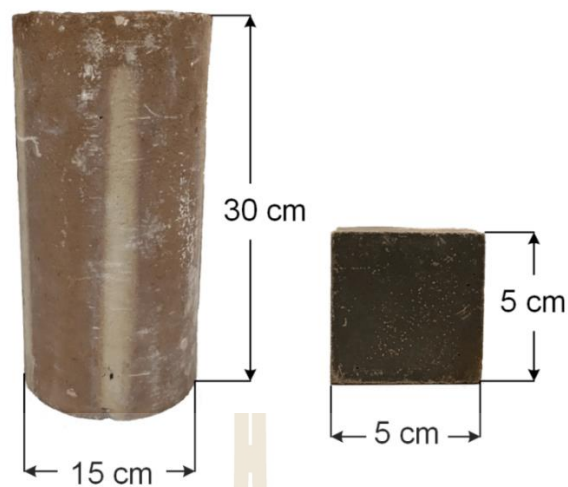
Figure 3.13   Example of concrete and mortar samples prepared for laboratory testing.

3.5   Basic parameter test

Some basic properties of aggregate and liquid concrete are tested in the laboratory including grain size distribution of fine and coarse aggregate, properties of liquid concrete and mortar properties. The details are as follows:

3.5.1   Grain size distribution of aggregate

Fine and coarse aggregates are cleaned and then dried before being tested to determine the mix size using sieves (ASTM C136) of sizes 3/4 inches, 1/2 inches, 3/8 inches, No. 4, 8, 16, 30, 50, 100, 200, and tray, respectively. The results are shown in Figure 3.14

3.5.2   Concrete slum test

In this test, a conical mold with a diameter of 10 cm at the top, 20 cm at the base, and a height of 30 cm. Liquid concrete is poured into the mold and divided into three layers, each layer standardized to the same volume. Each layer is tamped 25 times with a round rod to ensure consolidation. Subsequently, the base is leveled and set aside. The measurement of center collapse obtained from the concrete slum test is shown in Figure 3.15. The concrete subsides uniformly after the slump cone is removed. The slump values for the liquid concrete fall within the range of 18 to 20

cm (Table 3.1). The slump shape conforms to the "true slump pattern" which indicates an acceptable slump characteristic. A true slump indicates that the concrete mix has the appropriate water content and is suitable for its intended use. Tables 3.2 summarize the basic parameters of mortar samples prepared for the test by density-saturated mortar samples with dry surface conditions. Table 3.3 summarize the basic parameters of concrete samples prepared for the test.

Figure 3.14 Measurement of the collapse of fresh concrete.

Table 3.1 Slump test results obtained for liquid concrete.

Preparing Date (Date-Month-Year)	Collapse value (cm)	Mean collapse value (cm)
24-3-2022	18	19
25-3-2022	20	
26-3-2022	18	
27-3-2022	21	
29-3-2022	20	
30-3-2022	18	

Table 3.2 Mortar samples used for saline absorption and wave velocity test.

Sample No.	Preparing Date (D-M-Y)	Salinity (%)	Weight (kg)	Density-saturated (g/cm^3)
A1	5-4-2565	0	239.08	2.13
A2	4-4-2565	0	251.38	2.19
A3	6-4-2565	0	255.92	2.19
A4	7-4-2565	25	241.34	2.14
A5	29-3-2565	25	247.76	2.15
A6	7-4-2565	25	241.30	2.23
A7	4-4-2565	50	247.60	2.15
A8	25-3-2565	50	266.70	2.17
A9	5-4-2565	50	249.60	2.10
A10	31-3-2565	75	251.90	2.13
A11	4-4-2565	75	249.80	2.13
A12	5-4-2565	75	251.50	2.18
A13	24-3-2565	100	242.00	2.16
A14	4-4-2565	100	252.60	2.12
A15	24-3-2565	100	251.70	2.16

Table 3.3 Basic properties of concrete samples prepared for laboratory testing.

Sample No.	Preparing Date (D-M-Y)	Diameter (cm)	Length (cm)	Weight (kg)	Density (g/cm^3)
C-7-1	24-3-2565	14.86	30.16	11.14	2.13
C-7-2	24-3-2565	15.04	29.86	11.16	2.10
C-7-3	24-3-2565	14.88	30.17	11.44	2.18
C-14-1	24-3-2565	15.25	29.97	12.76	2.33
C-14-2	24-3-2565	15.08	29.91	12.54	2.35
C-14-3	24-3-2565	15.04	30.47	12.72	2.35
C-21-1	30-3-2565	15.19	30.26	12.44	2.27
C-21-2	30-3-2565	15.01	30.02	12.64	2.38
C-21-3	30-3-2565	15.05	30.13	13.06	2.44
C-28-1	24-3-2565	15.02	30.08	12.78	2.40
C-28-2	24-3-2565	15.00	30.00	12.62	2.37
C-28-3	24-3-2565	14.96	29.99	12.48	2.34
M0-0-1	24-3-2565	15.00	30.21	12.64	2.37
M0-0-2	24-3-2565	15.40	30.30	12.94	2.29
M0-0-3	24-3-2565	15.00	30.10	12.68	2.38
M1-0-1	27-3-2565	15.10	30.10	12.82	2.38
M1-0-2	27-3-2565	15.10	29.86	12.90	2.41
M1-0-3	27-3-2565	15.10	30.51	13.12	2.40
M1-25-1	29-3-2565	15.10	30.22	12.84	2.37
M1-25-2	29-3-2565	15.20	30.21	12.86	2.34
M1-25-3	29-3-2565	15.10	30.21	12.76	2.36
M1-50-1	24-3-2565	15.10	30.38	12.90	2.37
M1-50-2	26-3-2565	15.10	30.16	12.88	2.38
M1-50-3	26-3-2565	15.20	29.93	12.52	2.30
M1-75-1	26-3-2565	15.00	29.95	12.64	2.39
M1-75-2	26-3-2565	15.00	30.09	12.72	2.39
M1-75-3	26-3-2565	15.30	30.06	12.98	2.35

Table 3.3 Basic properties of concrete samples prepared for laboratory testing. (cont.)

Sample No.	Preparing Date (D-M-Y)	Diameter (cm)	Length (cm)	Weight (kg)	Density (g/cm^3)
M1-75-3	26-3-2565	15.30	30.06	12.98	2.35
M1-100-1	25-3-2565	15.10	30.08	12.70	2.36
M1-100-2	25-3-2565	15.10	30.10	12.86	2.38
M1-100-3	25-3-2565	15.20	30.02	12.96	2.38
M2-0-1	25-3-2565	15.04	30.02	12.70	2.38
M2-0-2	27-3-2565	15.19	30.07	12.80	2.35
M2-0-3	27-3-2565	14.93	30.30	12.90	2.43
M2-25-1	25-3-2565	15.00	29.96	12.74	2.41
M2-25-2	29-3-2565	14.98	30.06	12.82	2.42
M2-25-3	25-3-2565	15.00	29.78	12.68	2.41
M2-50-1	25-3-2565	14.84	30.06	12.60	2.42
M2-50-2	30-3-2565	15.27	30.09	12.84	2.33
M2-50-3	30-3-2565	15.00	30.14	12.62	2.37
M2-75-1	26-3-2565	15.08	29.68	12.74	2.40
M2-75-2	26-3-2565	15.00	30.16	12.70	2.38
M2-75-3	25-3-2565	15.02	30.06	12.70	2.38
M2-100-1	25-3-2565	15.14	29.97	13.06	2.42
M2-100-2	25-3-2565	15.10	29.96	12.70	2.37
M2-100-3	25-3-2565	14.99	30.08	12.80	2.42
M3-0-1	27-3-2565	15.06	29.99	12.82	2.40
M3-0-2	27-3-2565	15.08	30.08	12.82	2.39
M3-0-3	27-3-2565	15.03	29.94	12.80	2.42
M3-25-1	29-3-2565	15.09	30.01	12.86	2.40
M3-25-2	29-3-2565	15.11	30.44	13.10	2.40
M3-25-3	29-3-2565	15.10	29.74	12.76	2.39
M3-50-1	26-3-2565	15.10	30.38	13.18	2.42
M3-50-2	30-3-2565	15.10	29.75	12.70	2.38

Table 3.3 Basic properties of concrete samples prepared for laboratory testing. (cont.)

Sample No.	Preparing Date (D-M-Y)	Diameter (cm)	Length (cm)	Weight (kg)	Density (g/cm^3)
M3-50-3	30-3-2565	15.01	30.08	12.76	2.39
M3-75-1	26-3-2565	15.00	30.00	12.92	2.44
M3-75-2	25-3-2565	15.02	29.94	12.92	2.43
M3-75-3	26-3-2565	15.02	29.94	12.70	2.39
M3-100-1	25-3-2565	15.12	30.15	12.76	2.36
M3-100-2	24-3-2565	14.97	29.96	12.88	2.44
M3-100-3	24-3-2565	15.04	30.23	12.84	2.39
M6-0-1	27-3-2565	15.04	30.24	12.74	2.371
M6-0-2	27-3-2565	15.19	30.20	12.80	2.339
M6-0-3	27-3-2565	15.08	30.13	12.78	2.374
M6-25-1	29-3-2565	15.13	30.16	13.14	2.423
M6-25-2	29-3-2565	15.04	30.03	12.92	2.413
M6-25-3	29-3-2565	15.10	30.51	13.04	2.386
M6-50-1	25-3-2565	14.90	30.18	13.00	2.469
M6-50-2	25-3-2565	14.91	30.51	12.90	2.419
M6-50-3	30-3-2565	14.67	29.96	12.74	2.515
M6-75-1	26-3-2656	14.80	30.10	12.74	2.461
M6-75-2	26-3-2565	14.79	29.99	12.64	2.453
M6-75-3	26-3-2565	14.79	29.88	12.62	2.458
M6-100-1	24-3-2565	14.89	29.93	12.78	2.451
M6-100-2	25-3-2565	14.98	29.97	12.86	2.433
M6-100-3	25-3-2565	14.85	29.92	12.72	2.454
M12-0-1	27-3-2022	14.82	30.04	12.66	2.442
M12-0-2	27-3-2022	15.06	30.24	13.16	2.442
M12-0-3	24-3-2022	14.74	29.82	12.62	2.479
M12-25-1	29-3-2022	14.82	30.14	12.78	2.457
M12-25-2	29-3-2022	14.86	30.26	12.84	2.446

Table 3.3 Basic properties of concrete samples prepared for laboratory testing. (cont.)

Sample No.	Preparing Date (D-M-Y)	Diameter (cm)	Length (cm)	Weight (kg)	Density (g/cm^3)
M12-25-3	29-3-2022	14.94	29.98	12.76	2.427
M12-50-1	30-3-2022	14.90	30.50	13.14	2.470
M12-50-2	30-3-2022	14.88	30.04	12.82	2.453
M12-50-3	30-3-2022	14.94	30.32	13.16	2.475
M12-75-1	26-3-2022	14.82	29.90	12.80	2.481
M12-75-2	26-3-2022	14.84	30.32	12.90	2.459
M12-75-3	26-3-2022	14.76	30.16	12.82	2.483
M12-100-1	25-3-2022	14.96	29.90	12.90	2.454
M12-100-2	25-3-2022	14.84	30.04	12.78	2.459
M12-100-3	25-3-2022	14.82	30.00	12.80	2.472

CHAPTER IV

LABORATORY TESTS

4.1 Introduction

This chapter describes the test methods, apparatus, and calculations for the strength, elastic parameters, mineral composition, percent saline absorption, and wave velocities through specimens. The laboratory test includes the uniaxial compression test, X-ray diffraction analysis, saline absorption test, and ultrasonic pulse velocity measurements. The tests were conducted on both concrete and mortar specimens, as depicted in Figure 4.1.

4.2 Uniaxial compression test

After immersing in the saline solution for durations of 0, 1, 2, 3, 6, and 12 months, the saturated concrete samples, characterized by dry surface conditions, were tested to determine the compressive strength of the concrete. The concrete's compressive strength assessment within this study involved two distinct methodologies: 1) the indirect compressive strength evaluation, conducted using the Schmidt rebound hammer (ASTM C805), and 2) the direct compressive strength (ASTM C39) determination through the uniaxial compressive strength test.

4.2.1 Schmidt rebound hammer test

The Schmidt rebound hammer testing is a simple method and commonly used to determine the indirect compressive strength of concrete and rock due to its cost-effectiveness and ease of handling (Buyuksagis and Goktan, 2007). It can be performed either in the field or in the laboratory to obtain preliminary information about the relative quality of the material being examined. The mechanism involves a spring-loaded mass released against the piston, and the hammer is pressed against the

surface of the test material (Figure 4.2). During the impact of the piston against the surface, the resulting mass contraction leads to a rebound distance. This distance is directly proportionate to the total energy absorbed by the impacted surface. The rebound distance of the piston is read directly from the numerical scale on the instrument and is referred to as the rebound number (R) according to ASTM C805. Ten points are assessed using the Schmidt rebound hammer on both the end surface (a) and the outer surface (b) of the concrete sample (Figure 4.3). The compressive strengths are determined using the rebound hammer calibration chart as shown in Figure 4.4.
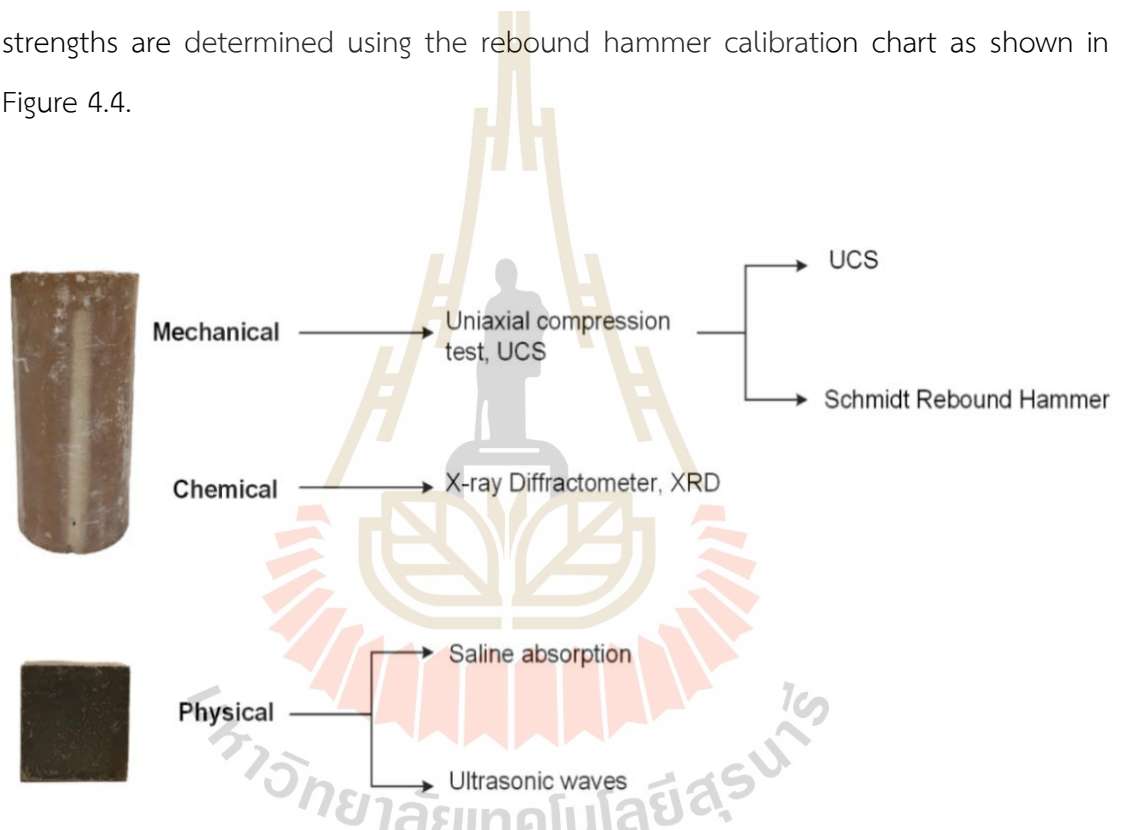
Figure 4.1 Concrete and mortar samples prepared for laboratory test.

Figure 4.2 Schmidt rebound hammer testing of a concrete sample.

a)   b)
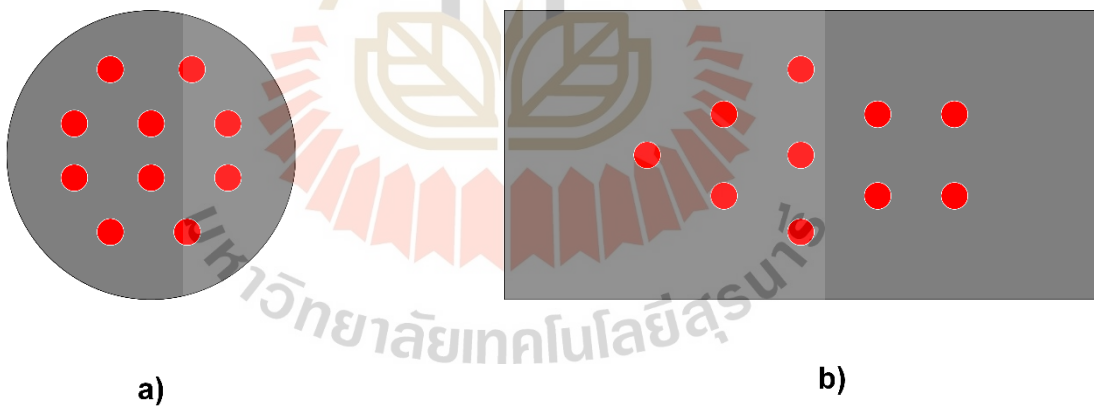
Figure 4.3 Ten points were assessed using the Schmidt rebound hammer on both the
end surface (a) and outer surface (b) of the concrete sample.
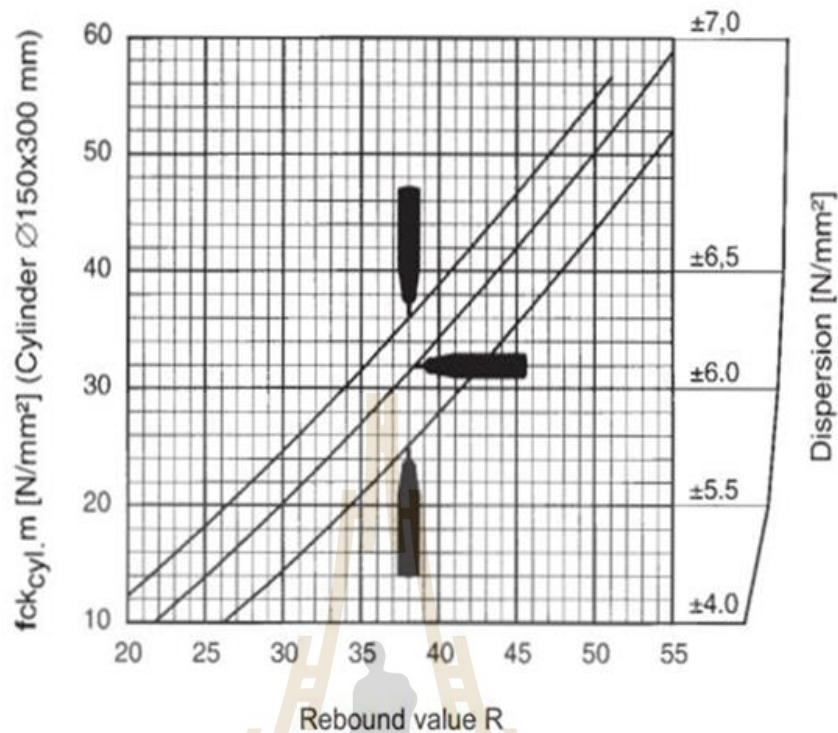
Figure 4.4 The rebound hammer calibration chart for determining the compressive strength (for the concrete cylinder dimensions of diameter = 150 mm and length = 300 mm).

4.2.2 Uniaxial compression test

The determination of uniaxial compressive strength and elastic parameters involves subjecting specimens to axial loading at a consistent rate of 0.1 MPa/s, as recommended in ASTM C39 standards. This process requires placing the concrete sample within a compression machine and applying axial stress until failure occurs. Throughout this procedure, the axial displacements are measured and recorded using dial gauges to monitor the specimen's behavior under load, which is used to calculate the elastic modulus of concrete samples. Figure 4.5 illustrates the setup utilized for conducting the concrete compressive strength test. The post-test concrete samples are shown in Figure 4.6. The sample experiences failure due to tension-induced fractures and shear failure modes.
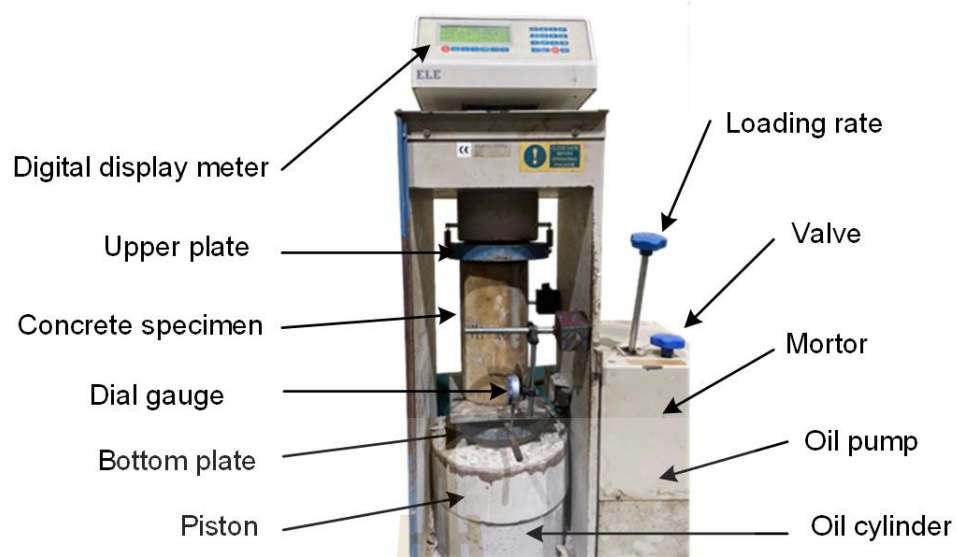
Figure 4.5 Test setup for the compressive strength tests of concrete sample.

The compressive strength of concrete (σ_c) can be calculated from the following equation.

$$\sigma_c = P/A \tag{4.1}$$

where P is the maximum pressure measured at the failure point of the concrete sample. A is the original cross-sectional area of the concrete sample (A = $\pi D^2/4$). The axial strain (ε) under uniaxial compression can be used to calculate the elastic modulus (E) of concrete based on a general equation 4.2 and 4.3, as follows:

$$\varepsilon = \Delta L/L \tag{4.2}$$

$$E = \sigma/\varepsilon \tag{4.3}$$

where ΔL is change in the length of the concrete sample within the original length (L).

Salinity (%)	Immersion time (month)									
	1		**2**		**3**		**6**		**12**	
	Before	After	Before	After	Before	After	Before	After	Before	After
0										
25										
50										
75										
100										
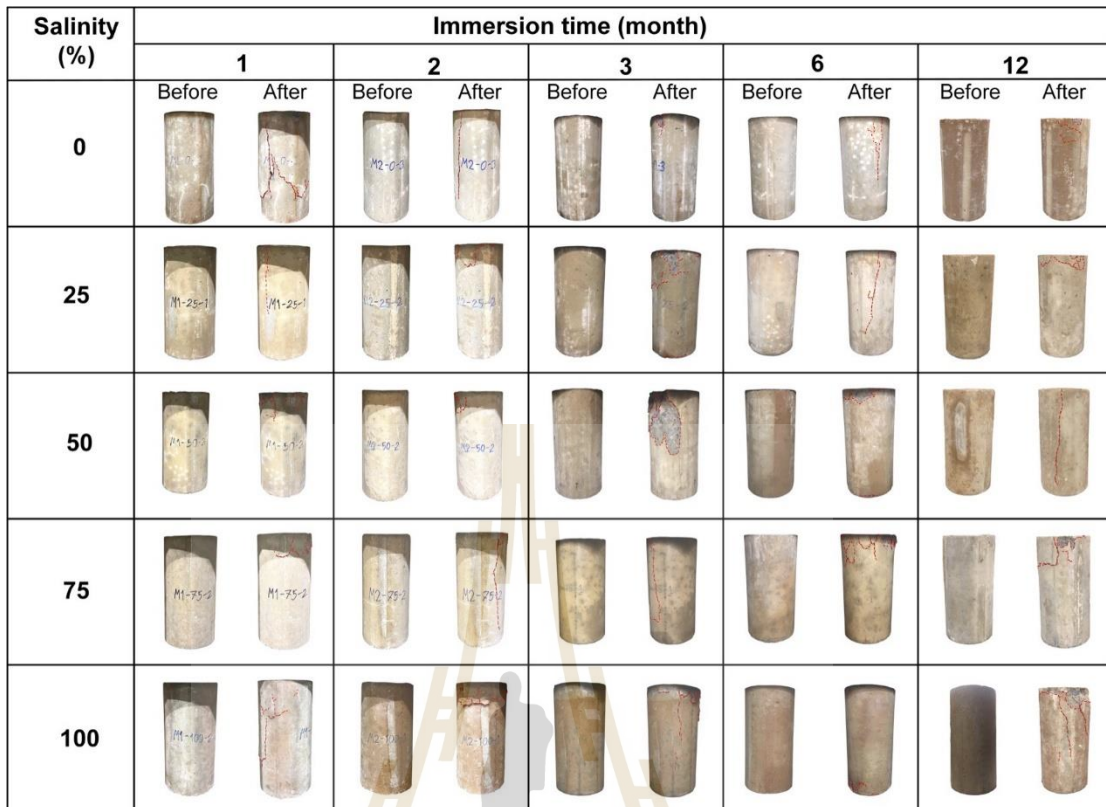
Figure 4.6 Pre-tested and post-tested concrete samples for the uniaxial compression tests.

4.3   X-ray diffraction analysis

The X-ray diffraction (XRD) is a method that utilizes X-rays for both qualitative and quantitative evaluation. This technique, tested according to ASTM C1365, determines the crystal structure of chemicals within a sample. The X-ray diffraction analysis method is based on directing an X-ray source towards a sample of concrete powder through a sieve, resulting in diffraction and reflection at various angles (typically ranging from 10 to 80 degrees in studies), with a detector serving as a receiver. The composition and structure of a substance can be revealed by different degrees of X-ray diffraction at these angles, based on its form and crystal nature. The sample's crystal structure is then studied using these findings, providing insights into the type of substance present.

Post-tested samples from the uniaxial compression test were then subsequently analyzed using X-ray diffraction (XRD). A representative specimen taken

from the outer surface of the sample is crushed to yield concrete powder particles smaller than 0.25 mm (mesh #60), totaling at least 20 grams. The mineral compositions of the powdered concrete specimen are analyzed using X-ray diffraction (XRD) via the X-ray Diffractometer-D8 phaser (Figure 4.7). The DIFFRAC.EVA software identifies the composition based on this fingerprint, subsequently quantified using TOPAS software. The results obtained here can be used to explain the concrete deterioration resulting from immersion in a saline solution.

In these testing methods, five primary minerals are examined: two forms of calcium silicate (C_3S, C_2S), tricalcium aluminate (C_3A), tetracalcium aluminoferrite (C_4AF), and Halite (NaCl), over immersion periods of 0, 1, 2, 3, 6, and 12 months. These minerals are the products induced from hydration reaction between cement compounds and water causes the formation and hardening of the concrete. The hydration reaction of calcium silicate (C_3S, C_2S) in cement occurs when it reacts with water to form Ca $(OH)^2$ and calcium silicate hydrate (CSH). The hydration reaction of tricalcium aluminate (C_3A) is instantaneous and contributes to the rapid hardening of the cement paste. The hydration reaction of tetracalcium aluminoferrite (C_4AF) is similar to the reaction in C_3A, but it is slower and generates less heat. Gypsum was found to retard the reaction of C_4AF more than that of C_3A.

a)   b)
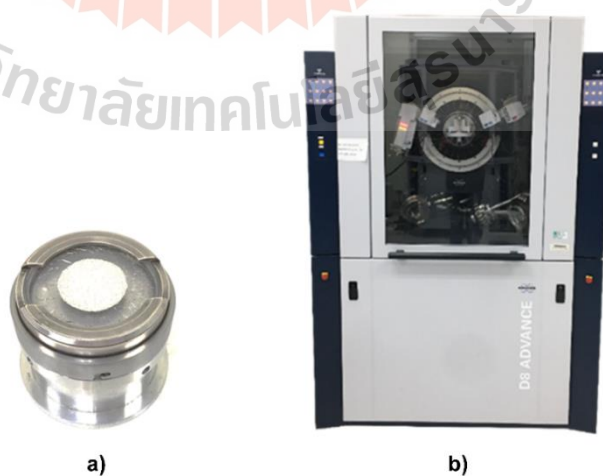
Figure 4.7 X-ray diffraction analysis equipment, (a) concrete powder, and (b) X-ray Diffractometer-D8 Phaser.

4.4   Saline absorption test

Saline absorption tests were performed on cubic mortar samples submerged in saline solutions of varying concentrations (0%, 25%, 50%, 75%, and 100%) throughout immersion periods of 0, 1, 2, 3, 6, and 12 months. The testing procedure followed ASTM 1585 standards. Initially, the saturated mortar samples with dry surface conditions were weighed. Following this, they were placed in an oven set at 80±5 °C for 24 hours.   This process aimed to measure the weight variations and saline absorption of mortar samples.

The percentage of saline absorption (by weight) was then calculated using Equation 4.4 to determine the brine absorption:

$$\%\text{Absorption} = ((W-D)/D) \times 100 \qquad\qquad (4.4)$$

where W is the weight of saturated mortar samples with dry surface conditions after immersion in saturated brine. D is the dry in oven weight of the mortar sample.

Throughout the test, the weight of the mortar samples was measured and recorded for each immersion time in saline solution to calculate the percentage of saline absorption (by weight). All the collected data were utilized to investigate the behavior of deteriorating mortar due to saline absorption.

4.5   Ultrasonic pulse velocity measurements

The wave velocity test was conducted using an OYO Sonic Viewer 170 (model 5338), as shown in Figure 4.8. This test utilizes a mortar sample to determine dynamic properties by measuring the velocities of primary and secondary waves as they pass through the specimen. The procedures adhere to ASTM C597-97 standards, and the results are used to analyze concrete deterioration.

Ultrasonic pulse velocity testing through solid materials or concrete involves generating two types of waves using wave generators: the primary wave, or P-wave, and the secondary wave, or S-wave. The wave velocities in different concrete types

are determined by the mechanical and physical properties of the concrete, expressed by Equations 4.5 and 4.6.

$$V_p = ((\lambda+2G)/\rho)^{0.5} \qquad (4.5)$$

$$V_s = (G/\rho)^{0.5} \qquad (4.6)$$

where V_P and V_S are the primary and secondary wave velocities, respectively. λ and G is the Lame's constant and ρ is the density of concrete.

The dynamic Poisson's ratio and dynamic elastic moduli are determined using Equations 4.7 and 4.8.

$$\nu_d = [(V_p^2-V_s^2)-2]/[2(V_p^2/V_s^2)-1] \qquad (4.7)$$

$$E_d = 2(1+\nu_d)\,\rho V_s^2 \qquad (4.8)$$

where V_P and V_S are the primary and secondary wave velocities, respectively. ν_d and the dynamic Poisson's ratio, and ρ is the density of concrete.

The ultrasonic pulse velocity measuring device consists of a signal transmitter and receiver connected to both ends of the concrete and a digital display screen showing the results from measurement (Figure 4.8). Preceding each wave velocity measurement, the contact surface of the mortar sample was dried, and the transmitter was positioned for the assessment, ensuring consistent and uniform pressure. Various research works have employed sonic rate techniques to evaluate concrete properties; however, these studies often neglected the assessment of concrete admixture parameters, such as water/cement ratio, on the propagation of ultrasonic waves in concrete (Abo-Qudais S.A., 2005). In this study, wave velocity measurement was employed to document and analyze the wave velocity of mortar samples across different immersion periods (0, 1, 2, 3, 6, and 12 months) immersed in saline solution, aiming to comprehend the physical behavior of the mortar.
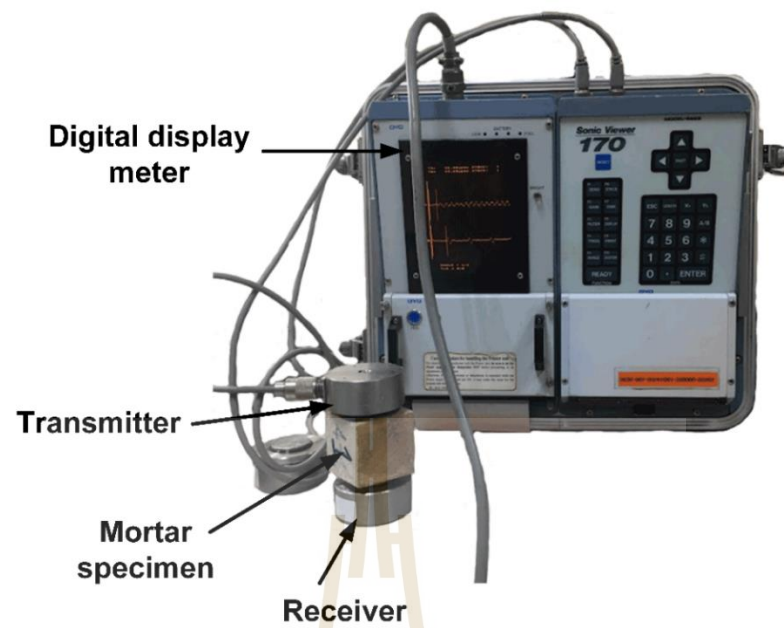
Figure 4.8 Wave velocity test apparatus performed using OYO Sonic Viewer 170 (Model5338).

CHAPTER V

TEST RESULTS

5.1 Introduction

The aim of this study is to investigate the time-dependent reduction in compressive strength of concrete when samples are constantly immersed in various concentrations of saline solutions. Moreover, X-ray diffraction (XRD) analysis was conducted to assess the change in mineral composition resulting from hydration reactions occurring within the concrete. The result is expected to reveal and support the cause behind the reduction in compressive strength of concrete. Two additional tests include saline absorption and ultrasonic pulse velocity tests on mortar samples. These tests were carried out to corroborate the progressive deterioration of concrete under immersion in saline solution over time. The study presents compressive strength, mineral composition variation, saline absorption, and P-wave and S-wave velocities as functions of saline concentration and immersion time.

5.2 Uniaxial compression test

The uniaxial compressive strength tests were conducted on concrete samples cured for 7, 14, 21, and 28 days to demonstrate a progressive increase in concrete compressive strength corresponding to the elapsed curing time. The compressive strength at 28 days of curing was utilized as a benchmark for comparing the compressive strength of concrete samples subjected to varying durations of submersion in saline solution. A summary of the test results is provided in Table 5.1. The compressive strength of concrete increases rapidly in the first seven days of curing. After that, it will gradually increase until reaches its peak at 28 days (Figure 5.1).

To study the effect of saline solution on compressive strength of concrete, after the 28-day curing period, the samples were subsequently immersed in a saline solution with varying concentrations of 0%, 25%, 50%, 75%, and 100%. The samples were continuously immersed in the saline solution for 0, 1, 2, 3, 6, and 12 months. Subsequently, non-destructive testing was performed on the samples using the Schmidt rebound hammer test and the uniaxial compressive strength test using a compression machine. The test results are summarized in Table 5.2. The results indicate the compressive strength of concrete obtained from direct and indirect methods decreases with increases in immersion time. High saline concentrations led to a more pronounced reduction in compressive strength compared to samples exposed to lower saline concentrations (Figure 5.2 and Figure 5.3). For samples immersed in 0% concentration (tap water), there was no observable alteration in the compressive strength of the concrete. The Schmidt rebound hammer test (indirect method) provides 1.6 times higher compressive strength values than the uniaxial compressive strength test (direct method).

Table 5.1 The compressive strength of concrete was obtained for concrete samples cured for 7, 14, 21, and 28 days.

Curing Time (day)	Compressive Strength, σ_c (ksc)
7	189 ± 27.73
14	218 ± 24.25
21	225 ± 9.46
28	242 ± 6.91
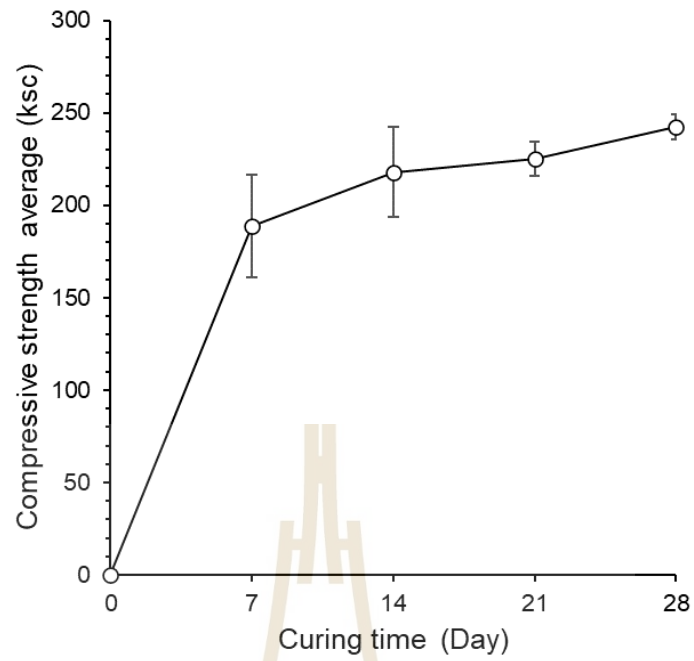
Figure 5.1 Development of concrete compressive strength and curing time.

Table 5.2   Direct and Indirect compressive strength and elasticity parameters of concrete.

Saline Concentration (%)	Immersion Time (month)	Compressive Strength, σ_c (ksc)		Elastic Modulus, E (GPa)
		Indirect Method	Direct Method	
0	0	283±13.32	181±8.96	5.350±1.84
	1	284±6.03	181±6.08	4.362±1.02
	2	283±8.00	181±5.51	3.824±0.52
	3	285±1.15	181±3.79	3.539±0.41
	6	284±7.21	181±2.89	3.349±0.47
	12	284±1.00	182±5.51	3.322 ±1.00
25	0	283±13.32	181±8.96	5.350±1.84
	1	272±6.43	178±16.52	4.191±2.42
	2	258±8.14	172±3.79	3.592±1.07
	3	249±6.43	164±7.51	3.284±0.54
	6	239±2.08	159±26.10	3.080±0.49
	12	194±23.46	150±10.02	2.957 ±1.00
50	0	283±13.32	181±8.96	5.350±1.84
	1	260±4.73	173±1.00	4.025±0.96
	2	244±5.51	161±11.59	3.233±0.70
	3	234±4.51	150±10.02	2.971±2.27
	6	223±3.79	141±16.52	2.799±2.81
	12	178±22.19	129±6.51	2.706 ±1.00
75	0	283±13.32	181±8.96	5.350±1.84
	1	247±4.73	169±0.58	3.902±1.60
	2	230±18.34	154±2.52	3.002±0.91
	3	219±22.37	141±9.29	2.693±0.38
	6	208±7.64	126±3.61	2.434±0.50
	12	161±10.41	117±6.03	2.346 ±1.00
100	0	283±13.32	181±8.96	5.350±1.84
	1	219±14.18	164±8.50	3.438±1.00
	2	205±16.97	147±9.64	2.537±0.98
	3	189±9.02	131±4.04	2.231±1.09
	6	178±1.00	114±1.00	2.000±0.32
	12	133±1.53	105±6.24	1.817 ±1.00
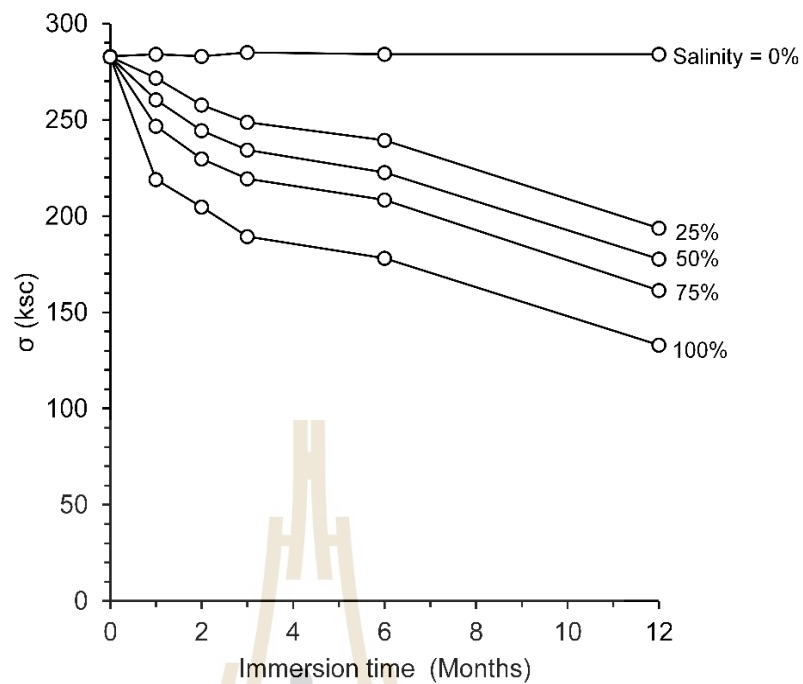
Figure 5.2 Compressive strength as a function of immersion time obtained from Schmidt rebound hammer test (indirect method) conducted on samples exposed to different levels of saline concentration.
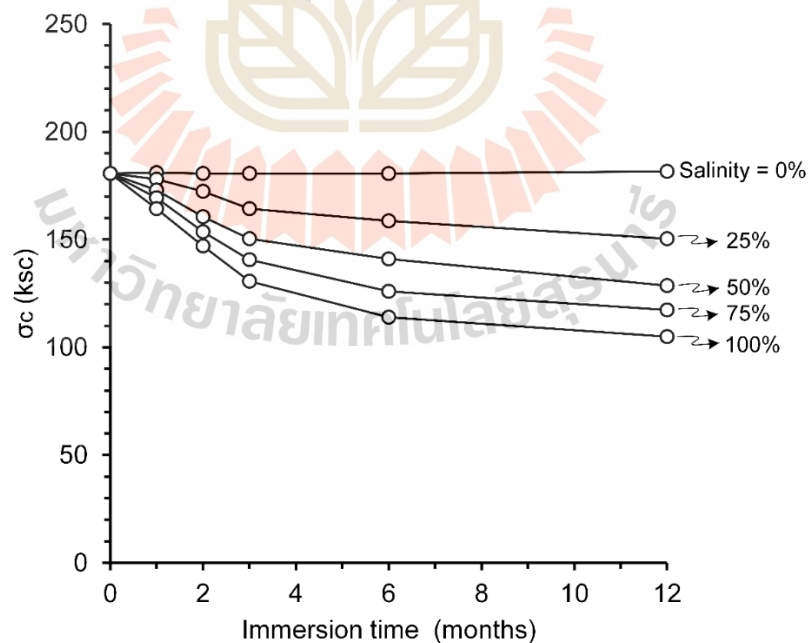
Figure 5.3 Compressive strength as a function of immersion time obtained from uniaxial compression test (direct method) conducted on samples exposed to different levels of saline concentration.

Figures 5.2 and 5.3 both demonstrate a consistent trend of decreasing compressive strength in correlation with prolonged immersion duration. Specifically, within the initial 0 to 3 months, there was a gradual decline in the concrete's compressive strength. During the 6 to 12-month period, a notable acceleration in the decrease of compressive strength in the concrete samples was observed. This highlights the influential impact of immersion time on concrete deterioration. Notably, under high saline concentrations, the compressive strength declined significantly faster compared to samples immersed into lower concentrations.

Several factors can contribute to the observed difference between the Schmidt rebound hammer and uniaxial compression tests. Some of these factors include:

1. Test Principle and Assumptions: The Schmidt rebound hammer test and the uniaxial compressive strength test are based on different principles and make different assumptions about the behavior of the material under stress. The underlying principles, test setup, and the specific properties being measured can result in variations in the measured values.

2. Testing Techniques: The two tests employ different techniques to assess the compressive strength of the material. The Schmidt rebound hammer test measures the rebound velocity of a hammer striking the surface of the material, while the uniaxial compressive strength test applies a uniaxial load until failure. The variations in the testing techniques can introduce differences in the measured values.

3. Loading Conditions: The loading conditions in the uniaxial compressive strength test involve applying a uniaxial load along a single axis until failure. On the other hand, the Schmidt rebound hammer test applies an impact load to the surface of the material. The difference in loading conditions can affect the stress distribution within the material and contribute to variations in the measured values.

The elastic modulus or modulus of elasticity is a material property that describes its stiffness or ability to deform under stress. It represents the ratio of stress to strain within the elastic range of a material. It was found that concrete's ability to

deform under stress when subjected to constant immersion in a sodium chloride solution resulted in a decrease in Young's modulus. As time progressed, there was a continual decrease in Young's modulus. Additionally, higher levels of salinity exacerbated this reduction, as shown in Figure 5.4. The observed decrease in Young's modulus poses a potential risk of inducing enduring damage to the concrete structure over the long-term period.
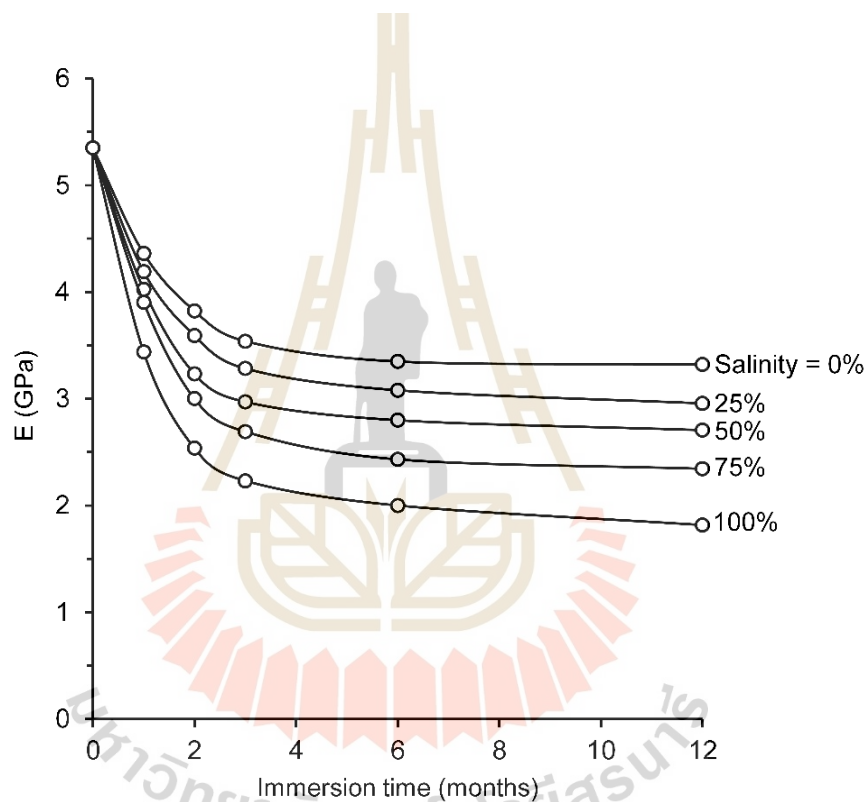
Figure 5.4 Correlation between Young's modulus and immersion time for concrete.

5.3   X-ray diffraction analysis

The X-ray diffraction analysis (XRD) can detect hydration reactions in concrete when certain mineral phases undergo structural changes due to the incorporation of water molecules into their crystal lattice. These hydration reactions primarily occur with cementitious materials, such as Portland cement, which is a key component of concrete. During the hydration process of cement, various mineral phases, including calcium silicates, calcium aluminate, and calcium hydroxide, react with water to form new hydrated compounds. The most significant hydration product in cement is calcium silicate hydrate (CSH) gel, which greatly contributes to the strength and durability of the mortar.

In this experiment, the mortar samples are immersed in a saline (NaCl) solution. The presence of chloride ions (Cl^-) results in chemical reactions with minerals within the mortar sample: calcium silicate (C_3S, C_2S), tricalcium aluminate (C_3A), and tetra calcium aluminoferrite (C_4AF), ultimately leading to the deterioration of the concrete sample. The XRD pattern of cement powder is presented in Figure 5.5.

The samples immersed in approximately 0% salinity have a higher C_3S and C_2S content compared to samples immersed in 100% salinity. The samples subjected to 100% salinity have the lowest proportions of C_3S at 44.74% and C_2S at 21.66%. Conversely, samples exposed to 0% salinity showcase the highest C_3S and C_2S percentages at 58.62% and 35.77%, respectively. This difference arises because 100% salinity conditions can prompt the formation of chloride-bearing phases like Friedel's salt (calcium chloride hydrate), ettringite (calcium aluminate sulfate hydrate), or other compounds containing chlorides within the concrete matrix. These findings illustrate a reduction in C_3S and C_2S content as salinity levels increase. Notably, the highest values are approximately 1.3 times greater than the lowest recorded values. Changes in the amount of C_3S and C_2S may be due to chemical reactions with chloride ions in saline solution, which causes changes in the mineral structure. This evidence strongly implies that a chemical reaction between chloride ions and C_3S and C_2S occurred during immersion.

Conversely, the results as shown in Table 5.3, indicate that the percentages of C_3A and C_4AF increased proportionally with the increasing in saline concentration. The sample tested under 0% saline concentration demonstrates C_3A and C_4AF percentages of roughly 3.66% and 1.95%, respectively. Conversely, the sample exposed to 100% saline concentration displays the highest recorded percentages, with C_3A at around 10.97% and C_4AF approximately at 11.58%. The highest values are about 3.0 and 6.0 times the lowest ones. The change in C_3A and C_4AF may be due to the hydration reaction of concrete occurring at the mineral phases consequently, the mineral is changed. These lead to the formation of chloroaluminate compounds and can react with tetra calcium alumino ferrite to form chloroaluminate hydrates, such as Friedel's salt. This indicates an increase in C_3A and C_4AF within the concrete.

According to the measurements documented in Table 5.3, there were no detectable traces of NaCl percentage found in the samples immersed in the 0% solution. The sample immersed in 100% saline concentration gives the highest NaCl percentage, measuring approximately 11.05%. This observation found that the NaCl content increased with increasing immersed times and salinity, as shown in Figure 5.5. The samples immersed in a high saline concentration will crystallize in large quantities. The salt crystals do not cause the concrete to increase in strength. On the other hand, it will cause the expansion of the concrete voids and lead to a decrease in the compressive strength of concrete.
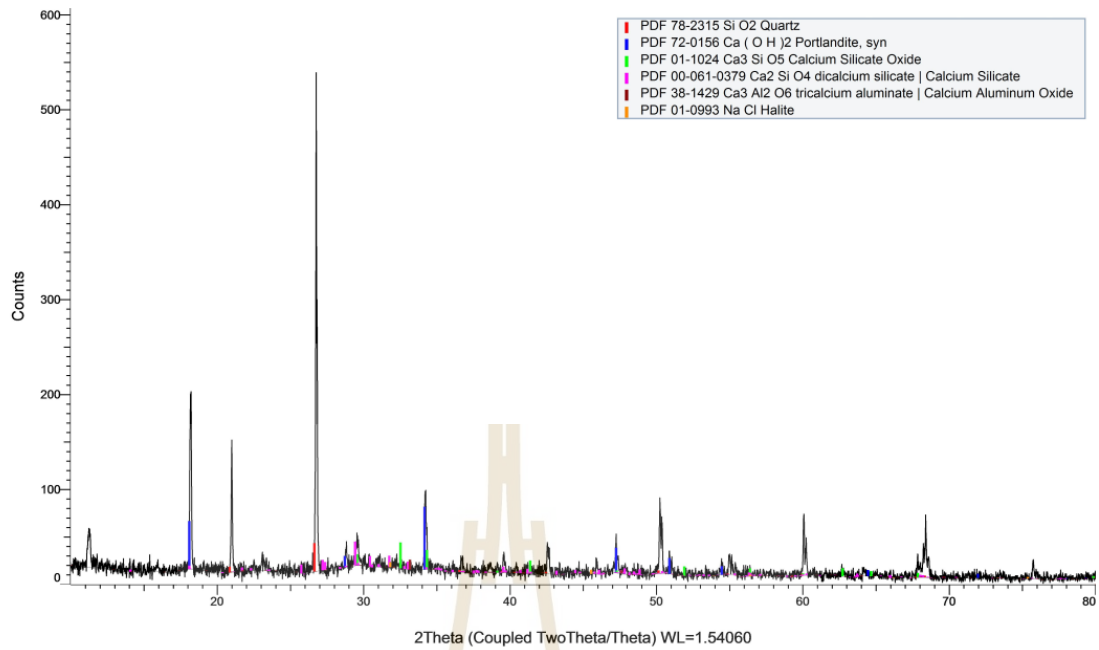
Figure 5.5   The XRD pattern of cement powder
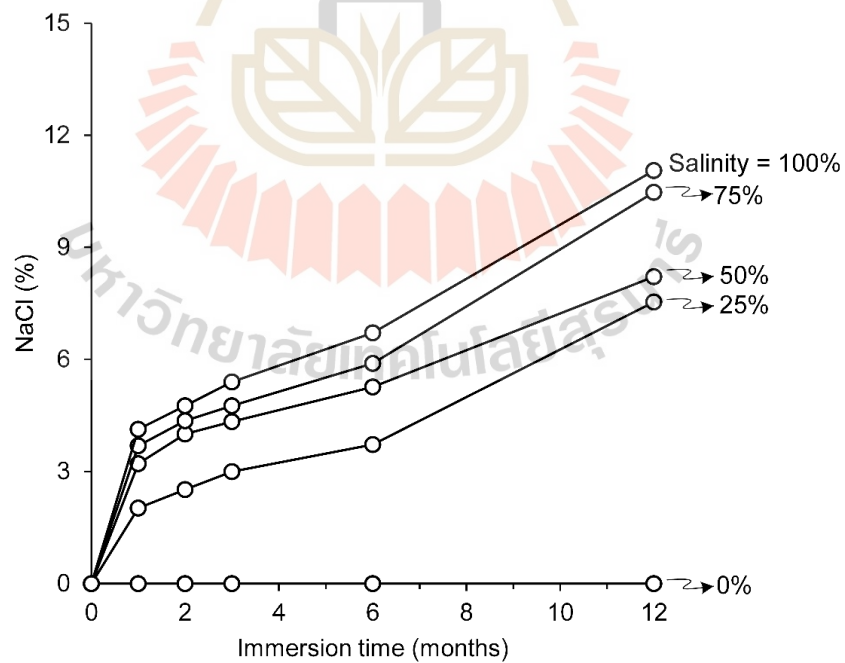
Figure 5.6   Correlation between percentage of sodium chloride (NaCl) and immersion

time under various saline concentrations.

Table 5.3 Mineral composition of concrete samples.

Immersion (months)	Salinity (%)	C_3S (%)	C_2S (%)	C_3A (%)	C_4AF (%)	NaCl (%)
Initial	-	58.62	35.77	3.66	1.95	0
1	0	58.58	35.41	3.98	2.03	0
2		58.25	34.66	4.64	2.45	0
3		58.02	33.84	5.24	2.90	0
6		57.34	32.73	6.37	3.56	0
12		55.56	30.19	8.75	5.50	0
1	25	58.38	33.41	4.00	2.19	2.02
2		58.14	31.38	5.06	2.90	2.52
3		57.88	29.13	6.97	3.02	3.00
6		56.98	28.09	7.33	3.88	3.72
12		50.06	27.55	8.43	6.42	7.54
1	50	58.23	32.06	4.21	2.29	3.21
2		57.90	29.48	5.48	2.94	4.20
3		57.28	27.89	7.20	3.20	4.43
6		55.39	27.44	7.96	3.95	5.26
12		49.83	26.96	9.12	5.88	8.21
1	75	58.03	30.54	5.17	2.37	3.89
2		57.70	29.07	5.64	3.23	4.36
3		56.33	27.80	7.69	3.62	4.56
6		54.21	26.80	8.43	4.67	5.89
12		47.30	22.24	10.09	9.90	10.47
1	100	57.07	30.51	5.61	2.68	4.13
2		56.87	28.57	6.38	3.72	4.46
3		55.63	27.65	7.35	3.97	5.40
6		53.51	25.65	9.05	5.08	6.71
12		44.74	21.66	10.97	11.58	11.05

5.4   Saline absorption

The experiment to measure saline absorption of mortar samples are performed under difference saline concentration and various immersion time. The results show that the saline absorption percentage tends to increase over time (Figure 5.7). For all saline concentrations, the absorption of saline during the initial 0 to 1 month immersion period showed a rapid increase. Subsequently, following this initial month, the saline absorption demonstrated a gradual increase before reaching a constant. The rise in saline absorption percentage directly contributed to an increase in the weight of the mortar samples, aligning with the observed trend of increased density in the mortar samples over prolonged soaking periods in high saline concentrations.

As shown in Figure 5.8, there was an evident increase in the density of the mortar samples over time. Normally, the loss of water from the mortar leads to a reduction in volume while maintaining a relatively constant mass. The decrease in volume with constant mass results in an increased density, indicating that the density of the mortar samples increases when immersed in the saline solution. It can be concluded that when the mortar is immersed in a saline solution, it allows to absorb and retain sodium chloride into its microstructure. The saline absorption test provides valuable information about the mortar's susceptibility to chloride ingress and its potential for corrosion and deterioration. The increased absorption of salts suggests that the mortar may be at a higher risk of chloride-induced corrosion in practical applications, particularly in environments where exposure to chloride-rich conditions is prevalent.
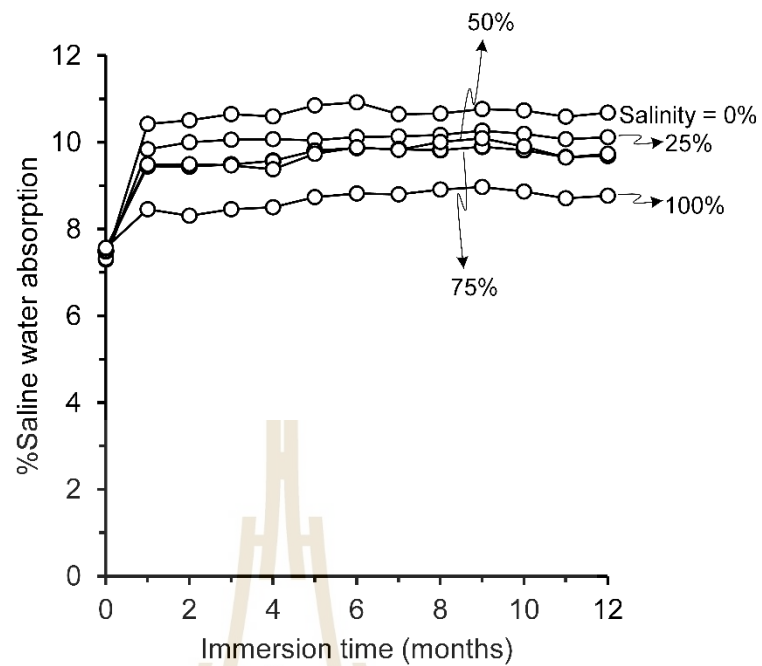
Figure 5.7   Correlation between saline absorption and immersion time under various saline concentrations.
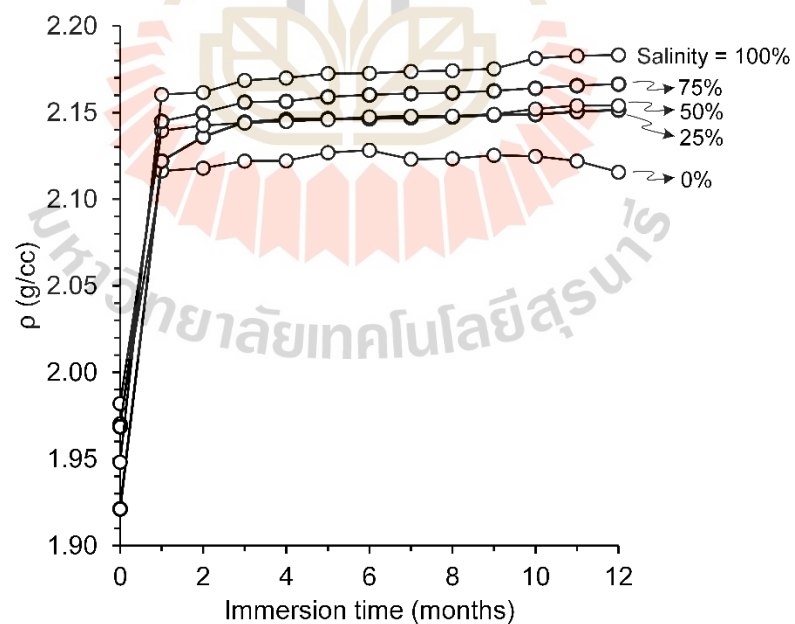
Figure 5.8   Correlation between density of mortar and immersion time under various saline concentrations.

Sodium chloride, as an ionic compound, dissociates into sodium ions (Na+) and chloride ions (Cl⁻) when in solution. The presence of these ions in the immersion solution enables interactions with the cementitious matrix of the mortar. The ions can diffuse into the mortar's pores and bond with the solid phase of the material. As the mortar absorbs the NaCl solution, leaching and diffusion processes occur. The soluble salts, including sodium chloride, dissolve in the water present in the mortar's pores. Over time, these salts can migrate deeper into the material through diffusion processes, resulting in an increase in salt content.

5.5   Ultrasonic pulse velocity

Mortar specimens are immersed in a saline solution, which can potentially affect their properties, including their ultrasonic pulse velocity (UPV). Sodium chloride is a salt, and its presence in the immersion solution can lead to chemical reactions and changes in the mortar's microstructure. Generally, higher pulse velocities indicate better quality and integrity of the material, while lower velocities may suggest the presence of defects or deterioration.

From Figure 5.9, the relationship between Ultrasonic pulse velocity and immersion time for concrete, considering the primary wave, shows that during the 0–1-month period, the wave propagation noticeably increased through the mortar sample. After the 1st-3rd month, the speed of the waves gradually increased and started to stabilize during the 3rd-12th month. It can be observed that the wave propagation speed increases as the sodium chloride solution concentration increases, and this is consistent with the secondary wave, indicating that the velocity of transmission through the mortar sample increases with time.
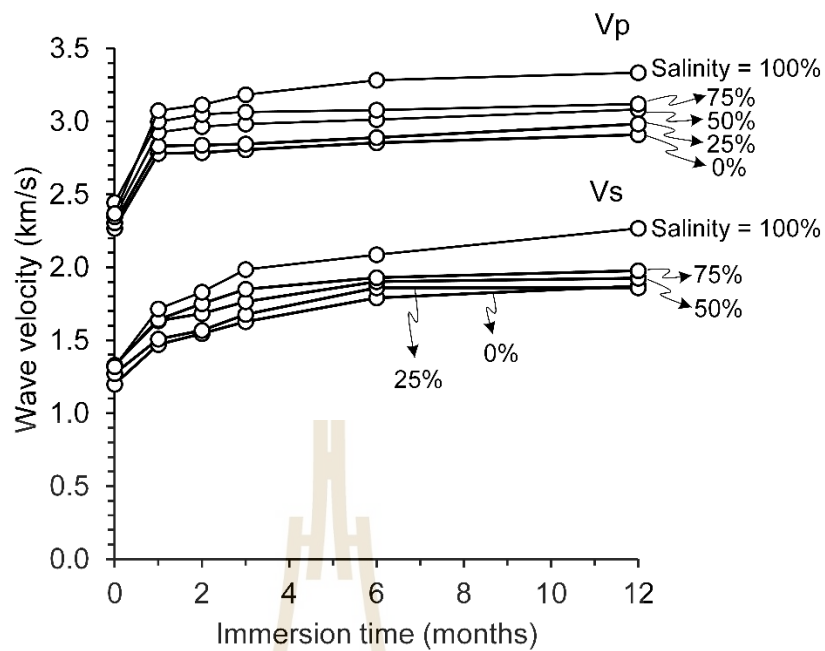
Figure 5.9 Correlation between ultrasonic pulse velocity and immersion time under various saline concentrations.

Sodium chloride exposure can lead to the degradation of the mortar's elastic properties, as shown in Figure 5.10. It was found that the mortar's elastic properties decreased with increasing time. In the first 3 months, the mortar's elastic properties gradually decreased, and from 3 to 12 months, a significant decrease in the mortar's elastic properties was observed. However, at 0% concentration, the mortar's elastic properties remained unchanged, as it was immersed in tap water. This indicates that chloride can penetrate the mortar and cause chemical reactions that result in the breakdown of cementitious bonds and the formation of expansive compounds. These processes can reduce the material's stiffness and increase its porosity, leading to a decrease in the wave propagation speed.

The dynamic Poisson's ratio (Figure 5.11) can be determined experimentally, and the physical situation of such a test is completely different from that of static loading. The value of the dynamic Poisson's ratio is always higher than the static Poisson's ratio, with an average value of about 0.24 which agrees with the results obtained by Teller (1956).

Figure 5.11 shows the relationship between the dynamic Poisson's ratio and immersion time for concrete. It was found that the Poisson's ratio value increased linearly with time, and after the third month, it began to stabilize in a straight line. Furthermore, when the concentration level varied, it was observed that the Poisson's ratio increased with an increase in concentration. When studying the immersion of sodium chloride in mortar, the concentration level of sodium chloride may affect various chemical and physical processes. Higher concentrations of sodium chloride can alter the properties of the solution, such as its ionic strength, pH, or osmotic pressure. These changes may influence the occurrence of specific events or reactions within the mortar, which could potentially follow a Poisson distribution.
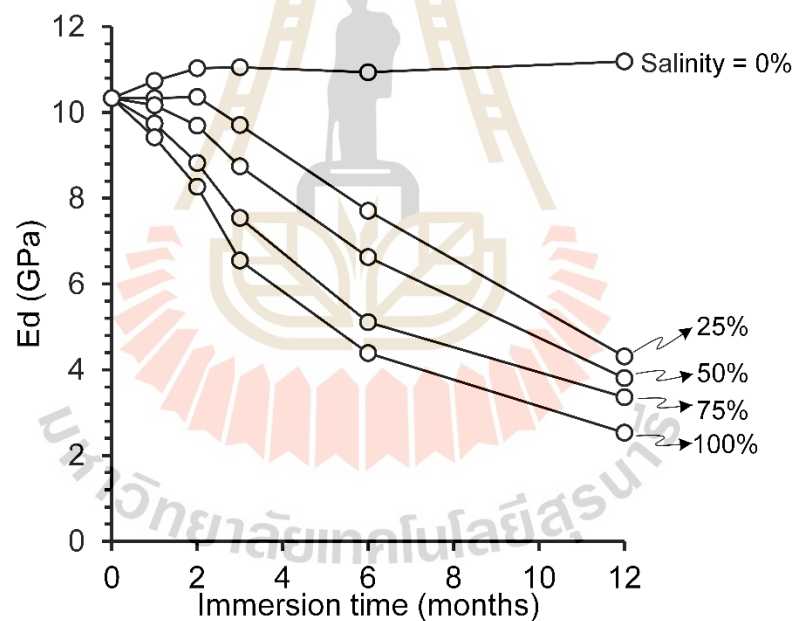
Figure 5.10 Elastic modulus dynamic (E_d) as a function immersion time for various saline concentrations.
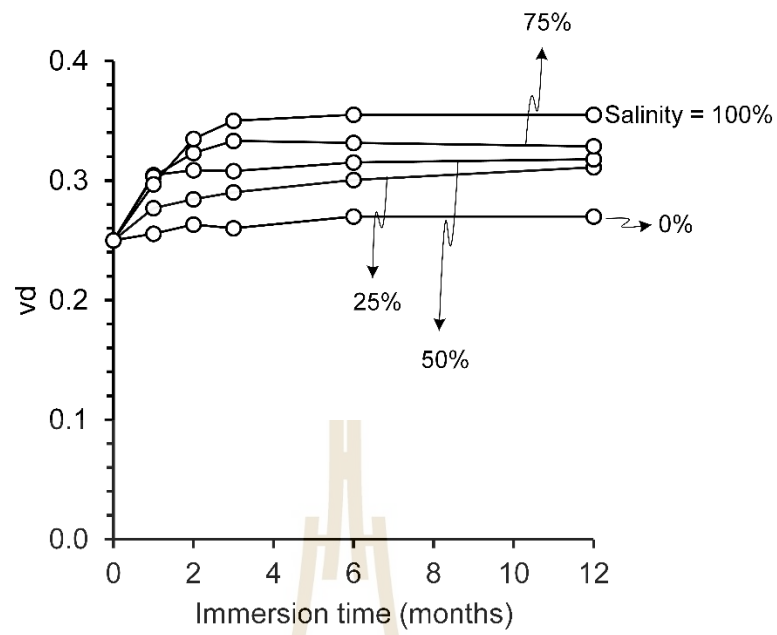
Figure 5.11 Dynamic Poisson's ratio (V_d) as a function immersion time for various saline concentrations
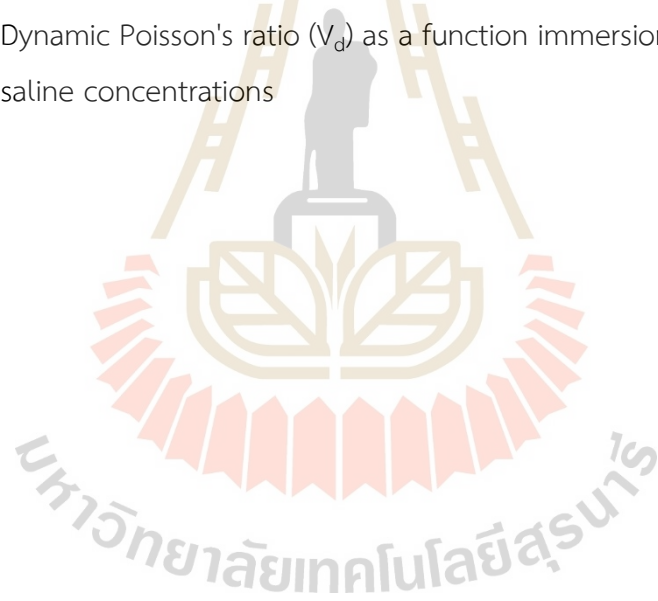
CHAPTER VI

ANALYSIS OF RESULTS

6.1 Introduction

The purpose of this chapter is to formulate the empirical equations that describe the relationship between compressive strength, saline concentration, and immersion time. The presented equations serve as predictive tools for estimating the reduction in the compressive strength of concrete subjected to varying concentrations of brine and immersion durations. The analysis involves the regression of the experimental test data utilizing IBM SPSS Statistics /software (Wendai, 2000). The final section of this chapter introduces the application of equations for estimating the lifespan of concrete under continuous immersion in saline water, which presents the relationship between the lifespan of the concrete and the saline concentration.

6.2 Compressive strength

To demonstrate the reduction in percentage of compressive strength of concrete over time, the normalized compressive strength (σ_c') are ploted as a fuction of immersion time for vaious of saline concentraion. The calculation of σ_c' is outlined as follows:

$$\sigma_c' = \frac{\sigma_c}{\sigma_{c0}} \times 100\% \tag{6.1}$$

where σ_{c0} is the compressive strength of concrete before immersion in saline solution (in ksc). This value represents the compressive at 28 days of curing time (σ_{c0} = 181 ksc). σ_c is the compressive strength of concrete after immersion in saline solution (in ksc), summaried in Chapter 5 (Table 5.2).

It is observed that the normalized compressive strength (σ_c') decreases from 100% of the original value (181 ksc) after immersion in salt water. At 0% salinity, there was no significant change in compressive strength; it seemed constant for all time. However, for the samples soaked in salt water at 25%, 50%, 75%, and 100%, the normalized concrete strength decreased to 88%, 78%, 70%, and 63%, respectively, after 12 months.

The exponential relationships are proposed to correlate the percentage normalized compressive strength (σ_c' in %) with immesion time (t in months). The increase in salinity decreases the percentage of normalized compressive strength. Good correlations are obtained, as shown in Figure 6.1. The following equations represent their relationship:

$$\sigma_c' = 100 + \left\{ \left(\frac{1}{\alpha} \right) \left(1 - e^{-\beta t} \right) \right\} \tag{6.2}$$

where β and γ are constants parameters (shown in Figure 6.1), and t is immersion time. Regressions analysis using SPSS software is performed to determine the above empirical constants from the test data. Figure 6.1 compares the test data with the predictions from Eq. (6.2). Good correlations are obtained ($R^2 > 0.98$).

The multiplier α and β increases with the salinity (%), as depicted by the linear equation illustrated in Figure 6.2.

$$\alpha = 0.0010X - 0.1018 \tag{6.3}$$

$$\beta = 0.0028X + 0.0648 \tag{6.4}$$

where X is salinity (%). Substituting Eq. (6.3) and (6.4) into (6.2) the percentage normalized compressive strength (%) under different salinity and immersion time can be represented by:

$$\sigma_c' = 100 + \left\{ \left(\frac{1}{0.0010X - 0.1018} \right) \left(1 - e^{-(0.0028X + 0.0648) \cdot t} \right) \right\} \tag{6.5}$$
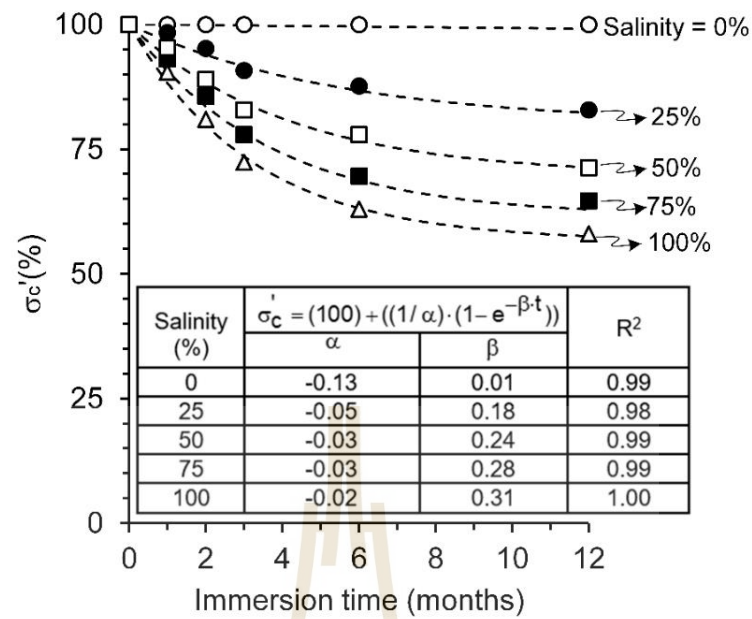
Figure 6.1 Relationships between normalized compressive strength (%) and immersion time for concrete subjected to different saline concentrations.
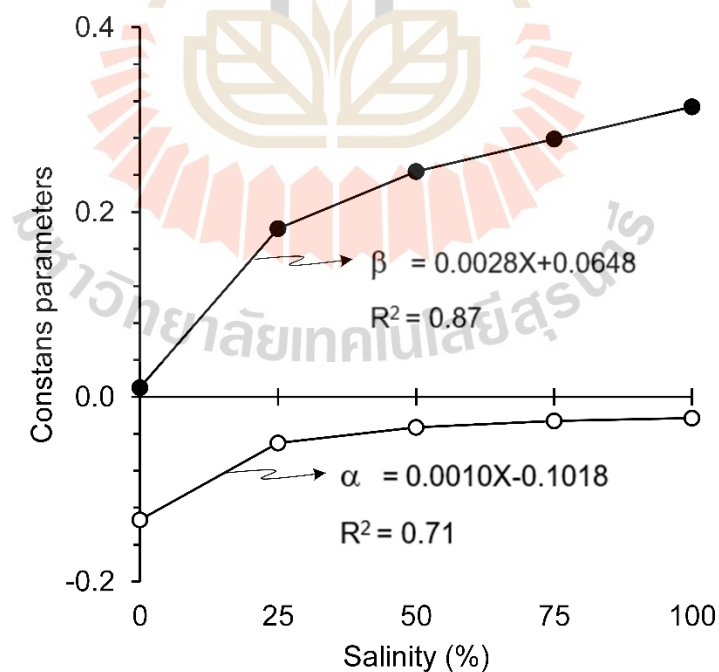
Figure 6.2 Constant parameters as a function of salinity (%).

The equation presented in Equation 6.5 serves as a tool to determine the percentage of concrete compressive strength at any given time relative to its initial strength before immersion in saline solution. This equation provides clear insight into the discernible trend of strength reduction over time.

6.3   Factor of Safety

The compressive strength of concrete is important for the stability of engineering structures that use concrete for construction. In general, the design lifespan of concrete is specified to be more than 100 years (Koh et al., 2014), and a general safety factor of 1.5 is specified according to EN 1992-1-1:2004 (E). The test results showed that the strength of concrete continuously immersed in saline water decreased with increasing time. At the same time, the inducing stresses on the concrete structure as initially designed remain the same and have not changed. Because of this, the safety factor (FS) set at the beginning also decreases over time. When the FS value decreases until it is equal to 1.0, it indicates that the structures fail under the design load. Hence, the ability to predict the lifespan of concrete in a saline environment holds practical significance for inspecting and monitoring concrete structure stability. Additionally, this predictive ability is helpful for engineers to plan and deal with future problems in a timely manner.

The mathematical expression for the factor of safety (FS) of concrete under applied uniaxial stress is given by:

$$FS = \sigma_c/\sigma \qquad\qquad (6.6)$$

where σ_c and σ are the ultimate compressive strength and compressive stress. With a safety factor of approximately 1.5, the average ultimate compressive strength (σ_c) is calculated as 181 ksc. Accordingly, the design load or compressive stress can be established at 120 ksc, considering variations in salinity and immersion time.

The compressive strength (σ_c) are plotted as a function of immersion time for various saline concentration as shown in Figure 6.3. The horizontal line extending along

the x-axis corresponds to a concrete strength of 120 MPa, representing the stress value for safety factor (FS) of 1.5. Drawing a vertical line from the intersection point of each concentration's test result with the horizontal line allows for the identification of the specific time (concrete lifespan) at which the compressive strength starts decreasing, reaching the critical point of FS = 1.0. This point marks the onset of concrete failure. However, the lifespan of concrete at the critical point (FS = 1.0) under different saline concentrations can be determined through the utilization of the empirical equation detailed below.

The exponential relationships are proposed to correlate the compressive stress (σ_c) with immersion time (t). Good correlations are obtained from compressive strength, as shown in Figure 6.3. The following equations represent their relationship:

$$\sigma_c = \sigma_{c0} + \left\{ \left(\frac{1}{\alpha'} \right) \left(1 - e^{-\beta' t} \right) \right\} \tag{6.7}$$

where α', β' and are empirical constant parameters (shown in Figure 6.3), σ_{c0} is compressive stength, equal to 181 ksc, for concrete sample before immesion in saline water, and t is immersion time. Regressions analysis using SPSS software is performed to determine the above empirical constants from the test data. Figure 6.3 compares the test data with the predictions from Eq. (6.7). Good correlations are obtained ($R^2 > 0.98$).

The multiplier α' and β' increases with the salinity (%), as depicted by the linear equation illustrated in Figure 6.4.

$$\alpha' = 0.0005X + 0.0544 \tag{6.8}$$

$$\beta' = 0.0028X + 0.0664 \tag{6.9}$$

where X is salinity (%). Substituting Eq. (6.8) and (6.9) into (6.10) the compressive strength under different salinity and immersion time can be represented by:

$$\sigma_c = \sigma_{c0} + \left\{ \left(\frac{1}{0.0005X + 0.0544} \right) \left(1 - e^{-(0.0028X + 0.0664) \cdot t} \right) \right\} \tag{6.10}$$

The lifespan of concrete can be calculated using Eq. (6.7) by substituting σ_{c0} = 181 ksc, σ_c = 120 ksc (the remained strength of concrete where for FS = 1.5), X is ranging between 0% to 100%. The calculated value of 't' is the lifespan of concrete represents in Figure 6.5. Relationships between lifespan for concrete and salinity, when subjected to immersion in highly concentrated salt water, the durability of a concrete structure is adversely affected, potentially leading to a shortened lifespan. Conversely, under immersion in low-concentration saltwater, the steadfastness of concrete structures is maintained.
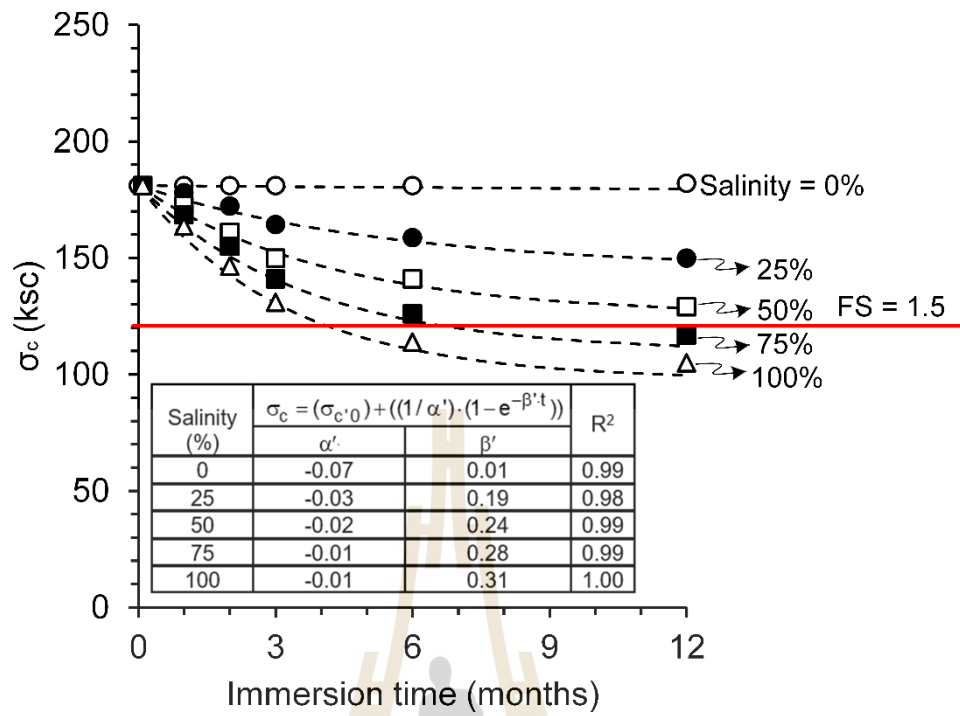
Figure 6.3   Compressive strength as a function of immersion time subjected to different
saline concentrations.
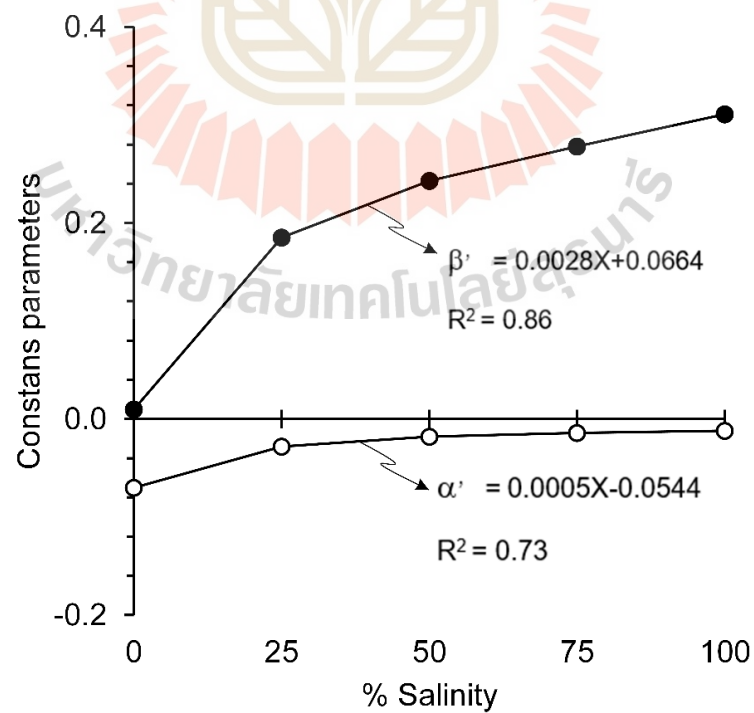
Figure 6.4   Constant parameters as a function of salinity (%).
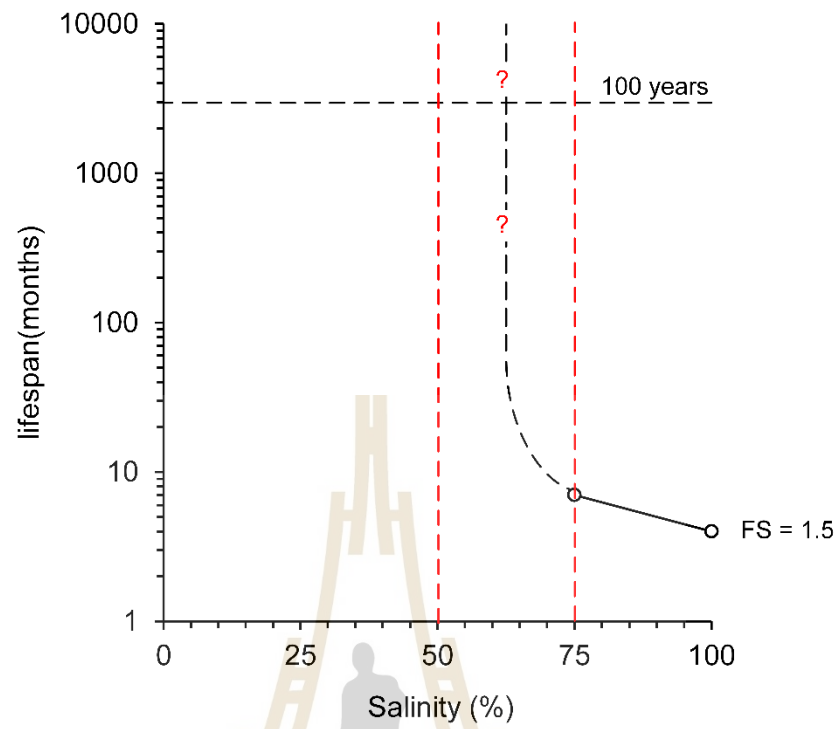
Figure 6.5   Relationships between lifespan for concrete and salinity (%).

CHAPTER VII

DISCUSSIONS AND CONCLUSIONS

7.1 Discussions

The presented results in Chapter V provide a comprehensive understanding of the time-dependent reduction in compressive strength of concrete under various concentrations of saline solutions. The study utilized a combination of tests, including uniaxial compression tests, X-ray diffraction (XRD) analysis, saline absorption tests, and ultrasonic pulse velocity tests, to assess the impact of saline exposure on concrete properties. The study highlights the importance of considering various factors, including mineral composition, elastic modulus, and dynamic properties, to comprehensively assess concrete behavior in saline environments. The key findings relevant to the test results are as follows.

The compressive strength of cured concrete rapidly increased during the first 7 days of the curing period and gradually reached its peak at the end of 28 days Gutteridge and Dalziel (1990). Subsequent immersion in saline solutions leads to a reduction in compressive strength, with higher concentrations causing more significant declines. The compressive strength exhibited a gradual decrease within the initial 0 to 3 months, followed by a notable acceleration in deterioration during the 6 to 12-month period. This time-dependent behavior emphasizes the importance of considering prolonged exposure when assessing the durability of concrete structures in saline environments. The study establishes a direct correlation between saline concentration and the reduction in compressive strength. This is evident in the observed trend where samples exposed to 100% saline concentration experience a faster and more pronounced reduction in compressive strength compared to those exposed to lower concentrations (Qasim et al., 2020). The concentration-dependent impact underscores the critical role of salinity levels in influencing the degradation of concrete. Several mechanisms contribute to the observed decrease in compressive

strength. The infiltration of chloride ions from saline solutions into the concrete matrix initiates chemical reactions with cementitious minerals, leading to the formation of deleterious compounds. The study indicates the potential formation of chloride-bearing phases like Friedel's salt and ettringite, contributing to the deterioration of the concrete structure (Yang et al., 2022).

Discrepancies in compressive strength values obtained through direct (uniaxial compression test) and indirect (Schmidt rebound hammer test) methods are highlighted. The indirect method consistently provides higher compressive strength values compared to the direct method. These variations can be attributed to differences in testing principles, assumptions, and techniques. Understanding these differences is essential for accurate assessment and interpretation of compressive strength data. The decrease in compressive strength is accompanied by a reduction in Young's modulus, indicating a decline in the material's stiffness. Higher salinity exacerbates this reduction, posing a potential long-term risk of enduring damage to the concrete structure. The interplay between compressive strength and Young's modulus provides insights into the overall mechanical behavior of the material under saline exposure.

The study investigates the impact of exposure to saline solutions on the mineral composition of concrete, focusing on dicalcium silicate (C_2S), tricalcium silicate (C_3S), tricalcium aluminate (C_3A), and tetracalcium aluminoferrite (C4AF). These minerals are crucial components that occur from the hydration reaction between water and cement, forming the primary constituents responsible for the strength and durability of concrete. As salinity increases, C_3S and C_2S content decreases, while C_3A and C_4AF increase. These alterations signify chemical reactions with chloride ions, indicating concrete degradation. C_3S and C_2S, vital components of Portland cement, undergo structural changes during immersion in saline, affecting concrete strength. Higher salinity leads to a decline in C_3S and C_2S, implying the formation of chloride-bearing compounds. Chloride ions react with C_3S and C_2S, contributing to the concrete matrix's deterioration. Additionally, C_3A and C_4AF increase with higher salinity, indicating hydration reactions. The study underscores the importance of understanding

mineralogical transformations in concrete exposed to saline environments for effective assessment and mitigation of structural degradation.

Saline absorption rapidly increased during the initial month and tends to stabilize, maintaining a relatively constant level over the subsequent 12 months. It decreases with an increase in saline concentration. Under high saline concentration, particularly at 100% (saturated brine), the concrete exhibits the lowest saline absorption. This may seem contradictory to the explanation that high concentrations cause high concrete corrosion, causing increased porosity to absorb more saline solution. This phenomenon occurs due to the crystallization of the saline solution within the voids of the samples under the highest saline concentration, which leads to a decrease in saline absorption. As a considerable quantity of salt crystallizes within the voids of the sample, the density of the sample rises proportionally to the increase in saline concentration. The results obtained here agree with those of Cao et al. (2019); Bai et al. (2021); Yang et al. (2022); and Vassuoni and Rahmam (2016) who study the absorption as affected by saline solution.

Both P- and S-wave velocities increase exponentially with increasing salinity. They move slowly through the sample when the wave propagates to mortar immersed in 0% of salinity (freshwater). On the other hand, they move with high speed when the wave propagates to mortar immersed in 100% salinity. This is due to reflection and refraction of wave velocity through the mortar sample which results in loss of wave energy. According to the reasons mentioned above, the samples immersed in a high saline concentration also have high density, resulting in a higher wave speed passing through the sample. The dynamic Poisson's ratio (ν_d) increases whereas the dynamic elastic moduli (E_d) decrease with increasing of saline concentration. The results obtained from this study are consistent with those of Su and Zhang (2014) and Rozgonyi-Boissinot et al. (2021) who studied the wave velocity as affected by saline water.

7.2   Conclusions

The effects of saline water on the mechanical properties of concrete are investigated based on uniaxial compressive strength, XRD, absorption, density, and wave velocity. All objectives and requirements of this study have been met. The results of laboratory testing and analyses can be concluded as follows:

1) The compressive strength of cured concrete increases rapidly during the initial 7 days of curing and gradually reaches its peak at 28 days. Subsequent immersion in saline solutions leads to a reduction in compressive strength, with higher concentrations causing more significant declines. The study reveals a time-dependent behavior, emphasizing the importance of prolonged exposure considerations in assessing concrete durability in saline environments.

2) A direct correlation between saline concentration and the reduction in compressive strength is established, with samples exposed to 100% saline concentration experiencing a faster and more pronounced decline compared to lower concentrations. Various mechanisms contribute to this reduction, including the infiltration of chloride ions, leading to chemical reactions and the formation of deleterious compounds.

3) Discrepancies in compressive strength values obtained through direct and indirect methods are highlighted, emphasizing the need for a nuanced interpretation of data. The decrease in compressive strength is accompanied by a reduction in Young's modulus, indicating a decline in material stiffness, exacerbated by higher salinity.

4) The study investigates the impact of saline exposure on the mineral composition of concrete, revealing alterations in C_2S, C_3S, C_3A, and C_4AF. These changes suggest chemical reactions with chloride ions, contributing to concrete degradation. Saline absorption trends indicate rapid increases in the initial month, stabilizing thereafter, and decreasing with higher saline

concentrations. The crystallization of saline solution within voids under the highest concentration leads to the lowest absorption.

5) Both P- and S-wave velocities increase exponentially with increasing salinity, showcasing variations in wave speed influenced by saline concentration. The dynamic Poisson's ratio increases, while dynamic elastic moduli decrease with rising salinity, consistent with prior studies.

6) The absorption characteristics and density of concrete under different saline water immersion conditions reveal noteworthy trends. Saline absorption tends to decrease, while density tends to increase with increasing saline concentration.

7) Empirical equations developed to correlate the relationship between the compressive strength of concrete and immersion time under various saline concentrations can be used to predict the lifespan of the concrete.

In summary, this study provides valuable insights into the multifaceted impact of saline exposure on concrete properties, emphasizing the need for a holistic understanding to assess and mitigate degradation in concrete structures in saline environments. The findings contribute to the existing body of knowledge and support informed decision-making in the realm of concrete engineering. The results align with previous studies, reinforcing the consistency and reliability of the observed trends in response to saline water exposure.

7.3 Recommendations for future studies

The experimental study focused on a single concrete and mortar mixture, limiting its representativeness to other concrete mixtures. Additionally, the test duration was confined to 12 months and conducted solely under immersion in saline water conditions. To enhance the accuracy and comprehensiveness of the analysis and conclusions, and acknowledging the limitations in sample numbers and test parameters employed in this study, the following recommendations for future studies are proposed:

1) To advance the understanding of concrete deterioration and enhance the reliability and accuracy of concrete's strength predictions, it is recommended that future studies focus on extending the duration of the testing period. A prolonged testing period will allow for a more in-depth analysis of the long-term effects of sample soaking time on concrete strength. This extended duration will capture subtle changes and potential trends that may not be evident in shorter-term experiments. Moreover, it will provide a more realistic representation of the concrete's behavior under varying environmental conditions, contributing to the robustness of the findings.

2) The concrete sample should be systematically prepared with variations in water/cement ratio (w/c), concrete admixture, cement type, and aggregate size. This approach aims to represent the variety of concrete for actual engineering structures.

3) To comprehensively investigate concrete deterioration, it is recommended to carry out experiments across diverse environmental conditions, encompassing changes in temperature, humidity, and cyclic wetting and drying cycles. This approach aligns with the goal of enhancing the realism and applicability of research findings to real-world construction scenarios.

4) Field studies should be conducted to verify the accuracy of the laboratory results in their application in actual concrete structures. This provides a connection between controlled laboratory conditions and real-world situations. It creates a more holistic understanding.

5) The depth of brine penetration into the concrete sample should be measured during immersion in the saline solution. The obtained test results offer valuable data that can be employed to precisely define the depth of reinforcement within the concrete structure.

6) The analysis of mineral composition by XRD analysis of concrete samples for each test condition (each immersion time and saline concentration) is

recommended immediately following the completion of the compression test. Suppose the samples cannot be tested immediately and must be left for several days. In this case, the potential for additional chemical reactions exists, leading to analysis results that may not accurately reflect the results of each test condition. The concrete samples should be dried thoroughly before testing. This drying process can stop any ongoing chemical reactions and ensure the test results are accurate for those conditions.

7) More measurement techniques should be conducted to assess various concrete deteriorations, such as visual examination for the presence of cracks on the concrete surface, inspection for the loss of surface material due to weathering or other environmental factors, use high-frequency sound waves to detect internal flaws, voids, or changes in material properties, utilizes radar pulses to detect subsurface features, such as cracks and void, assesses the concentration of chloride ions in concrete, as high levels can lead to reinforcement corrosion, and Utilizes techniques like scanning electron microscopy (SEM) to observe microstructural changes, including the formation of cracks and the deterioration of cement paste.

By addressing these recommendations in future studies, researchers can advance the understanding of concrete behavior under saline exposure, leading to more robust and applicable conclusions for the construction and maintenance of structures in saline environments

.

REFERENCES

Abalaka, A.E., & Babalaga, A.D. (2011). Effects of sodium chloride solutions on compressive strength development of concrete containing rice husk ash. *ATBU Journal of Environmental Technology*, 4(1): 33-40.

Abo-Qudais, S. A. (2005). Effect of concrete mixing parameters on propagation of ultrasonic waves. *Construction and Building Materials*, 19(4): 257-263.

Althoey, F. (2021). Compressive strength reduction of cement pastes exposed to sodium chloride solutions: secondary ettringite formation. *Construction and Building Materials*, 299(1): 123965.

Althoey, F., & Farnam, Y. (2020). Performance of calcium aluminate cementitious materials in the presence of sodium chloride. *Journal of Materials in Civil Engineering*, 32(10), 04020277.

American Society for Testing and Materials. (2020). *Annual Book of ASTM Standards: Standard Test Method for Compressive Strength of Hydraulic Cement Mortars (Using 2-in. or 50-mm Cube Specimens)* (Vol. 04.01). West Conshohocken, PA: ASTM International.

American Society for Testing and Materials. (2012). *Annual Book of ASTM Standards: Standard Specification for Portland Cement.* (Vol. 04.01). West Conshohocken, PA: ASTM International.

American Society for Testing and Materials. (2021). *Annual Book of ASTM Standards: Standard Test Method for Compressive Strength of Cylindrical Concrete Specimens* (Vol. 04.01). West Conshohocken, PA: ASTM International.

American Society for Testing and Materials. (1997). *Annual Book of ASTM Standards: Standard Test Method for Pulse Velocity Through Concrete* (Vol. 04.02). West Conshohocken, PA: ASTM International.

American Society for Testing and Materials. (2002). Annual Book of ASTM Standards: *Standard Test Method for Rebound Number of Hardened Concrete.* (Vol. 04.02). West Conshohocken, PA: ASTM International.

American Society for Testing and Materials. (2018). Annual Book of ASTM Standards: *Standard Test Method for Determination of the Proportion of Phases in Portland Cement and Portland-Cement Clinker Using X-Ray Powder Diffraction Analysis*. (Vol.04.01). West Conshohocken, PA: ASTM International.

American Society for Testing and Materials. (2013). Annual Book of ASTM Standards: *Standard Test Method for Measurement of Rate of Absorption of Water by Hydraulic Cement Concretes.* (Vol. 04.02). West Conshohocken, PA: ASTM International.

Bai, L., Xie, J., Liu, J., & Xie, Y. (2021). Effect of salt on hygroscopic properties of cement mortar. *Construction and Building Materials*, 305(1): 124746.

Barret, P., Ménétrier, D., & Bertrandie, D. (1983). Mechanism of C3S dissolution and problem of the congruency in the very initial period and later on. *Cement and Concrete Research*, 13(5), 728-738.

Bassuoni, M. T., & Rahman, M. M. (2016). Response of concrete to accelerated physical salt attack exposure. *Cement and concrete research*, 79(1): 395-408.

Bérubé, M. A., Dorion, J. F., Duchesne, J., Fournier, B., & Vézina, D. (2003). Laboratory and field investigations of the influence of sodium chloride on alkali–silica reactivity. *Cement and Concrete Research*, 33(1), 77-84.

Buyuksagis, I. S., & Goktan, R. M. (2007). The effect of Schmidt hammer type on uniaxial compressive strength prediction of rock. *International Journal of Rock Mechanics and Mining Sciences*, 44(2): 299-307.

Cao, Y., Guo, L., & Chen, B. (2019). Influence of sulfate on the chloride diffusion mechanism in mortar. *Construction and Building Materials*, 197(1): 398-405.

Chalee, W., Thikhawanich M., Jaturapitakkul, C., & Utsahpanich, P. (2007). The effect of seawater on compressive strength chloride permeation and corrosion of steel reinforcement in fly ash concrete in marine environment for 4 years. *KMUTT R&D Journal*, 30 (1): 153-166.

Chandra, S., & Xu, A. (1992). Influence of presaturation and freeze-thaw test conditions on length changes of Portland cement mortar. *Cement and concrete research*, 22(4), 515-524.

Dhondy, T., Xiang, Y., Yu, T., & Teng, J. G. (2021). Effects of mixing water salinity on the properties of concrete. *Advances in Structural Engineering*, 24(6): 1150-1160.

Fink, J. (2021). Petroleum engineer's guide to oil field chemicals and fluids. Gulf Professional Publishing. Texas, United States.

European standard. (2004). British-Adopted European Standard: *Desing of concrete structures- part 1-1: General rules and rules for buildings.* (EN 1992-1-1). Brussels, Belgium.

Gauffinet-Garrault, S. (2012). The rheology of cement during setting. Woodhead publishing. Sawston, Cambridge. 96-113p.

Goñi, S., Frías, M., de la Villa, R. V., & García, R. (2013). Sodium chloride effect on durability of ternary blended cement. Microstructural Characterization and Strength. *Composites Part B: Engineering*, 54(1): 163-168.

Gopalakrishnan, R., & Jeyalakshmi, R. (2020). The effects on durability and mechanical properties of multiple nano and micro additive OPC mortar exposed to combined chloride and sulfate attack. *Materials Science in Semiconductor Processing*, 106(1): 104772.

Guo, Q., Chen, L., Zhao, H., Admilson, J., & Zhang, W. (2018). The effect of mixing and curing sea water on concrete strength at different ages. *Proceedings of the MATEC Web of Conferences*. Les Ulis, France.

Gutteridge, W. A., & Dalziel, J. A. (1990). Filler cement: the effect of the secondary component on the hydration of Portland cement: part I. A fine non-hydraulic filler. *Cement and Concrete Research*, 20(5), 778-782.

Haynes, H., & Bassuoni, M. T. (2011). Physical salt attack on concrete. *Concrete international*, 33(11): 38-42.

He, P., Yu, J., Wang, R., Du, W., Han, X., Gu, S., & Liu, Q. (2020). Effect of ion chelator on pore structure, mechanical property, and self-healing capability of seawater exposed mortar. *Construction and Building Materials*, 246(1): 118480.

Homwuttiwong, S. (2016). Concrete abrasion and testing ASTM C1138 (under water method), *Thailand Concrete Association E-magazine*, 10: 1-9.

Islam, M. M., Islam, M. S., Mondal, B. C., & Islam, M. R. (2010). Strength behavior of concrete using slag with cement in sea water environment. *Journal of Civil Engineering (IEB)*, 38(2): 129-140.

Jahandari, S., Toufigh, M. M., Li, J., & Saberian, M. (2018). Laboratory study of the effect of degrees of saturation on lime concrete resistance due to the groundwater level increment. *Geotechnical and Geological Engineering*, 36(1): 413-424.

Koh, H. M., Park, W., & Choo, J. F. (2014). Lifetime design of long-span bridges. *Structure and Infrastructure Engineering*,10(4), 521-533.

Lee, B. Y., & Kurtis, K. E. (2017). Effect of pore structure on salt crystallization damage of cement-based materials: consideration of w/b and nanoparticle use. *Cement and Concrete Research*, 98(1): 61-70.

Liu, J., Tang, K., Qiu, Q., Pan, D., Lei, Z., & Xing, F. (2014). Experimental investigation on pore structure characterization of concrete exposed to water and chlorides. *Materials*, 7(9), 6646-6659.

Lyman, J. & Fleming, R. (1940). Composition of seawater. *Journal of Marine Research*, 3(1): 134-146.

Mbadike, E. M., & Elinwa, A. U. (2011). Effect of salt water in the production of concrete. *Nigerian Journal of Technology*, 30(2): 105-110.

Ming, F., Du, C., Liu, Y., Shi, X., & Li, D. (2017). Concrete durability under different circumstances based on multi-factor effects. *Sciences in Cold and Arid Regions*, 9(4): 384-391.

Nadelman, E. I., & Kurtis, K. E. (2019). Durability of Portland-limestone cement-based materials to physical salt attack. *Cement and Concrete Research*, 125: 105859.

Neamluang, T., Khwankaew, J., Rujiphonphiphat, J., Samphao, W., & Onura, W. (2018). The study of effects of saline water on irrigation structures: a case study of Chonlahan Phichit operation and maintenance project. *Chonlasarn Research Journal of Irrigation Management*, 6(1): 52-62.

Nehdi, M. L., Suleiman, A. R., & Soliman, A. M. (2014). Investigation of concrete exposed to dual sulfate attack. *Cement and Concrete Research*, 64, 42-53.

Nelson, E. & Guillot, D. (2006). Oilwell Cementing. Schlumberger publications. 773p.

Nonat A, & Mutin JC. (1992). From hydration to setting. *Proceedings of the International RILEM Workshop*. London, England.

Qasim, O. A., Maula, B. H., Moula, H. H., & Jassam, S. H. (2020). Effect of salinity on concrete properties. *Materials Science and Engineering*, 745(1): 012171.

Qiao, C., Suraneni, P., & Weiss, J. (2018). Damage in cement pastes exposed to NaCl solutions. *Construction and Building Materials*, 171, 120-127.

Riley, K. F., Hobson, M. P., & Bence, S. J. (1998). Mathematical methods for physics and engineering: a comprehensive guide. Cambridge University Press. Sawston, Cambridge.

Rodrigues, A. S. (2014). Deterioration of Concrete. *Journal of Civil Engineering and Environmental Technology*, 1(4): 14-19.

Rozgonyi-Boissinot, N., Khodabandeh, M. A., Besharatinezhad, A., & Török, Á. (2021). Salt weathering and ultrasonic pulse velocity: condition assessment of salt damaged porous limestone. *Earth and Environmental Science*, 833(1): 012070.

Sakr, M., & Bassuoni, M. T. (2019). Surface treatments for concrete under physical salt attack. *Proceedings of the Sixth International Conference on the Durability of Concrete Structures.* Leeds, United Kingdom.

Saleh, F. K., Teodoriu, C., & Sondergeld, C. H. (2019). Investigation of the effect of cement mixing energy on cement strength and porosity using NMR and UPV methods. Journal of Natural Gas Science and Engineering, 70, 102972.

Shi, X., Fay, L., Gallaway, C., Volkening, K., Peterson, M., Pan, T., & Nguyen, T. A. (2009). Evaluation of alternative anti-icing and deicing compounds using sodium chloride and magnesium chloride as baseline deicers, phase I. *Proceedings of the Colorado Department of Transportation*. Denver, United States of America.

Shi, X., Fay, L., Peterson, M. M., Berry, M., & Mooney, M. (2011). A FESEM/EDX investigation into how continuous deicer exposure affects the chemistry of Portland cement concrete. *Construction and building materials*, 25(2), 957-966.

Shoukry, S. N., William, G. W., Downie, B., & Riad, M. Y. (2011). Effect of moisture and temperature on the mechanical properties of concrete. *Construction and Building Materials*, 25(2), 688-696.

Su, X. P., & Zhang, L. (2014). Comparing tests on the durability of concrete after long-term immersion in different salt solution. *Applied Mechanics and Materials*, 501, 1087-1091.

Sui, S., Wang, F., Wu, M., Li, S., Liu, Z., Gao, S., & Jiang, J. (2023). Influence of sodium chloride on the hydration of C3S blended paste. *Construction and Building Materials*, 369, 130543.

Sutter, L., Van Dam, T., Peterson, K. R., & Johnston, D. P. (2006). Long-term effects of magnesium chloride and other concentrated salt solutions on pavement and structural Portland cement concrete. *Transportation Research Record*, 1979(1), 60-68.

Taylor, M.A. (1978). Effects of ocean salts on the compressive strength of concrete, *Cement and Concrete Research*, 8 (4): 491-500.

Teller, L. W. (1956). Elastic properties, in significance of tests and properties of concrete and concrete aggregates. *ASTM Special Technical Publication*, 169(1): 94-103.

Thongwat, W., & Terakulsatit, B. (2019). Using GIS and map data for the analysis of the relationship between soil and groundwater quality at saline soil area of Kham Sakaesaeng district, Nakhon Ratchasima, Thailand. *International Journal of Materials and Metallurgical Engineering*, 13(1): 32-39.

Tiwari, P., Chandak, R., & Yadav, R. (2014). Effect of salt water on compressive strength of concrete. I*nternational Journal of Engineering Research and Applications*, 4(4): 38-42.

Valenza, J.J., Vitousek, S., & Scherer, G.W. (2005). Expansion of hardened cement paste in saline solutions, creep, shrinkage and durability mechanics of concrete and other quasi-brittle materials, *Proceedings of the Hermes Science*, London, United Kingdom.

Wang, Y., Ueda, T., Gong, F., & Zhang, D. (2019). Meso-scale mechanical deterioration of mortar due to sodium chloride attack. *Cement and Concrete Composites*, 96, 163-173.

Wendai, L. (2000). Regression analysis, linear regression and profit regression. 13chapters. *SPSS for Windows: statistical analysis: Publishing House of Electronics Industry*, Beijing, China.

Xie, Y., Xie, J., Bai, L., & Liu, J. (2023). Experimental study on the effect of salt on the water absorption characteristic of cement mortar. *Journal of Building Engineering*, 73, 106693.

Xiong, L. X., & Yu, L. J. (2015). Mechanical properties of cement mortar in sodium sulfate and sodium chloride solutions. *Journal of Central South University*, 22(3): 1096-1103.

Yang, D., Yan, C., Liu, S., Jia, Z., & Wang, C. (2022). Prediction of concrete compressive strength in saline soil environments. *Materials*, 15(13): 4663.
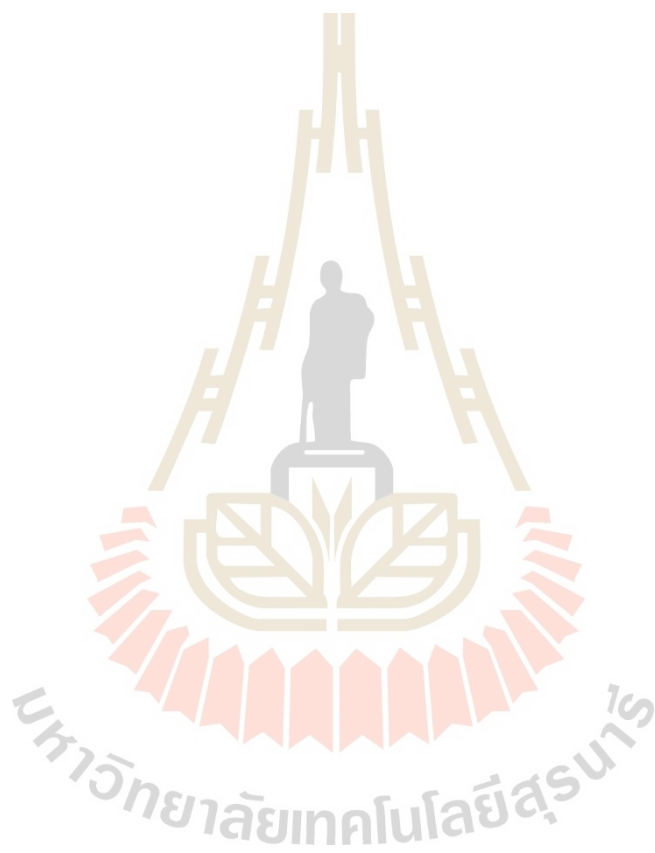
APPENDIX A

LIST OF PUBLICATION
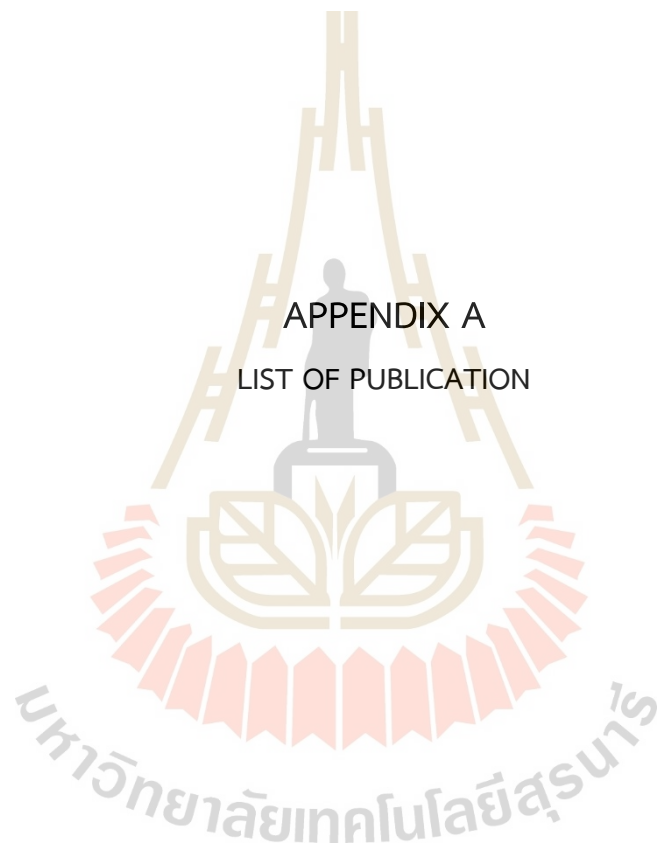
บทความวิจัย

ผลกระทบจากความเค็มของน้ำเกลือต่อคุณสมบัติทางกลศาสตร์ของคอนกรีต
Effects of Salinity of Salt Water on Mechanical Properties of Concrete

บุรินทร์ ทองเกลี้ยง,* เดโช เผือกภูมิ และ กิตติเทพ เฟื่องขจร

สาขาวิชาเทคโนโลยีธรณี สำนักวิชาวิศวกรรมศาสตร์ มหาวิทยาลัยเทคโนโลยีสุรนารี

111 ถนนมหาวิทยาลัย ตำบลสุรนารี อำเภอเมืองนครราชสีมา จังหวัดนครราชสีมา 30000, E-mail: Burin1997th@gmail.com

บทคัดย่อ

วัตถุประสงค์ของงานวิจัยนี้คือ เพื่อประเมินผลกระทบจากความเค็มของน้ำเกลือ (สารละลายโซเดียมคลอไรด์) และระยะเวลาในการสัมผัสกับน้ำเกลือต่อสมบัติทางวิศวกรรมของคอนกรีต ตัวอย่างคอนกรีตและมอร์ต้าร์ที่ผ่านการบ่มเป็นเวลา 28 วัน ถูกนำไปแช่ในน้ำเกลือที่มีระดับความเค็มเท่ากับ 0%, 25%, 50%, 75% และ 100% เป็นระยะเวลา 0, 1, 2, 3, และ 6 เดือน ตามลำดับ หลังจากนั้นจึงนำตัวอย่างคอนกรีตไปทดสอบเพื่อหากำลังอัดและวัดความสามารถในการดูดซับน้ำเกลือของตัวอย่างมอร์ต้าร์ ผลการทดสอบพบว่ากำลังอัดกำลังอัดของคอนกรีตมีค่าลดลงอย่างต่อเนื่องตามระยะเวลาที่เพิ่มขึ้น และผลกระทบดังกล่าวจะยิ่งรุนแรงขึ้นเมื่อตัวอย่างถูกแช่น้ำเกลือที่มีระดับความเค็มสูงขึ้น นอกจากนี้ยังพบว่าความสามารถในการดูดซับน้ำของตัวอย่างมอร์ต้าร์มีค่าเพิ่มขึ้นตามระยะและระดับความเค็มที่เพิ่มขึ้น ผลการทดสอบการเลี้ยวเบนด้วยรังสีเอ็กซ์ยังระบุว่าแร่ที่เป็นผลผลิตของปฏิกิริยาไฮเดรชันมีการเปลี่ยนแปลงเมื่อตัวอย่างแช่ในน้ำเค็มนานขึ้น ซึ่งเหล่านี้สนับสนุนว่าตัวอย่างคอนกรีตเกิดการกัดกร่อนด้วยน้ำเค็มอย่างต่อเนื่องจนมีผลทำให้เกิดการเสื่อมสภาพในเชิงเวลา

คำสำคัญ : ความเค็ม; กำลังอัด; ความทนทานของคอนกรีต; การดูดซับน้ำ; การวิเคราะห์การเลี้ยวเบนด้วยรังสีเอ็กซ์

Abstract

The purpose of this study is to assess the effects of salinity of saline water (NaCl solution) and duration of exposure to saline water on the engineering properties of concrete. Concrete and mortar samples cured for 28 days were immersed in saline water with different salinity levels of 0%, 25%, 50%, 75%, and 100% for 0, 1, 2, 3, and 6 months, respectively. Then, the concrete samples were tested to determine the compressive strength and the mortar samples were measured the ability to absorb saline water. The test results showed that the compressive strength of concrete continuously decreased with increasing time. This effect tends to be severe when the samples were immersed in saline water with higher salinity levels. It was also found that the water absorption of the mortar samples increased with increasing immersed time and salinity. The X-ray diffraction test also indicated that the minerals involved in the hydration reaction changed with prolonged immersion in saline water. These allow the concrete samples to undergo continuous

Keywords: Salinity; Compressive strength; Concrete durability; Water absorption; X-ray diffraction analysis.

1. บทนำ

คอนกรีตถูกนำมาใช้อย่างแพร่หลายตั้งแต่อดีตจนถึงปัจจุบัน เนื่องจากเป็นวัสดุที่เหมาะสมทั้งในด้านราคาและคุณสมบัติด้านกำลังอัดสูง คอนกรีตถูกนำมาใช้ในงานก่อสร้างหลายประเภท ทั้งอาคาร ถนน เขื่อน สะพาน อนุสาวรีย์ และงานก่อสร้างอื่น ๆ ที่สามารถพบเห็นได้ในงานก่อสร้างทั่วไป โครงสร้างคอนกรีตที่เสื่อมสภาพจะแสดงอาการดังต่อไปนี้ แตกร้าว สีซีด สึกกร่อน โก่งงอ และสึกกร่อน โดยที่ปัจจัยหลักที่มีผลต่อการเสื่อมสภาพของคอนกรีตที่พบบ่อยที่สุด คือ ปัจจัยด้านสิ่งแวดล้อมที่นำไปสู่การสึกกร่อนของคอนกรีต [1] และอาจพบเห็นได้ชัดเจนกับโครงสร้างที่สัมผัสกับน้ำเค็มบริเวณชายทะเล Tiwari et al. [2] และ Islam et al. [3] ได้ระบุว่าความเค็มของน้ำทะเลทั่วโลกเฉลี่ยประมาณ 3.5% (35 g/L)

นอกจากสภาพความเค็มของน้ำทะเลแล้วนั้น ความเค็มของชั้นดินและผิวดินที่กระจายตัวในพื้นที่ภาคอีสานของประเทศไทย ซึ่งเป็นผลจากการที่ภาคอีสานมีชั้นเกลือและโดมเกลือ รวมถึงมีการทำนาเกลืออีกด้วย [4] ส่งผลให้พื้นที่ดังกล่าวมีน้ำเค็มจากสารละลายโซเดียมคลอไรด์ โดยที่ Lyman and Fleming [5] พบว่าเกลือส่วนใหญ่เป็นโซเดียมคลอไรด์ (NaCl) โดยที่คลอไรด์ไอออนสามารถแพร่ซึมผ่านเนื้อคอนกรีตแล้วทำปฏิกิริยาระหว่างปูนซีเมนต์ และมวลรวม Bassuoni and Rahman [6] อธิบายไว้ว่าปัจจัยที่ส่งผลต่อการเสื่อมสภาพจากการตกผลึกของเกลือในวัสดุที่มีรูพรุน ได้แก่ ชนิดและความเข้มข้นของเกลือ การเปลี่ยนแปลงเฟสไฮเดรชันของเกลือ อัตราการระเหย แรงตึงผิว ความดันไอ สภาวะแวดล้อม และคุณสมบัติรูพรุน ปัจจัยเหล่านี้ก่อให้คอนกรีตที่ใช้ในการก่อสร้างเกิดการเสื่อมสภาพ โดยการเสื่อมสภาพอาจส่งผลต่องานคอนกรีตในระยะยาว [7]

ในการศึกษานี้มีวัตถุประสงค์เพื่อ ประเมินการเสื่อมสภาพของคอนกรีตอันเป็นผลมาจากความเค็มหรือสภาพความเป็นคลอไรด์ ซึ่งเป็นสาเหตุให้คุณสมบัติทางกายภาพและกลศาสตร์มีการเปลี่ยนแปลง และเป็นสาเหตุต่อเนื่องที่ทำให้โครงสร้างทางวิศวกรรมเกิดการวิบัติ ดังนั้นจึงจำเป็นต้องมีศึกษาผลกระทบการเสื่อมสภาพของคอนกรีตจนทำให้คุณสมบัติทางกายภาพและทางกลศาสตร์ ได้แก่ กำลังอัดของคอนกรีต การดูดซับน้ำเกลือ ความเร็วคลื่น และการเปลี่ยนแร่องค์ประกอบ เมื่ออยู่ในสภาวะที่สัมผัสกับน้ำบาดาลเค็มแบบตลอดเวลา (เป็นสภาวะที่อยู่ใต้ระดับน้ำบาดาลเค็ม) การทดสอบได้มีการแปรผันความเข้มข้นน้ำเกลือตั้งแต่ 0% ถึง 100% โดยตัวอย่างจะถูกแช่ในน้ำเค็มเป็นเวลา 0 ถึง 6 เดือน ตามลำดับ ผลที่ได้จะนำมาสร้างสมการทางคณิตศาสตร์เพื่อประเมินกำลังของกรีตที่สัมผัสกับน้ำใต้ดินที่มีความเค็มและเวลาที่แตกต่างกัน

2. วัสดุ อุปกรณ์ และวิธีการวิจัย
2.1 ตัวอย่างคอนกรีต มอร์ตาร์ และน้ำเกลือ

ตัวอย่างคอนกรีตทรงกระบอกที่มีขนาดเส้นผ่าศูนย์กลาง 15 เซนติเมตรและยาว 30 เซนติเมตร ซึ่งผสมจากปูนซีเมนต์ปอร์ตแลนด์สามัญ (ประเภทที่ 1) กับมวลรวมละเอียด มวลรวมหยาบ และน้ำ ตามลำดับ ซึ่งการจัดเตรียมตัวอย่างเป็นไปตามมาตรฐานผลิตภัณฑ์อุตสาหกรรม (มอก. 15 เล่ม 1) โดยคิดเป็นอัตราส่วนซีเมนต์-มวลรวมละเอียด-มวลรวมหยาบ-น้ำ เท่ากับ 1:2:4:0.5 โดยน้ำหนัก โดยตัวอย่างเมื่อเทเข้าไปในแบบหล่อคอนกรีต จะถูกทิ้งไว้ให้ก่อตัวเป็นเวลา 24 ชั่วโมง แล้วทำการแกะแบบและนำตัวอย่างไปบ่มในน้ำจืดระยะเวลา 28 วัน

ตัวอย่างมอร์ตาร์มีรูปทรงสี่เหลี่ยมขนาด 5×5×5 ลูกบาศก์เซนติเมตร โดยทำการผสมปูนซีเมนต์ปอร์ตแลนด์สามัญ (แบบที่ 1) กับมวลรวมที่ละเอียด (ทราย) และน้ำ โดยคิดเป็นอัตราส่วนซีเมนต์-ทราย-น้ำ เท่ากับ 1:2.75:0.5 ตัวอย่างในกลุ่มนี้เมื่อหล่อในแบบแล้ว ทำการเกาะออกจากแบบหลังจาก 24 ชั่วโมง และบ่มเป็นระยะเวลา 28 วัน เช่นเดียวกับตัวอย่างคอนกรีต

น้ำเกลือที่ใช้ในการทดสอบได้จากการนำเกลือสินเธาว์ที่ผลิตได้ในพื้นที่จังหวัดนครราชสีมา ละลายในน้ำจืดให้มีความเข้มข้นหลายระดับ ได้แก่ 0% (น้ำจืด), 25%, 50%, 75% และ 100% (น้ำเกลือเข้มข้น) ในสัดส่วนของเกลือสินเธาว์ 0.00, 89.75, 179.50, 269.25 และ 359.00 กรัม/ลิตร ตามลำดับ ระหว่างการทดสอบ ระดับความเค็มของน้ำเกลือได้มีการตรวจวัดโดยใช้เครื่องวัดความเค็ม (Salinity Refractometer) อย่างต่อเนื่อง ซึ่งจะดำเนินการทุก 1 สัปดาห์

2.4 เครื่องมือและวิธีการทดสอบ

ตัวอย่างคอนกรีตและมอร์ตาร์ที่ผ่านการบ่มในน้ำจืดเป็นเวลา 28 วัน เพื่อสอดคล้องกับสภาพแวดล้อมหลังการก่อสร้างที่ต้องบ่มอย่างน้อย 7 วัน โดยตัวอย่างคอนกรีตและมอร์ตาร์ถูกนำไปแช่ในน้ำเกลือที่ระดับความเข้มข้นแตกต่างกันเป็นระยะเวลา 0, 1, 2,3 และ 6 เดือน เมื่อครบระยะเวลาที่กำหนด ตัวอย่างจะถูกนำมาทดสอบเพื่อหา 1) กำลังกดในแกนเดียว (Uniaxial compressive strength, UCS) 2) กำลังกดในแกนเดียวด้วยวิธี Schmidt Rebound Hammer 3) การทดสอบเพื่อปริมาณแร่องค์ประกอบที่เปลี่ยนไปด้วยเทคนิควิเคราะห์การเลี้ยวเบนของรังสีเอ็กซ์หรือ X-ray Diffractometer (XRD) ในการทดสอบ จะทำการเก็บชิ้นส่วนของคอนกรีต (ไม่เอาหิน) จากตัวอย่างที่แตกบดให้ได้ขนาดแล้วค่อยนำไปทดสอบต่อไป 4) การทดสอบเพื่อวัดความสามารถในการดูดซับน้ำเกลือ (saline absorption) ในการทดสอบสอบจะใช้ตัวอย่างมอร์ตาร์ และ 5) การทดสอบเพื่อประเมินความเร็วในการเคลื่อนตัวของคลื่น โดยการทดสอบนี้ดำเนินการทดสอบกับตัวอย่างมอร์ตาร์เช่นเดียวกัน

3. ผลการทดสอบ
3.1 กำลังกดในแกนเดียว

ในการทดสอบแบ่งการทดสอบออกเป็น 2 แบบ คือการหากำลังกดในแกนเดียว (ASTM C39) [8] และการหากำลังกดด้วยวิธี Schmidt Rebound Hammer (ASTM C805) [9] ได้การคำนวณหากำลังรับแรงอัดของคอนกรีตและระยะเวลาการแช่น้ำเค็มที่มีการแปรผันระดับความเข้มข้น 0% ถึง 100% จนได้ความสัมพันธ์ระหว่างกำลังกดแกนเดียวและระยะเวลาการแช่ที่แปรผันระดับความเข้มข้นในรูปที่ 1 และรูปที่ 2 ตามลำดับ
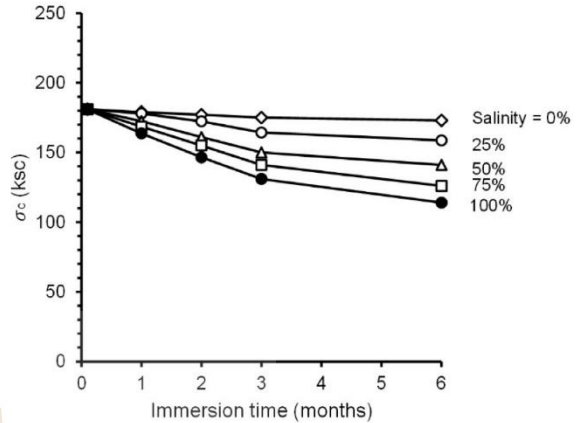
รูปที่ 1 ความสัมพันธ์ระหว่างกำลังกดแกนเดียวและระยะเวลาการแช่ที่แปรผันระดับความเข้มข้น
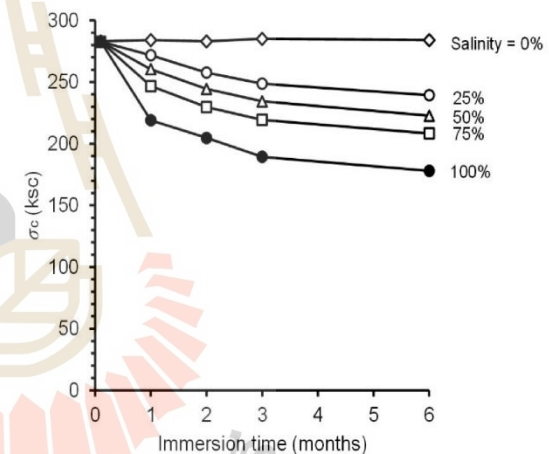
รูปที่ 2 ความสัมพันธ์ระหว่างกำลังกดแกนเดียวด้วยวิธี Schmidt Rebound Hammer และระยะเวลาการแช่ที่แปรผันระดับความเข้มข้น

จากรูปจะเห็นได้ว่า กำลังกดอัดของคอนกรีตลดลงเชิงเวลาและยิ่งความเข้มข้นเพิ่มขึ้นกำลังกดแกนเดียวลดลงอย่างมาก ซึ่งผลการทดสอบทั้ง 2 แบบมีความสอดคล้องกัน โดยการทดสอบด้วย Schmidt Rebound Hammer ให้กำลังกดมากกว่า UCS ถึง 1.6 เท่า บริเวณที่มีปริมาณคลอไรด์สูง Neamluang et.al. [10] พบการลดลงของกำลังกดแกนเดียวเป็นผลมาจากลักษณะการสลายตัวของคอนกรีต เป็นเหตุผลที่ความเข้มข้น 0 % (น้ำจืด) ถูกกัดกร่อนน้อยกว่าความเข้มข้นอื่นๆ ซึ่งสอดคล้องกับ Qasim et al. [11] ได้ระบุว่ากำลังรับแรงอัดของคอนกรีตลดลงตามปริมาณเกลือที่เพิ่มขึ้น เนื่องมาจากเกลือค่อยๆ เข้าไปตกผลึกในรูพรุนอย่างต่อเนื่อง การเปลี่ยนแปลงปริมาตรภายในตัวอย่างคอนกรีตด้วยผลึกเกลือ ทำให้คอนกรีตแสดงลักษณะการหลุดร่อนและการร่วนเนื่องจากการขยายตัวของปริมาตร ส่งผลให้เกิดการวิบัติ โดยสังเกตได้ว่าระยะเวลา

ที่แช่น้ำเกลือมากขึ้น กำลังรับแรงอัดของคอนกรีตยิ่งลดลง กำลังรับแรง
ของคอนกรีตเพิ่มขึ้นสำหรับปริมาณเกลือต่ำและกำลังรับแรงลดลง
สำหรับปริมาณเกลือสูง

    เมื่อได้ความสัมพันธ์ระหว่างกำลังกดแกนเดียวและระยะเวลา
การแช่ที่แปรผันระดับความเข้มข้น จะเห็นได้ว่ากำลังรับแรงอัดแกนเดียว
ลดลงแบบลอการิทึม จึงได้มีการพัฒนาสมการให้สอดคล้องกับผลการ
ทดสอบกำลังกดแกนเดียว เพื่อทำนายกำลังกดแกนเดียวเชิงเวลาที่มีการ
แปรันระดับความเข้มข้นของน้ำเกลือ จากรูปที่ 3 สมการทางคณิตศาสตร์
ระหว่างกำลังกดแกนเดียวในคอนกรีตและระยะเวลาการแช่ที่แปรผัน
ระดับความเข้มข้นดังสมการที่ (1)

$$\sigma_c = A \cdot \ln(x) + B \qquad (1)$$

โดยที่ σ_c คือ กำลังกดแกนเดียวสูงสุด
          A และ B คือ ค่าคงที่
          x คือ ระยะเวลาการแช่น้ำเกลือ

    ความเหมือน (Mean misfit) และความคลาดเคลื่อน
(R-squared) ระหว่างผลการทดสอบและการคาดการณ์ของสมการ
สามารถประเมินได้โดยใช้ค่าเฉลี่ยที่ไม่เหมาะสมเป็นตัวบ่งชี้ คำนวณโดย
[12] ดังในสมการที่ (2)

$$s = \frac{1}{m}\left(\sum_i^m s_i\right) \qquad (2)$$

เมื่อ $s_i = \left[\left(\frac{1}{n}\right)\left(\sum_{j=1}^n \left(X_{j,p} - X_{j,t}\right)^2\right)\right]^{1/2} \qquad (3)$

โดยที่ $X_{j,p}$ และ $X_{j,t}$ คือ กำลังรับแรงอัดแกนเดียวที่คาดการณ์และวัดได้
n คือ จำนวนของเดือนที่ใช้สำหรับการแช่ตัวอย่างคอนกรีต และ m คือ
จำนวนของความเข้มข้น

    เมื่อนำสมการที่ (1) มาคาดการณ์กำลังกดแกนเดียวในอนาคต
จากนั้นคำนวณจากสมการที่ 2 ซึ่งสามารถทราบค่า Mean misfit ได้เท่ากับ
5.11 และค่าความคลาดเคลื่อนเท่ากับ 0.907 สามารถใช้สมการที่ (1) ใน
การคาดการณ์กำลังกดแกนเดียวในอนาคตได้ เมื่อโครงสร้างคอนกรีตถูก
แช่น้ำเกลือที่ความเข้มข้นต่าง ๆ

3.2 X-Ray Diffractometer (XRD)

    เทคนิควิเคราะห์การเลี้ยวเบนของรังสีเอ็กซ์ (XRD) ถูก
นำมาใช้วิเคราะห์เพื่อระบุปริมาณของสารประกอบ (แร่ประกอบ) ใน
ตัวอย่างคอนกรีตที่สัมผัสกับน้ำเกลือที่ระดับความเข้มข้นและเวลาต่าง ๆ
กัน ในการทดสอบได้สนใจสารประกอบแคลเซียมซิลิเกต (C_3S, C_2S)
ไตรแคลเซียมอะลูมิเนต (C_3A) เตตระแคลเซียมอะลูมิโนเฟอร์ไรต์
(C_4AF) และแฮไลท์ (NaCl) ตามลำดับ ผลที่ได้สรุปไว้ในตารางที่ 1 จาก
ผลการทดสอบพบว่า C_3S และ C_2S มีแนวโน้มลดลงเมื่อระยะเวลาที่

สัมผัสกับน้ำเกลือนานขึ้น ซึ่งสิ่งนี้สนับสนุนว่าคอนกรีตถูกกัดกร่อนจาก
น้ำเกลือจนทำให้สารประกอบเหล่านี้มีค่าลดลงในเชิงเวลา

$\sigma_c = A \times \ln(\text{Immersion time}) + B$
$R^2 = 0.905$

A = [-0.1415 × ln (%salinity)] -1.9624
B = [-0.2673 × ln (%salinity)] +177.82

Salinity = 0 %
25 %
50 %
75 %
100 %
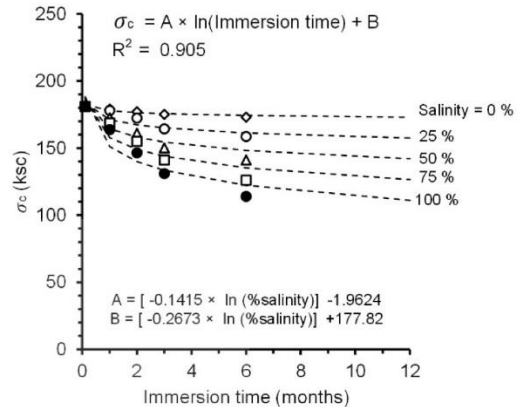
รูปที่ 3 ความสัมพันธ์ระหว่างสมการคณิตศาสตร์กำลังกดแกนเดียวและ
ระยะเวลาการแช่ที่แปรผันระดับความเข้มข้น

ตารางที่ 1 แร่องค์ประกอบของตัวอย่างคอนกรีตตามระยะเวลาแช่น้ำเกลือ

Salinity (%)	ระยะเวลา (เดือน)	แร่องค์ประกอบ (%)				
		C_3S	C_2S	C_3A	C_4AF	Halite
	initial	58.62	35.77	3.66	1.95	0.00
	1	58.58	35.41	3.98	2.03	0.00
0	2	58.25	34.66	4.64	2.45	0.00
	3	58.02	33.84	5.24	2.9	0.00
	6	57.34	32.73	6.37	3.56	0.00
	initial	58.62	35.77	3.66	1.95	0.00
	1	58.38	33.41	4.00	2.19	2.02
25	2	58.14	31.38	5.06	2.9	2.52
	3	57.88	29.13	6.97	3.02	3.00
	6	56.98	28.09	7.33	3.88	3.72
	initial	58.62	35.77	3.66	1.95	0.00
	1	58.23	32.06	4.21	2.29	3.21
50	2	57.9	29.48	5.48	2.94	4.2
	3	57.28	27.89	7.20	3.20	4.43
	6	55.39	27.44	7.96	3.95	5.26
	initial	58.62	35.77	3.66	1.95	0.00
	1	58.03	30.54	5.17	2.37	3.89
75	2	57.70	29.07	5.64	3.23	4.36
	3	56.33	27.8	7.69	3.62	4.56
	6	54.21	26.8	8.43	4.67	5.89
	initial	58.62	35.77	3.66	1.95	0.00
	1	57.07	30.51	5.61	2.68	4.13
100	2	56.87	28.57	6.38	3.72	4.46
	3	55.63	27.65	7.35	3.97	5.40
	6	53.51	25.65	9.05	5.08	6.71

บทความวิจัย

การประชุมวิชาการวิศวกรรมศาสตร์และเทคโนโลยี มทร.พระนคร ครั้งที่ 7
Proceedings of the 7th RMUTP Conference on Engineering and Technology

3.3 การดูดซับน้ำเกลือ

ในการทดสอบนี้ จะใช้ตัวอย่างลูกบาศก์มอร์ตาร์จำนวน 5 ตัวอย่างที่แช่ในน้ำเกลือที่มีการแปรผันระดับความเข้มข้น (0%, 25%, 50%, 75%, และ 100%) ตลอดระยะเวลา 6 เดือน โดยตัวอย่างมอร์ตาร์ที่ถูกแช่ในน้ำเกลือ เรียกว่ามวลอิ่มตัว จากนั้นนำตัวอย่างอบในเตาอบที่อุณหภูมิ 80±5 °C จนกระทั่งความแตกต่างของมวลในช่วงเวลา 24 ชั่วโมง สามารถคำนวณการดูดซับน้ำเกลือได้ดังสมการที่ (4)

$$\%Absorption = \frac{W - D}{D} \times 100 \qquad (4)$$

โดยที่ W คือ น้ำหนักตัวอย่างมอร์ตาร์ที่แช่ในน้ำเกลือมวลอิ่มตัวผิวแห้ง และ D คือ น้ำหนักแห้งของตัวอย่างมอร์ตาร์

จากรูปที่ 4 ความสัมพันธ์ระหว่างเปอร์เซ็นต์การดูดซับน้ำและระยะเวลาการแช่น้ำเกลือที่มีการแปรผันระดับความเข้มข้นในช่วงเดือนที่ 0-1 เปอร์เซ็นต์การดูดซับน้ำเกลือจะเพิ่มขึ้นอย่างเห็นได้ชัด หลังจากเดือนที่ 1 เปอร์เซ็นต์การดูดซับน้ำเกลือจะค่อย ๆ เพิ่มขึ้นเชิงเวลา เมื่อพิจารณาที่ความเข้มข้น 0% ซึ่งไม่มีผลึกเกลือเข้าไปทดแทนในช่องว่างจึงทำให้มีเปอร์เซ็นต์การดูดซับน้ำมากกว่าความเข้มข้นอื่น และเมื่อได้พิจารณาที่ความเข้มข้น 100% พบว่ามีเปอร์เซ็นต์การดูดซับน้ำน้อยสุด Choi et al. [13] โดยทั่วไปการดูดซับจะลดลง เมื่อสัมผัสกับสภาพน้ำเกลือเมื่อเทียบกับสภาพน้ำประปา เนื่องจากมีผลึกเกลือเข้าไปแทรกตัวในช่องว่างของตัวอย่างปูนมอร์ตาร์ จึงเป็นเหตุผลที่ว่าเกลือเข้าไปตกผลึกในช่องว่าง ทำให้เกิดการดูดซับน้ำน้อย เมื่อผลึกเกลือเข้าไปในตัวอย่างมากขึ้นเท่าใด ตัวอย่างมอร์ตาร์เกิดการเสื่อมสภาพอันเนื่องมาจากปริมาตรของมอร์ตาร์เพิ่มขึ้นด้วยผลึกของเกลือ จึงเป็นสาเหตุให้กำลังกดแกนเดียวมีกำลังรับแรงลดลงเมื่อความเข้มข้นน้ำเกลือเพิ่มขึ้น

3.4 การทดสอบความเร็วคลื่น

ในการทดสอบความเร็วของคลื่น (Pulse velocity) ผ่านวัสดุที่เป็นของแข็งหรือเนื้อคอนกรีต (ASTM C597-97) [14] จะมีคลื่นที่สร้างขึ้นจากเครื่องกำเนิดคลื่น 2 ชนิด ได้แก่ คลื่นปฐมภูมิ (Primary wave หรือ P-wave) และคลื่นทุติยภูมิ (Secondary wave หรือ S-wave) ความเร็วคลื่นของทั้งสองในคอนกรีตชนิดต่าง ๆ จะกำหนดโดยคุณสมบัติเชิงกลศาสตร์และคุณสมบัติทางกายภายของหินนั้น ๆ ซึ่งคำนวณโดยใช้สมการ (5) และ (6)

$$V_P = \sqrt{\frac{\lambda + 2G}{\rho}} \qquad (5)$$

$$V_S = \sqrt{\frac{G}{\rho}} \qquad (6)$$

โดยที่ V_P และ V_S คือ ความเร็วคลื่นปฐมภูมิและคลื่นทุติยภูมิ ตามลำดับ λ และ G คือ ค่า Lame's constants และ ρ คือ ความหนาแน่นของคอนกรีต

จากรูปที่ 5 ความสัมพันธ์ระหว่างความเร็วคลื่น (P-wave และ S-wave) และระยะเวลาแช่น้ำเกลือ ที่เคลื่อนที่ผ่านตัวอย่างมอร์ตาร์มีค่าเพิ่มขึ้นตามระยะเวลาที่สัมผัสกับน้ำเค็มนานขึ้น ผลกระทบนี้จะเด่นชัดขึ้นที่ระดับความเข้มข้นสูง สอดคล้องกับผลการทดสอบของ Ramírez-Ortíz et al. [15] กล่าวว่า เมื่อความเข้มข้นเพิ่มขึ้น ความหนืดเพิ่มขึ้นเช่นกัน ส่งผลให้ความเร็วคลื่นเพิ่มขึ้นแบบเชิงเส้น จากรูปที่ 6 เมื่อความหนาแน่นของสารละลายเพิ่มขึ้น เนื่องจากความเข้มข้นของ NaCl สูงขึ้น ผลกระทบของเวลาในการแช่น้ำเกลือนั้น สามารถอธิบายได้จากความจริงที่ว่า มีความสัมพันธ์แบบผกผันระหว่างปริมาตรรูพรุน และความเร็วของคลื่นพัลส์ ปริมาตรของรูพรุนในมอร์ตาร์จะลดลงตามเวลา เนื่องจากระดับของความอิ่มน้ำของซีเมนต์ขึ้นอยู่กับระยะเวลา เมื่อเนื้อคอนกรีตถูกกัดกร่อนจนเป็นช่องว่าง จะทำให้คลื่นเคลื่อนที่ผ่านตัวกลางได้ช้าลง แต่เนื่องจากในการทดสอบพบว่ามีเกลือตกผลึกในช่องว่างรวมถึงมีน้ำเกลืออยู่ จึงเป็นผลที่ส่งเสริมทำให้คลื่นเคลื่อนเคลื่อนที่ได้เร็วขึ้น

รูปที่ 4 ความสัมพันธ์ระหว่างเปอร์เซ็นต์การดูดซับน้ำและระยะเวลาแช่น้ำเกลือ
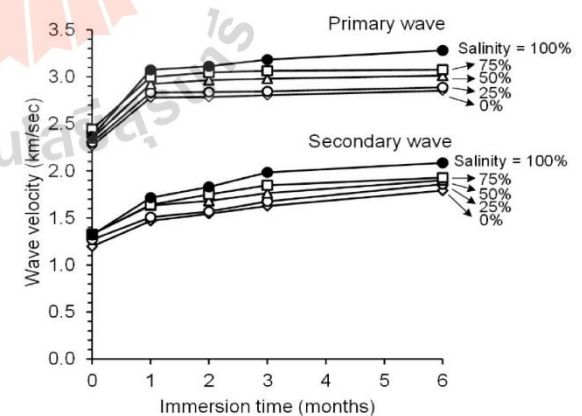
รูปที่ 5 ความสัมพันธ์ระหว่างความเร็วคลื่น (P-wave และ S-wave) และระยะเวลาแช่น้ำเกลือ
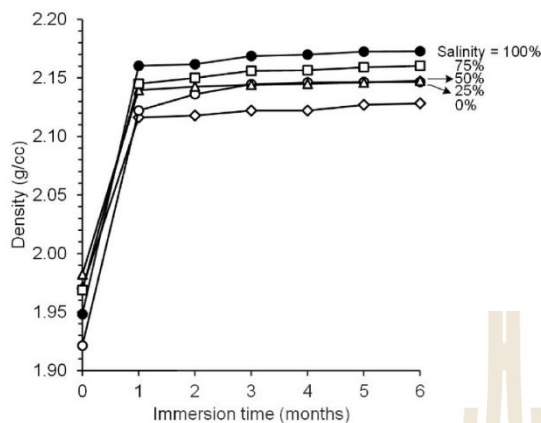
รูปที่ 6 ความสัมพันธ์ระหว่างความหนาแน่นและระยะเวลา
แช่น้ำเกลือ

4. สรุป

จากการศึกษาผลกระทบของน้ำเค็มต่อการเสื่อมสภาพของคอนกรีต ซึ่งประเมินจากการเปลี่ยนแปลงของกำลังอัดของคอนกรีต ค่าความสามารถในการดูดซับน้ำ และการเปลี่ยนแปลงของแร่ที่เกิดจากปฏิกิริยาไฮเดรชัน โดยที่ตัวอย่างคอนกรีตถูกแช่อยู่ในน้ำเค็มที่มีระดับความเค็ม 0%, 25%, 50% 75% และ 100% เวลาเป็นช่วงเวลาจาก 0 ถึง 6 เดือน จากผลการทดสอบสามารถสรุปผลได้ดังนี้

1) กำลังอัดกำลังอัดของคอนกรีตมีค่าลดลงอย่างต่อเนื่องตามระยะเวลาและระดับความเค็มที่เพิ่มขึ้น ทั้งนี้เนื่องจากเกิดการกัดกร่อนของตัวอย่างคอนกรีต โดยที่แร่ที่เกิดจากปฏิกิริยาไฮเดรชัน ได้แก่ ไดแคลเซียมซิลิเกต (C_2S) ไตรแคลเซียมซิลิเกต (C_3S) ไตรแคลเซียมอะลูมิเนต (C_3A) และเตตระแคลเซียมอลูมิโนเฟอร์ไรต์ (C_4AF) เกิดการผุกร่อนจากการทำปฏิกิริยาเคมีระหว่างคลอไรด์กับแร่แคลเซียมซิลิเกต (C_2S และ C_3S) จนทำให้คอนกรีตมีกำลังลดลง

2) ความสามารถในการดูดซับน้ำของตัวอย่างมอร์ตาร์ มีค่าเพิ่มขึ้นเมื่อระยะและความเค็มเพิ่มขึ้น ซึ่งสนับสนุนว่าตัวอย่างมีช่องว่างเพิ่มขึ้นจากการที่แร่แคลเซียมซิลิเกต (C_2S และ C_3S) ผุกร่อนไปจนเป็นรูพรุนมากขึ้น

3) แร่แฮไลต์ (Halite) ที่ละลายในน้ำเค็มแทรกเข้าไปในเนื้อคอนกรีตและตกผลึกในช่องว่างที่เกิดจากการผุกร่อนของแร่แคลเซียมซิลิเกต (C_2S และ C_3S) ซึ่งมีแนวโน้มเพิ่มขึ้นตามระยะเวลาและความเข้มข้น บ่งชี้ว่าตัวอย่างเกิดการเสื่อมสภาพจากผลกระทบของน้ำเค็มในเชิงเวลา

4) ความเร็วคลื่น (P-wave และ S-wave) ที่เคลื่อนที่ผ่านตัวอย่างมอร์ตาร์มีค่าเพิ่มขึ้นตามระยะเวลาที่สัมผัสกับน้ำเค็มนานขึ้น ผลกระทบนี้จะเด่นชัดขึ้นที่ระดับความเข้มข้นสูง ผลดังกล่าวอาจขัดแย้งเหตุผลที่ว่าเมื่อเนื้อคอนกรีตถูกกัดกร่อนจนเป็นช่องว่าง จะทำให้คลื่นเคลื่อนที่ผ่านตัวกลางได้ช้าลง แต่เนื่องจากในการทดสอบพบว่ามีเกลือตกผลึกในช่วงว่างรวมถึงมีน้ำเกลืออยู่ จึงเป็นผลที่ส่งเสริมทำให้คลื่นเคลื่อนเคลื่อนที่ได้เร็วขึ้น

5) สมการทางคณิตศาสตร์ที่พัฒนาขึ้นในความสัมพันธ์ของกำลังอัดของคอนกรีต ระดับความเค็ม และเวลาที่สัมผัสกับน้ำเค็ม สามารถนำไปประเมินกำลังของคอนกรีตที่จมอยู่ในน้ำเกลือเป็นเวลาต่าง ๆ กัน

5. กิตติกรรมประกาศ

เอกสารอ้างอิง

[1] Austin Socorro Rodrigues. (2014). Deterioration of Concrete. *Civil Engineering.* 1(4): pp. 1-6

[2] Tiwari, P., Chandak, R. and Yadav, R. (2014). Effect of salt water on compressive strength of concrete. *International Journal of Engineering Research and Applications*, 4(4): 38-42.

[3] Islam, M. M., Islam, M. S., Mondal, B. C. and Islam, M. R. (2010). Strength behavior of concrete using slag with cement in sea water environment. *Journal of Civil Engineering (IEB)*, 38(2): 129-140.

[4] สำนักงานนโยบาย และ แผนสิ่งแวดล้อม. (2016). *การประชุมคณะอนุกรรมการพิจารณาสถานที่ทำงานของหน่วยราชการ ในเขตกรุงเทพมหานคร และ เมือง หลัก ครั้ง ที่ 8/2543 วัน ที่ 9 มิถุนายน 2543* (No. 136962).

[5] Lyman, J. and Fleming, R. (1940) Composition of seawater. *Journal of Marine Research*, 3: 134-146.

[6] Bassuoni, M. T. and Rahman, M. M. (2016). Response of concrete to accelerated physical salt attack exposure. *Cement and concrete research*, 79: 395-408.

[7] Althoey, F. (2021). Compressive strength reduction of cement pastes exposed to sodium chloride solutions: Secondary ettringite formation. *Construction and Building Materials*, 299: 123965.

[8] ASTM C39/C39M-14 (2014). Standard Test Method for Compressive Strength of Cylindrical Concrete Specimens. *Annual Book of ASTM Standards*, American Society for Testing and Materials, West Conshohocken, PA.

[9] ASTM C805-2 (2010). Standard Test Method for Rebound Number of Hardened Concrete. *Annual Book of ASTM Standards*, American Society for Testing and Materials, West Conshohocken, PA.

[10] Neamluang, T., Khwankaew, J., Rujiphonphiphat, J., Samphao, W. and Onura, W. (2018). The study of effects of saline water on irrigation structures: A case study of Chonlahan Phichit operation and maintenance project. *Chonlasarn Research Journal of Irrigation Management*, 6(1): 52-62.

[11] Qasim, O. A., Maula, B. H., Moula, H. H., and Jassam, S. H. (2020). Effect of Salinity on Concrete Properties. *Materials Science and Engineering.* 745(1): 012171.

[12] K. Riley, M. Hobson, and S. Bence, "Mathematical methods for physics and engineering," *A Comprehensive Guide. [Quantum operators]*, pp. 648-712, 1998.

[13] Choi, S. I., Park, J. K., Han, T. H., Pae, J., Moon, J. and Kim, M. O. (2022). Early-age mechanical properties and microstructures of Portland cement mortars containing different admixtures exposed to seawater. *Case Studies in Construction Materials*, 16, 01041.

[14] ASTM C597-97 (2017). Standard Test Method for Pulse Velocity Through Concrete. *Annual Book of ASTM Standards*, American Society for Testing and Materials, West Conshohocken, PA.

[15] Ramírez-Ortíz, A. E., Castellanos, F. and Cano-Barrita, P. F. D. J. (2018). Ultrasonic detection of chloride ions and chloride binding in Portland cement pastes. *International Journal of Concrete Structures and Materials*, 12(1), 1-12.

บุรินทร์ ทองเกลี้ยง
นักศึกษาระดับบัณฑิตศึกษา สาขาวิชา
เทคโนโลยีธรณี สำนักวิชาวิศวกรรมศาสตร์
มหาวิทยาลัยเทคโนโลยีสุรนารี

เดโช เผือกภูมิ
อาจารย์ประจำ สาขาวิชาเทคโนโลยีธรณี สำนัก
วิชาวิศวกรรมศาสตร์ มหาวิทยาลัยเทคโนโลยี
สุรนารี วศ.ด. เทคโนโลยีธรณี มหาวิทยาลัย
เทคโนโลยีสุรนารี

BIOGRAPHY

Miss Burin Thongkliang was born on December 1, 1997 in Buriram Province, Thailand. She received her Bachelor's Degree in Engineering (Geological Engineering) from Suranaree University of Technology in 2019. For her post-graduate, she continued to study with a Master's degree in the Geological Engineering Program, Institute of Engineering, Suranaree University of Technology. During graduation, 2020-2023, she was a part time worker in position of research assistant at the Geomechanics Research Unit, Institute of Engineering, Suranaree University of Technology. She published a technical paper related to concrete mechanics, titled effects of salinity of salt water on mechanical properties of concrete in the proceeding of the 7th RMUTP Conference on Engineering and Technology 2023, Rajamangala University of Technology Phra Nakhon, Bangkok, Thailand.